

**An Anatomical and Physiological Investigation of  
Ectomycorrhizal *Pinus banksiana* (Lamb.) and  
*Eucalyptus grandis* (W. Hill ex Maiden) Roots**

by

**Jeff H. Taylor**

**A thesis**

**Presented to the University of Waterloo  
in fulfillment of the thesis requirement for the degree of  
Doctor of Philosophy  
in  
Biology**

**Waterloo, Ontario, Canada, 2000**

**©Jeff H. Taylor 2000**



National Library  
of Canada

Acquisitions and  
Bibliographic Services

395 Wellington Street  
Ottawa ON K1A 0N4  
Canada

Bibliothèque nationale  
du Canada

Acquisitions et  
services bibliographiques

395, rue Wellington  
Ottawa ON K1A 0N4  
Canada

*Your file* *Votre référence*

*Our file* *Notre référence*

The author has granted a non-exclusive licence allowing the National Library of Canada to reproduce, loan, distribute or sell copies of this thesis in microform, paper or electronic formats.

The author retains ownership of the copyright in this thesis. Neither the thesis nor substantial extracts from it may be printed or otherwise reproduced without the author's permission.

L'auteur a accordé une licence non exclusive permettant à la Bibliothèque nationale du Canada de reproduire, prêter, distribuer ou vendre des copies de cette thèse sous la forme de microfiche/film, de reproduction sur papier ou sur format électronique.

L'auteur conserve la propriété du droit d'auteur qui protège cette thèse. Ni la thèse ni des extraits substantiels de celle-ci ne doivent être imprimés ou autrement reproduits sans son autorisation.

0-612-51231-2

**Canada**

**The University of Waterloo requires the signatures of all persons using or photocopying this thesis. Please sign below, and give address and date.**

## Abstract

Tree roots have a very unique anatomy. It was only recently discovered that woody roots possess three distinct anatomical regions, the white, condensed tannin and cork zones. Additionally, many tree roots naturally form symbiotic associations with soil fungi. The resulting ectomycorrhizal root tips that are formed represent a fourth root region that must be considered as well. The distinct anatomy of each root region results in very different capacities for ion acquisition. In the present work, various aspects of ectomycorrhizal *Pinus banksiana* (Lamb.) and *Eucalyptus grandis* (W. Hill ex Maiden) root anatomy were examined, and the impacts of the results on potential for nutrient acquisition were considered. Firstly, the vitality of the extramatrical hyphae of growth-pouch grown *P. banksiana* ectomycorrhizae were investigated. It was found that while a large fraction of the hyphae are alive, most are encased in impermeable walls. Secondly, the permeability of *P. banksiana* and *E. grandis* ectomycorrhizal mantles to physiologically significant ions was tested, and the mantles were found to be impermeable to sulphate ions. Similarly, the permeability of the outer surface of the cork zone of both these tree species was tested. The phellem proved to be permeable to sulphate ions, though sparingly so. Lastly, the anatomy of ectomycorrhizal growth-chamber grown *E. grandis* seedlings and growth-chamber and field-grown *P. banksiana* seedlings were investigated to assess each root regions contribution to nutrient uptake. For both species, a considerable amount of the root tissue most suited for ion uptake is located within the ectomycorrhizal mantle. Because the remainder of the root system is rather poorly suited and situated for soil mineral uptake, it was concluded that the vast majority of the ions absorbed by the root system are supplied

by the fungal partner and fed to the root tips within the fungal mantle. The remainder of the root system serves only as conduits from the root tips to the above ground portions of the tree.

## Acknowledgements

I would like to thank my Supervisor Dr. Carol A. Peterson, for teaching me how to be a scientist, and for financial support through her Natural Sciences and Engineering Research Council of Canada (NSERC) grant. I also thank my other committee members, Dr. Larry Peterson, Dr. Gina Mohammed and Dr. Wayne Hawthorn for their time and efforts.

I must thank NSERC for their financial support through a Postgraduate Industrial Scholarship and PGS B award. I also thank Mikro-Tek and Mark Kean for sponsoring the Industrial scholarship, and Wayne Smith, and Kerry Fisher for all their help while I was in Timmins.

I thank my lab mates, especially Daryl Enstone for her expertise with everything in the lab. A special thanks to “Captain” Dave Barrowclough, for increasing the quotient of beer in my life, and his unyielding resilience in the struggle of man. Thanks also to Jon Van Hamme, who led the revolution against university bureaucracy.

I must thank Ms. Lynn Hoyles for keeping the growth chamber functional and my plants alive, and Dr. Greenberg and Dr. Carlson for trusting me with their equipment.

Most importantly, I want to thank my wife, Susanne, for her help, support, and understanding in academics and in life. Without her love, I could not be where I am today. Thanks, Susanne. I love you.

This thesis was brought to you by the letter M and the number 3.

## TABLE OF CONTENTS

<b>ABSTRACT.....</b>	<b>iv</b>
<b>ACKNOWLEDGEMENTS.....</b>	<b>vi</b>
<b>LIST OF TABLES.....</b>	<b>xi</b>
<b>LIST OF FIGURES.....</b>	<b>xii</b>
<b>CHAPTER 1: Introduction.....</b>	<b>1</b>
<b>CHAPTER 2: Permeability of the cork and fungal mantle in ectomycorrhizal tree roots to berberine, PTS and sulphate ions.....</b>	<b>15</b>
<b>2.1. Abstract.....</b>	<b>15</b>
<b>2.2. Introduction.....</b>	<b>16</b>
<b>2.3. Methods.....</b>	<b>17</b>
<b>2.3.1. Organisms and cultural conditions.....</b>	<b>17</b>
<b>2.3.2. Berberine permeability tests.....</b>	<b>18</b>
<b>2.3.3. PTS and sulphate permeability tests.....</b>	<b>22</b>
<b>2.4. Results.....</b>	<b>29</b>
<b>2.4.1. Periderm and polyderm.....</b>	<b>29</b>
<b>2.4.1.1. Permeability to berberine.....</b>	<b>29</b>
<b>2.4.1.2. Permeability to PTS and sulphate ions.....</b>	<b>32</b>
<b>2.4.2. Fungal mantle.....</b>	<b>33</b>
<b>2.4.2.1. Permeability to berberine.....</b>	<b>33</b>
<b>2.4.2.2. Permeability to PTS and sulphate ions.....</b>	<b>40</b>
<b>2.5. Discussion.....</b>	<b>40</b>
<b>2.5.1. Permeability of the phellem.....</b>	<b>40</b>
<b>2.5.2. Permeability of the fungal mantle.....</b>	<b>46</b>
<b>2.5.3. Conclusions.....</b>	<b>48</b>

<b>CHAPTER 3: Maturation of the tracheary elements in the roots of <i>Pinus banksiana</i> (Lamb.) and <i>Eucalyptus grandis</i> (W. Hill ex Maiden)</b> .....	<b>49</b>
3.1. Abstract.....	49
3.2. Introduction.....	50
3.3. Methods.....	52
3.4. Results and Discussion.....	54
<b>CHAPTER 4: Morphometric analysis of <i>Pinus banksiana</i> Lamb. root anatomy during a three-month field study</b> .....	<b>64</b>
4.1. Abstract.....	64
4.2. Introduction.....	65
4.3. Methods.....	68
4.3.1. Plant material.....	68
4.3.1.1. Growth chamber.....	68
4.3.1.2. Field.....	69
4.3.2. Root sampling.....	70
4.3.3. Root structure.....	70
4.3.4. Root measurements.....	71
4.3.5. Calculations of CPSA.....	72
4.3.5.1. Cortical cells.....	72
4.3.5.2. Passage cells.....	73
4.4. Results.....	73
4.4.1. Field conditions.....	73
4.4.2. Root anatomy.....	73
4.4.3. Contributions of the anatomical zones to total root length.....	78
4.4.4. Root tip frequency and structure.....	79
4.4.5. CPSA.....	82
4.5. Discussion.....	90
4.5.1. Anatomy.....	90



4.5.2. Root composition and growth.....	93
4.5.3. Metacutization.....	94
4.5.4. Ion uptake capacity.....	95
<b>CHAPTER 5: Morphometric study of ectomycorrhizal <i>Eucalyptus grandis</i></b>	
<b>(W. Hill ex Maiden) seedling roots.....</b>	<b>98</b>
<b>5.1. Abstract.....</b>	<b>98</b>
<b>5.2. Introduction.....</b>	<b>98</b>
<b>5.3. Methods.....</b>	<b>101</b>
<b>5.3.1. Plant material.....</b>	<b>101</b>
<b>5.3.2. Root sampling.....</b>	<b>102</b>
<b>5.3.3. Root structure.....</b>	<b>102</b>
<b>5.3.4. Root measurements.....</b>	<b>103</b>
<b>5.3.5. Calculations of APSA.....</b>	<b>105</b>
<b>5.3.5.1. Epidermal and cortical cells.....</b>	<b>105</b>
<b>5.3.5.2. Root hairs.....</b>	<b>106</b>
<b>5.3.5.3. Passage cells.....</b>	<b>107</b>
<b>5.4. Results.....</b>	<b>107</b>
<b>5.4.1. Root anatomy.....</b>	<b>107</b>
<b>5.4.2. APSA.....</b>	<b>111</b>
<b>5.5. Discussion.....</b>	<b>118</b>
<b>CHAPTER 6: Viability and wall permeability of the extramatrical hyphae of</b>	
<b>the ectomycorrhizal fungus <i>Hebeloma cylindrosporum</i> (Romagnesi).....</b>	<b>121</b>
<b>6.1. Abstract.....</b>	<b>121</b>
<b>6.2. Introduction.....</b>	<b>121</b>
<b>6.3. Methods.....</b>	<b>123</b>
<b>6.3.1. Organisms and cultural conditions.....</b>	<b>123</b>
<b>6.3.2. Reagents and techniques.....</b>	<b>124</b>

6.3.3. Influence of the age of the ectomycorrhizal association.....	126
6.3.4. Wall permeability of the extramatrical hyphae.....	126
6.4. Results.....	127
6.5. Discussion.....	130
<b>CHAPTER 7: Conclusions.....</b>	<b>138</b>
7.1. Novel developments.....	138
7.1.1. Fungal vitality tests.....	139
7.1.2. Tissue surface permeability.....	140
7.2. A model of woody root structure and function.....	142
7.3. Pertinent questions raised by this thesis.....	145
7.4. Summary.....	146
<b>REFERENCES.....</b>	<b>148</b>

**LIST OF TABLES**

<b>Table 2.1: The treatment and receiver solutions for the cork and ectomycorrhizal IPT tests under the three conditions (1 experimental, 2 control) examined with both PTS and radiolabeled sulphate.....</b>	<b>28</b>
<b>Table 2.2: Flow of PTS and sulphate through the intact phellem. ....</b>	<b>39</b>
<b>Table 4.1: Average dimensions and numbers (#) of living cortical cells (CC), passage cells (PC), and average calculated CPSA per millimeter root length for each root zone.....</b>	<b>89</b>
<b>Table 5.1: Living cell plasmalemma surfaces accessibility by the soil solution in ectomycorrhizal eucalypt roots.....</b>	<b>108</b>

## LIST OF FIGURES

<b>Figure 1.1:</b> Representation of three anatomical zones found in a <i>Pinus banksiana</i> (Lamb.) root. ....	2
<b>Figure 1.2:</b> Representation of an <i>Eucalyptus grandis</i> root in median longitudinal section.....	4
<b>Figure 1.3:</b> Representation of an endodermis/exodermis in cross-section.....	7
<b>Figure 1.4:</b> Representation of an ectomycorrhizal, non-exodermal root in both cross- (a) and longitudinal-section (b).....	9
<b>Figure 2.1:</b> A schematic face view of ectomycorrhizal root tips prepared for exposure to berberine. ....	20
<b>Figure 2.2 a, b:</b> Sketches of cork zone (a) and ectomycorrhizal roots (b) prepared for the internal perfusion technique (IPT). ....	24
<b>Figure 2.3a:</b> Cross-section of a cork zone <i>P. banksiana</i> root in white light.....	30
<b>Figure 2.3b:</b> Cross-section of a cork zone <i>E. grandis</i> root in white light.....	30
<b>Figure 2.3c:</b> Cross-section of a <i>P. banksiana</i> cork zone root following treatment with B/KSCN.....	30
<b>Figure 2.3d:</b> Cross-section of an <i>E. grandis</i> cork zone root following treatment with B/KSCN.....	30

<b>Figure 2.3e:</b> Cross-section of a <i>P. banksiana</i> cork zone root in which the phellem was severed before treatment with B/KSCN.....	30
<b>Figure 2.3f:</b> Cross-section of an <i>E. grandis</i> cork zone root in which the phellem was severed before treatment with B/KSCN. ....	30
<b>Figure 2.3g:</b> Cross-section of a <i>H. cylindrosporum/P. banksiana</i> ectomycorrhizal root following treatment with B/KSCN. ....	30
<b>Figure 2.3h:</b> Cross-section of a <i>H. cylindrosporum/P. banksiana</i> ectomycorrhizal root in which the mantle surface was severed before B/KSCN treatment.....	30
<b>Figure 2.3i:</b> Cross-section of a <i>H. cylindrosporum/P. banksiana</i> ectomycorrhiza in which B/KSCN was allowed access to the root tissue basipetal to the mantle.	30
<b>Figure 2.4:</b> The average apparent volume ( $\mu\text{l}$ ) of PTS solution ( $\pm$ S.E.) that entered the receiver solution at various times during the IPT experiment for both intact and wounded cork zone roots of <i>E. grandis</i> and <i>P. banksiana</i> (n=4).....	34
<b>Figure 2.5:</b> The average apparent volume ( $\mu\text{l}$ ) of $^{35}\text{SO}_4^{-2}$ solution ( $\pm$ S.E.) that entered the receiver solution at various times during the IPT experiment for both intact and wounded cork zone roots of <i>E. grandis</i> and <i>P. banksiana</i> .....	36
<b>Figure 2.6:</b> The average apparent volume ( $\mu\text{l}$ ) of PTS solution ( $\pm$ S.E.) that entered the receiver solution at various times during the IPT experiment for both intact and injured ectomycorrhizal <i>H. cylindrosporum / P. banksiana</i> roots.....	41

<b>Figure 2.7:</b> The average apparent volume ( $\mu\text{l}$ ) of $^{35}\text{SO}_4^{-2}$ solution ( $\pm$ S.E.) that entered the receiver solution at various times during the IPT experiment for both intact and injured ectomycorrhizal <i>H. cylindrosporum</i> / <i>P. banksiana</i> roots.....	43
<b>Figure 3.1:</b> The average growth rates (solid bar), and distances from the tip at which CBE (diagonal line bar) and cellufluor (wavy line bar) detected tracheary elements in <i>Pinus banksiana</i> and <i>Eucalyptus grandis</i> roots. ....	55
<b>Figure 3.2a:</b> <i>E. grandis</i> white root tip treated with cellufluor.....	58
<b>Figure 3.2b:</b> <i>E. grandis</i> brown root tip treated with cellufluor.....	58
<b>Figure 3.2c:</b> <i>P. banksiana</i> white root tip treated with cellufluor.....	58
<b>Figure 3.2d:</b> <i>P. banksiana</i> ectomycorrhizal root tip treated with cellufluor.....	58
<b>Figure 3.2e:</b> <i>E. grandis</i> short lateral root tip treated with CBE.....	58
<b>Figure 3.2f:</b> <i>E. grandis</i> brown root tip treated with CBE.....	58
<b>Figure 3.2g:</b> <i>P. banksiana</i> ectomycorrhizal root tip treated with CBE.....	58
<b>Figure 3.2h:</b> <i>P. banksiana</i> brown root tip treated with CBE.....	58
<b>Figure 3.3:</b> Relationship between the distance from the root tip the trachieds/ vessel members mature and the growth rate of the white root for <i>Pinus banksiana</i> and <i>Eucalyptus grandis</i> .....	61
<b>Figure 4.1:</b> Percent moisture ( $\pm$ SD) of the soil 0.15 m below the surface at the Kamiskotia Lake site over the time course of the experiment .....	74

<b>Figure 4.2: Soil temperature (<math>\pm</math> SD) 0.15 m below the surface from the Kamiskotia Lake site over the time course of the experiment.....</b>	<b>76</b>
<b>Figure 4.3: Lengths of cork, condensed tannin, white, and mycorrhizal root zones in roots of field- and chamber-grown seedlings.....</b>	<b>80</b>
<b>Figure 4.4: Numbers of brown, white, and mycorrhizal root tips in field- and chamber-grown seedlings. ....</b>	<b>83</b>
<b>Figure 4.5: The percent of metacutized root tips in field-grown seedlings.....</b>	<b>85</b>
<b>Figure 4.6: The percent of metacutized root tips among the three root tip types (white, brown, and mycorrhizal) in field-grown seedlings.....</b>	<b>87</b>
<b>Figure 4.7: The average total CPSA (cortical plasmalemma surface area) per seedling root system and the contribution of three root regions (condensed tannin, white, and mycorrhizal) in field- and chamber-grown seedlings.....</b>	<b>91</b>
<b>Figure 5.1: The average number of roots of each type (<math>\pm</math>S.D.) observed on an <i>E. grandis</i> seedling .....</b>	<b>109</b>
<b>Figure 5.2: The average length of each root region (<math>\pm</math>S.D.) in an <i>E. grandis</i> seedling root system.....</b>	<b>112</b>
<b>Figure 5.3: The average APSA (<math>\text{mm}^2</math>) per millimeter root length for each white root region of the main/tap, side, fine roots, and the ectomycorrhizal roots of the <i>E. grandis</i> seedlings.....</b>	<b>114</b>

<b>Figure 5.4: The average total APSA (mm<sup>2</sup>) for each white root region of the main/tap, side and fine roots, and the ectomycorrhizal roots of an <i>E. grandis</i> seedling .....</b>	<b>116</b>
<b>Figures 6.1-8: Whole mounts of <i>Hebeloma cylindrosporum</i> extramatrical hyphae (Figures 6.1-5) and <i>Pinus banksiana</i> white roots (Figures 6.6-8). .....</b>	<b>128</b>
<b>Figure 6.1: Extramatrical hyphae stained with fluorescein diacetate showing stained and unstained regions.....</b>	<b>128</b>
<b>Figure 6.2: Unstained extramatrical hyphae.....</b>	<b>128</b>
<b>Figure 6.3-5: Extramatrical hyphae stained with ethidium bromide.</b>	
<b>Figure 6.3: Concentrated ethanol pretreatment, showing fluorescing nuclei.</b>	<b>128</b>
<b>Figure 6.4: Heat pretreatment.....</b>	<b>128</b>
<b>Figure 6.5: Control (no pretreatment).....</b>	<b>128</b>
<b>Figures 6.6-8: Roots stained with EB.....</b>	<b>128</b>
<b>Figure 6.6: Ethanol pretreatment, fluorescing nuclei.....</b>	<b>128</b>
<b>Figure 6.7: Heat pretreatment, fluorescing nuclei.....</b>	<b>128</b>
<b>Figure 6.8: No pretreatment. Few fluorescing nuclei were present.....</b>	<b>128</b>
<b>Figure 6.9: Fraction of hyphae showing the fluorescence of the vitality stains ethidium bromide (EB), disodium fluorescein (DF) and fluorescein diacetate (FDA) at various ages of association.....</b>	<b>131</b>



**Figure 10: The number of fluorescing (ethidium bromide-stained) nuclei observed per millimeter of hyphae, following three pretreatments for extramatrical hyphae of a four week old association.....133**

## **CHAPTER 1**

### **Introduction**

Plant roots have evolved to serve two primary purposes. The first is to anchor the plant, and the second is to absorb the necessary nutrients from the soil solution. A wide variety of plant root systems have developed, each adapted to the specific environment in which the plant lives. A particularly interesting class of root is the woody roots, typically associated with trees, that undergo a series of unique modifications.

One special aspect of these roots is the production of wood, from which they obtained their name. Wood, which is made up of secondary xylem produced by the inward derivatives of the vascular cambium (Esau 1977), gives these roots their characteristic toughness. However, not all the roots of a woody root system are woody (McKenzie and Peterson 1995a,b). The young, growing tips of a woody root system are very similar to herbaceous roots, and they gradually mature to woody roots some distance behind the tip.

A second characteristic feature of woody roots is the presence of distinct anatomical zones (Figures 1.1, 1.2). These zones are produced by a developmental pattern responsible for the gradual metamorphosis of young root tips to mature, woody roots (McKenzie and Peterson 1995a,b). The root zone that includes the growing root tip is the white zone. It is characterized by the presence of viable cells in the cortex and epidermis. In addition, the apoplast of this zone is permeable from the surface of the root to the exodermis (if present) or endodermis (if no exodermis is present). Behind the white zone is the condensed tannin

**Figure 1.1: Representation of three anatomical zones found in a *Pinus banksiana* (Lamb.) root. Not drawn to scale.**

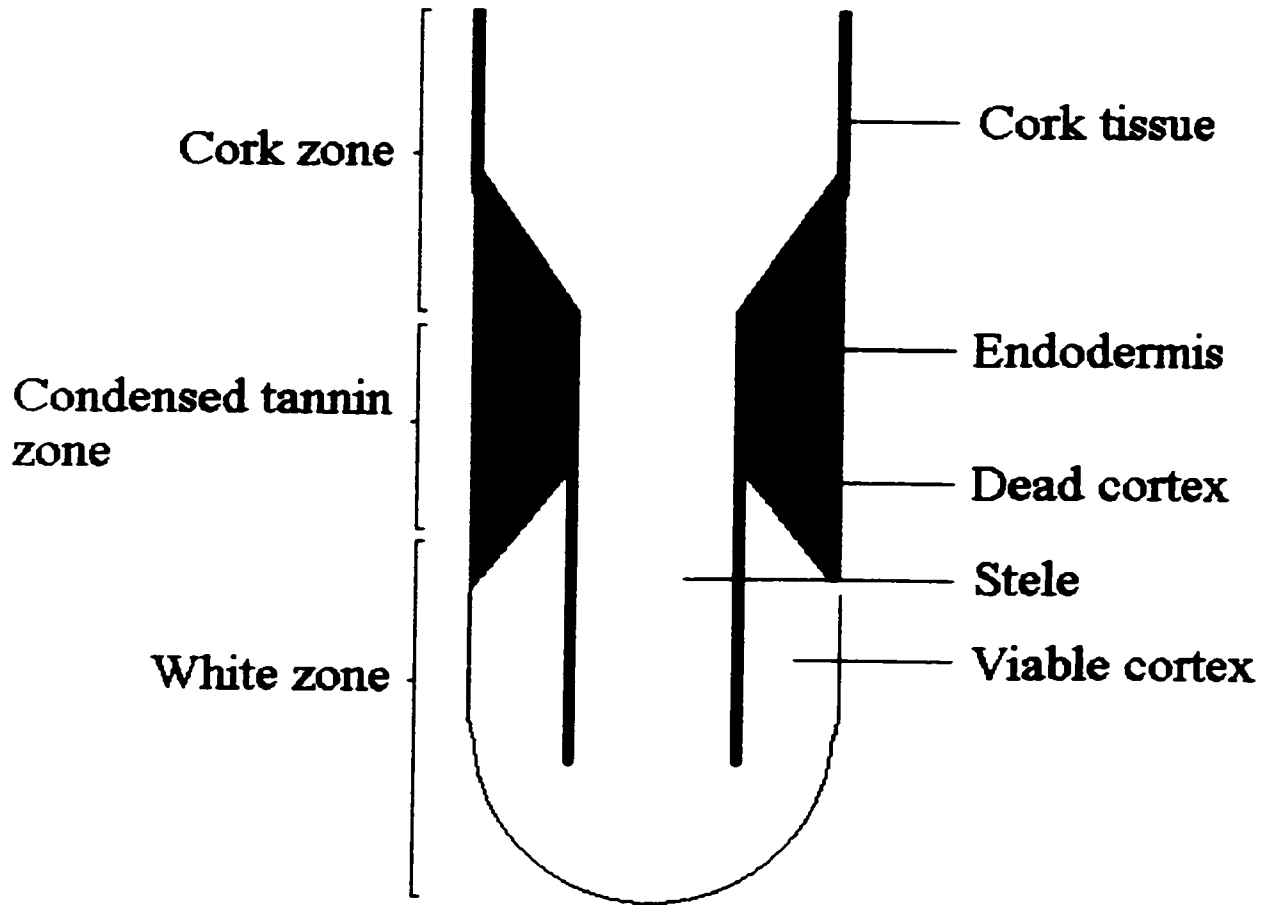


Figure 1.1

**Figure 1.2: Representation of an *Eucalyptus grandis* root in median longitudinal section. Not drawn to scale. The portion of the exodermis and endodermis drawn with dotted lines represents the root region in which the exodermis and endodermis have Casparian bands but no suberin lamellae.**

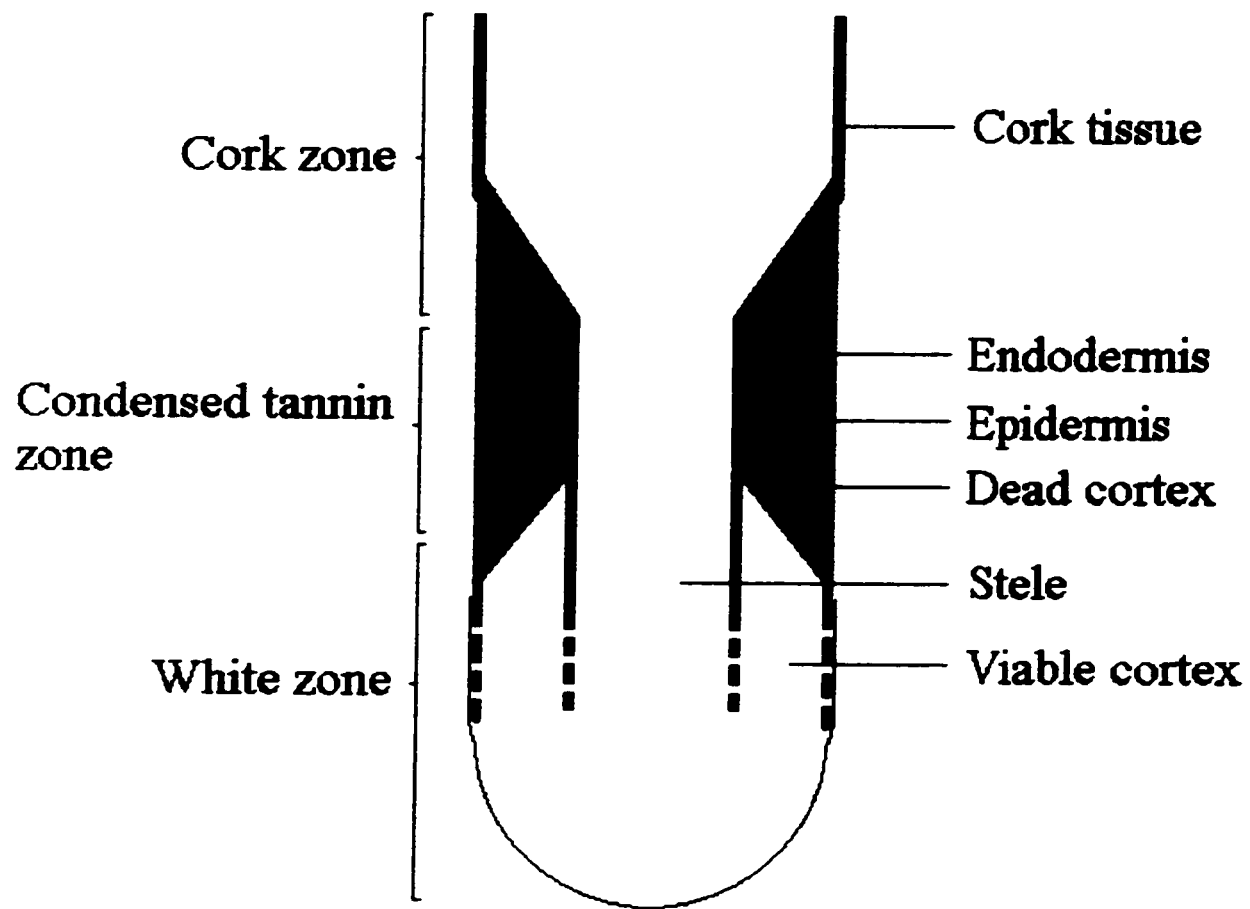


Figure 1.2

zone. Here, the epidermis and cortex (excluding the endodermis) are dead, and the accumulation of condensed tannins gives the roots a brown colour. The endodermis is still alive, and the passage cells (endodermal cells lacking suberin lamellae [Figure 1.3]) still provide a viable plasmalemmae surface area (Peterson and Enstone 1996). The most mature root zone is the cork zone. It begins at the point the first layer of phellem, located within the endodermis, is mature. Eventually, the cortex is shed and the dead, suberized cork cells become the outer surface of the root. Superficially, it is impossible to distinguish the young cork zone from the condensed tannin zone, and this has resulted in a great deal of confusion in the literature (e.g. Kramer 1946, Chung and Kramer 1974, Van Rees and Comerford 1990).

A third feature commonly, though not always, present on woody root systems is ectomycorrhizae (Figure 1.4 a,b). An ectomycorrhiza is an association between a root and a soil-borne fungus (see Smith and Read 1997). The root portion of this association resembles a white zone root. The fungal portion may be divided into three distinct components. Present between but not penetrating the root cells are the Hartig net hyphae. In an exodermal root, the Hartig net is only present in the epidermal layer, while in a non-exodermal root, the Hartig net hyphae are present among the epidermal and cortical cells (excluding the endodermis). Ensheathing the root tip, embedded in an extrahyphal matrix are the hyphae of the fungal mantle. Radiating out from the mantle into the soil solution are the extramatrical (or extraradical) hyphae and rhizomorphs. An ectomycorrhiza is a symbiotic union, as both partners benefit from the association. The fungus receives fixed

**Figure 1.3: Representation of an endodermis/exodermis in cross-section.**



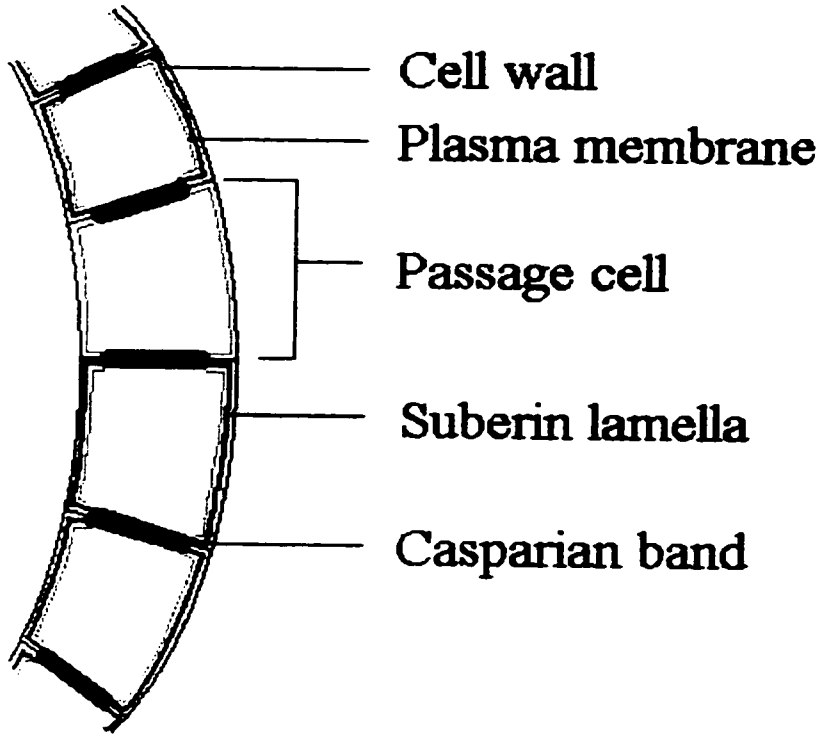


Figure 1.3

**Figure 1.4: Representation of an ectomycorrhizal, non-exodermal root in both cross- (a) and longitudinal-section (b).**

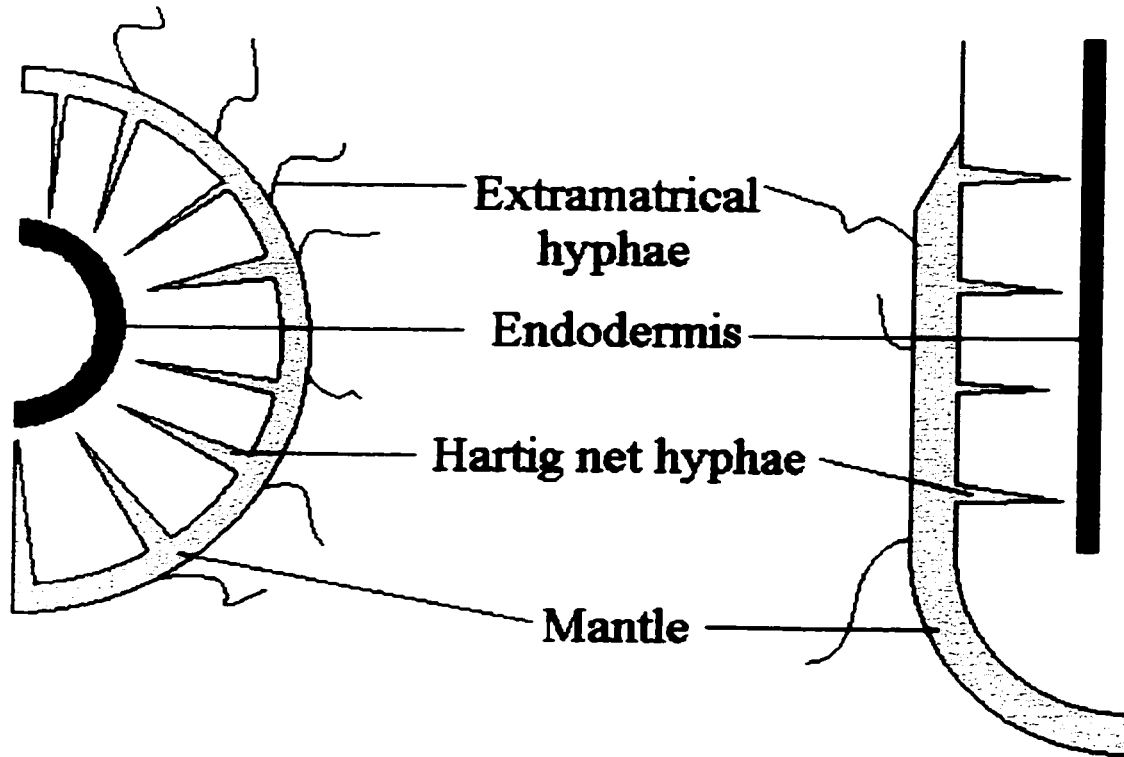


Figure 1.4

carbohydrates from the plant that it uses as food (Smith and Read 1997). Conversely, the plant receives mineral ions absorbed by the fungus. The exchange occurs between the cortical and/or epidermal cells of the plant and the Hartig net hyphae. Other physiological and ecological benefits have been proposed (see Smith and Read 1997), but the exchange of sugars and minerals is the best defined.

The acquisition of ions from the soil by roots has been intensively studied, which is not surprising given the basic significance and economic importance of the topic. However, an overwhelming proportion of this work involved herbaceous crop plants (see the references in Marschner 1986), leaving proposals of mineral absorption by woody roots highly speculative. This is significant, especially in light of the different root zones which woody roots possess that are not present in herbaceous roots. In addition, those studies which have examined ion uptake in woody species have been highly fractured, with root physiologists and mycorrhizal researchers working nearly isolated from each other. As a result, there is to date no strong model of ion uptake in woody systems.

There are three characteristics that a cell must have to be capable of absorbing an ion from the surrounding medium. First, the cell must be alive. Second, it must be exposed to the medium. In the case of plant root cells, the plasmalemmae must be exposed to the soil solution by a permeable apoplast. These criteria would eliminate suberized cells, such as mature cells of the exodermis or endodermis, as well as cells completely bounded by impermeable walls, such as the cells of the stele which are surrounded by the endodermis (Baker 1971; Robards and Robb 1974). Lastly, the cell must have the membrane transport proteins required to absorb the nutrient ion(s) in question.

The aim of this study was to examine the pathways of ion uptake. However, the molecular examinations necessary to verify the presence of plasmalemmae transport proteins were outside the scope of the project. Therefore, cells that were both alive and exposed to the soil solution by a permeable apoplast were considered to be potentially capable of absorbing ions. This condition applied to both plant and fungal cells. In the case of the fungal cells, the potential for ion uptake was quantified by measuring the plasmalemmae surface area of those cells potentially capable of absorbing ions.

In the course of this thesis, ectomycorrhizal *Pinus banksiana* (Lamb.) and *Eucalyptus grandis* (W. Hill ex Maiden) seedlings were studied with regard to various features relating to ion acquisition. These two species were chosen for a number of reasons. Firstly, both genera are very common, and of wide global distribution. Secondly, both are of great economic importance as harvestable timber. Lastly, *P. banksiana* is a gymnosperm, while *E. grandis* is an angiosperm and thus, they represent the two primary classes of trees (Esau 1977). To serve as inoculum, the common fungi *Hebeloma cylindrosporum* (Romagnesi) and *Pisolithus tinctorius* (Coker & Couch) were chosen for the pine and eucalypt, respectively. These are both very common ectomycorrhizal fungi, which have been used in numerous studies (e.g. Malajczuk et al. 1989, Oh et al. 1995).

A number of aspects relating to potential for nutrient acquisition from the soil were studied in this work, and, the research may be divided into three broad categories. One feature that was examined was surface permeability, specifically the permeability of the ectomycorrhizal mantle, and the phellem to sulphate ions. The permeability of these layers was very important in regard to nutrient uptake. If they were impermeable, then ions would

be unable to diffuse through them and the underlying tissues would be incapable of absorbing ions. In the case of the roots surrounded by the ectomycorrhizal mantle, the root cells would still contribute to ion uptake, but only those mineral ions passed to them by the fungal partner. Conversely, if these layers were permeable, then these root zones would be potentially capable of nutrient acquisition. The permeability of both these layers has been debated in the literature, but without consensus. In the case of the ectomycorrhizal mantle, permeability work had been performed with dyes only, employing a variety of techniques of varying suitability (Ashford et al. 1988, Behrmann and Heyser 1992). Likewise, the cork permeability work was often suspicious, particularly with regard to the means by which a piece of root was determined to be from the cork zone (e.g. Van Rees and Comerford 1990). Clearly, an accurate determination of the permeability of each of these root surfaces to nutrient ions was timely.

A second broad field that was examined was the maturation of the conductive xylem tissues. The tracheids of both angiosperms and gymnosperms, along with the vessel members of angiosperms, are responsible for the rapid longitudinal transport of ions absorbed by the root to the upper regions of the plant. However, these conductive cells develop some distance behind the tip (Wilcox 1962a). Portions of the root near the tip in which the vessel members and/or tracheids are not mature will not be very efficient at supplying ions to the remainder of the plant, as they will be dependent on slow diffusion of ions through cortex and stele cells until they contact the mature conducting xylem tissues. In this study, the distance behind the tip at which the xylem matured in various root types was determined, along with an assessment of the effect of root growth rate on xylem

maturation. Additionally, a comparison was made between the deposition of the secondary wall and the region in which the tracheids/vessel members become functional.

The final general field of study in this thesis was a determination of the potential for ion uptake in various regions of an ectomycorrhizal root system. This was estimated by measuring the plasmalemma surface area of living cells exposed to the soil solution. For the root portion, this work was done on ectomycorrhizal *P. banksiana* and *E. grandis* seedlings grown in a growth chamber. In addition, a time-course field study was done on *P. banksiana* seedlings. To the best of our knowledge, such measurements had only been performed previously on herbaceous systems. A separate study produced an estimate of the fraction of the extramatrical hyphae that were potentially capable of ion uptake. Taken together, a clear picture of where ion uptake potentially occurred in the entire woody root system was obtained.

The overall aim of this thesis was to produce a model of ion uptake in ectomycorrhizal tree roots. This was obtained by combining the results of the studies performed (see Discussion). This represents the most complete study of potential for ion uptake in woody root systems to date. While a number of assumptions were necessary, the predictions of this model will provide focus and, hopefully, serve as a catalyst for future studies in this area of plant physiology.

## CHAPTER 2

### **Permeability of the cork and fungal mantle in ectomycorrhizal tree roots to berberine, PTS and sulphate ions.**

#### **2.1 Abstract**

For a root zone to be capable of ion uptake, it must possess viable cells which can be contacted by the soil solution. While such cells clearly exist in the white non-mycorrhizal and condensed tannin zones, the presence of such cells is uncertain in the cork and white ectomycorrhizal zones, since the latter two are invested with a potentially impermeable outer tissue layer. In this study, the permeability of the cork (phellem) of *Pinus banksiana* (Lamb.) and *Eucalyptus grandis* (W. Hill ex Maiden) and the fungal mantle of *Hebeloma cylindrosporum* (Romagnesi)/ *P. banksiana* to berberine, trisodium 8-hydroxy-1,3,6-pyrenetrisulfonate (PTS) and sulphate ions was tested. A novel method, named the internal perfusion technique, was employed to examine the permeability of the outer tissue layers to PTS and sulphate. Both the cork and fungal mantles were impermeable to berberine. The ectomycorrhizal mantle also proved to be impermeable to PTS and sulphate ions, with the latter result being especially significant as it represents the first time an ectomycorrhizal mantle has been found to be impermeable to a nutrient ion. However, the cork surfaces of both species proved to be sparingly permeable to both PTS ( $0.0081 \mu\text{l} \cdot \text{mm}^{-2} \cdot \text{h}^{-1}$ ) and sulphate ions ( $1.3 \mu\text{l} \cdot \text{mm}^{-2} \cdot \text{h}^{-1}$ ). The implications of these results on ion uptake by the woody root system are discussed.



## 2.2 Introduction

Several researchers have observed ion acquisition by “brown”, “woody” or “suberized” roots, implying that the phellem is permeable to nutrient ions (Kramer 1946, Chung and Kramer 1974, Van Rees and Comerford 1990). However, two issues call this work into question. First, soil-grown roots were employed, and it is possible that the phellem was damaged in an attempt to unearth them. Second, these studies came before the work of McKenzie and Peterson (1995a,b) who subdivided the brown region into the condensed tannin zone and the cork zone. The former zone should be capable of ion uptake by passage cells in the endodermis (see Chapters 4 and 5 for a full discussion of tree root anatomy), but ion uptake by the cork zone is debatable. The cork zone differentiates from the condensed tannin zone at the point where a complete ring of dead, suberized phellem cells is produced within the endodermis. In most woody species, a layer of suberized cells (sometimes several cells in thickness), termed a periderm, is produced. However, in some cases (i.e., *Eucalyptus* sp.) several concentric rings, alternating between suberized and non-suberized cells are formed, and this is termed a polyderm (Esau 1977). In both cases, the young cork zone is superficially indistinguishable from the condensed tannin zone. Were the macroscopically-similar cork and condensed tannin zones formerly mistakenly treated as the same zone by researchers measuring ion uptake? McKenzie and Peterson (1995b) found cork zone roots to be impermeable to tracer dyes at their outer surface, an observation that is expected given the dead, suberized nature of the phellem. Of course, results with tracer dyes, which are larger than nutrient ions, cannot be extrapolated to

physiologically significant ions. Clearly, the question of cork zone permeability to nutrient ions has not been answered by prior studies.

The results of previous investigations into the permeability of the ectomycorrhizal mantle have been controversial. Ashford et al. (1988) established that *Pisonia* ectomycorrhizal mantles were impermeable to cellufluor, a fluorochrome that binds strongly to cellulose. However, their work was criticized by Behrmann and Heyser (1992) because of the slow diffusion of cellufluor within the apoplast. The latter authors found that ectomycorrhizal mantles in the *Suillus bovinus/Pinus sylvestris* association were permeable to sulphorodamine G and lanthanum nitrate. Their results were supported by later work (Kuhn et al. 1999, Vesik et al. 2000) in which the permeability of fungal mantles to calcium and magnesium, and lanthanum, respectively, were tested. However, in none of the latter studies was the mantle-covered root area properly sealed off from the remainder of the root. As a result, the tracer observed internal to the mantle may have entered the condensed tannin zone and diffused longitudinally to that point. Thus, the question of mycorrhizal mantle permeability to nutrient ions remains open.

In the current work, we determined the permeability of the phellem surface of cork roots of *P. banksiana* (Lamb.) and *E. grandis* (Hill ex Maiden) to dyes and sulphate ions. These species were chosen so that the permeability of a periderm (*P. banksiana*) and polyderm (*E. grandis*) would be tested. The permeability of the fungal mantle from *Hebeloma cylindrosporum* (Romagnesi)/*P. banksiana* ectomycorrhizae to these substances was also established. All roots were developed in growth pouches (Piché et al. 1983) to avoid damage during isolation. One of the dyes used was berberine (B), which was

precipitated in place with thiocyanate (KSCN), as described by Enstone and Peterson (1992). Berberine is a fluorescent alkaloid (molecular weight 384.4, monovalent cation) that can be easily visualized by fluorescence microscopy, allowing a rapid assessment of permeability or gross damage. The permeability to both trisodium 8-hydroxy-1,3,6-pyrenetrisulfonate (PTS; molecular weight 524.4, trivalent anion) and radiolabelled sulphate ( $^{35}\text{SO}_4^{2-}$ ) was then determined using a novel, internal perfusion technique (IPT). The impact of these permeability results on ion uptake in the cork and ectomycorrhizal zones will be discussed.

## **2.3 Methods**

### *2.3.1 Organisms and cultural conditions*

Seeds of *Pinus banksiana* (Lamb.) and *Eucalyptus grandis* (W. Hill ex Maiden) were supplied by Mikro-Tek (36 Emerald Street, P.O. Box 2120, Timmins, ON). The seeds were stratified in 4°C water for 2 days, sterilized in 33% (for *P. banksiana*) or 16.5% (for *E. grandis*) hydrogen peroxide with a drop of Tween 80 for 30 min, and then germinated on 1.5% Bactoagar. When the seedlings were 20 mm long (with roots and shoots being about equal length) they were transferred to sterile growth pouches (Fortin et al. 1980), which forced the root system to develop in a two-dimensional manner. Water and nutrient solutions were held on a paper insert within the pouch, and the system was aerated by a vertically oriented pipette. The pouches were held in a growth chamber where the temperatures were maintained at 25-23°C (day-night), daylength 16 h, photosynthetic photon flux density  $300 \mu\text{mol}\cdot\text{m}^{-2}\cdot\text{s}^{-1}$ , and relative humidity 75-85%. Seedlings were

watered twice weekly with 5-7 mL of sterile, distilled water; every fourth watering was with 25% Knop's solution (Loomis and Schull 1937).

The ectomycorrhizal fungus, *Hebeloma cylindrosporum* (obtained from Mikro-Tek), was maintained on plates of modified Melin-Norkrans medium at 22°C. Cultures were allowed to grow to a diameter of 60 mm. To inoculate the plants, three agar cuttings of 5 mm<sup>2</sup> were taken from the periphery of the fungal cultures and placed within 5 mm of white roots. Hyphal contact with the root generally occurred within 3 days of inoculation. Ectomycorrhizal establishment was considered complete at the time the mantle was mature (10 weeks, as established by preliminary studies).

### 2.3.2 *Berberine permeability tests*

The permeabilities of the phellem and fungal mantle were first assessed using the berberine thiocyanate technique developed by Enstone and Peterson (1992). For the cork zone, root segments (with no laterals) from the appropriate region (as determined by a sample cross-section) were cut under water, blotted and the ends sealed with a mix of 90% anhydrous lanolin and 10% paraffin wax (modified from Cruz et al. 1992). The segments were then immersed in 0.05% (w/v; 1.3 mM) berberine hemisulphate (Sigma, St. Louis, Mo.) in phosphate buffer (50 mM, pH 6.0) for 45 min. The specimens were removed from the berberine and rinsed with buffer, gently blotted, and placed in 50 mM potassium thiocyanate (J.T. Baker Inc, Phillipsburg, N.J.) for 45 min. At the end of this treatment period, half the thiocyanate solution was removed and replaced with buffer. To assess the permeability of the fungal mantle to berberine, ectomycorrhizal roots were oriented in a well as described above so that only the mantle-covered roots were situated in the center of

**Figure 2.1:** A schematic face view of ectomycorrhizal root tips prepared for exposure to berberine. Root “a” has only the mantle exposed to the berberine, while root “b” also has the root tissue basipetal to the mantle exposed.

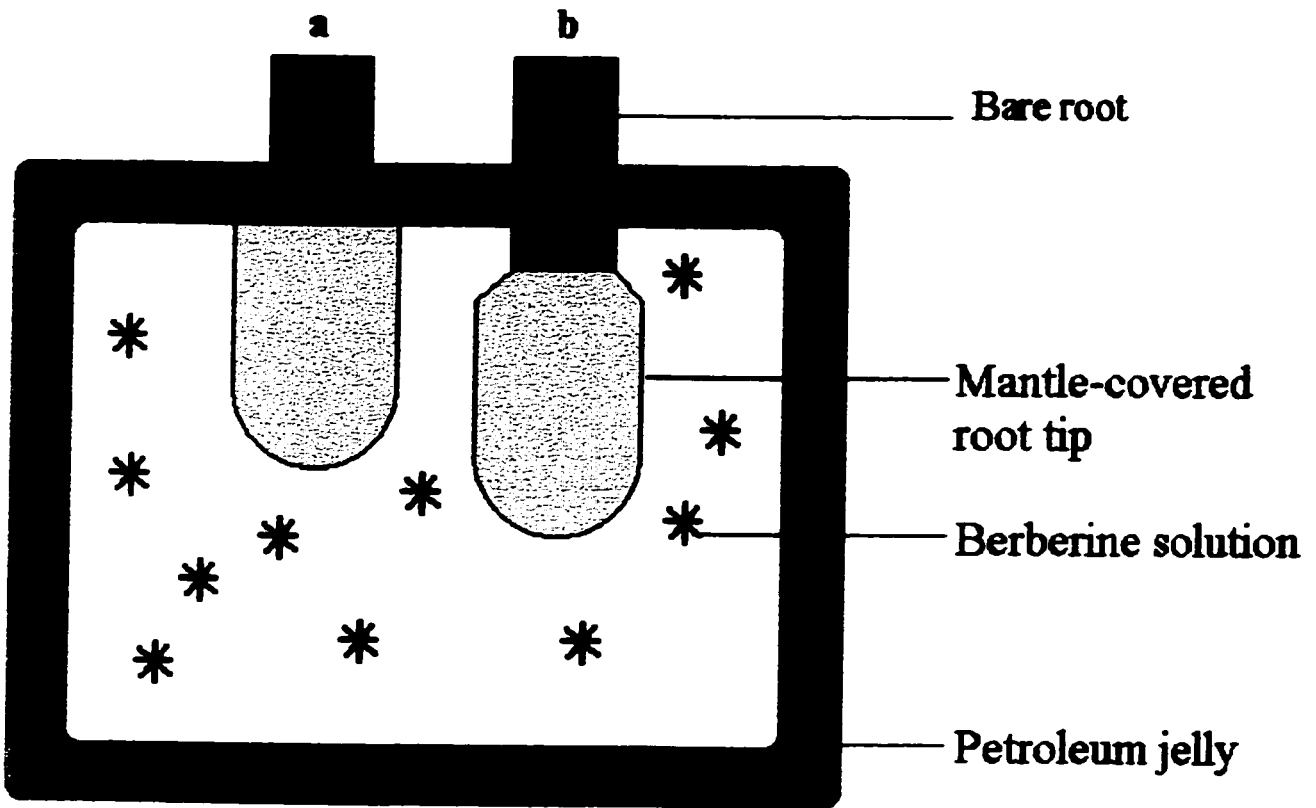


Figure 2.1

the well. Therefore, only the ensheathing mantle was exposed to the tracer (a in Figure 2.1). Additional roots were orientated in the petroleum jelly so that the root tissues basipetal to the mantle were also exposed to the treatment solution (b in Figure 2.1). The root tips were then processed as described above.

Two controls were employed for both the cork and ectomycorrhizal roots. In the first, the roots were exposed only to the phosphate buffer for the entire treatment time. In the second, a shallow longitudinal incision was made in the phellem (cork roots) or mantle (ectomycorrhizal roots) by a razor blade to expose the underlying tissue. These second root segments were otherwise treated as described above.

In preparation for observation, segments were rinsed briefly with thiocyanate, gently blotted and cut with a clean, dry double-edged razor blade. Sections were observed with violet light using a Zeiss Axiophot microscope (Carl Zeiss Canada, Don Mills, ON) equipped with an Osram HBO 100W mercury lamp and epifluorescence optics. The filter set consisted of exciter filter BP395-440, chromatic beam splitter FT460, and barrier filter LP470. Images were recorded on Kodak Ektachrome Elite II 100 film and developed into slides. The plate was made in Corel Draw 7.0.

### *2.3.3 PTS and sulphate permeability tests*

To test the phellem's and fungal mantle's permeability to PTS (a common apoplastic tracer) and mobile sulphate anions, an internal perfusion technique (IPT) was developed. In cork zone segments, the tracer solution in the micropipette was free to enter the root tissue, but due to the sealant coating between the root and micropipette tip and on the distal

end of the root, could only exit the root through the phellem surface (Figure 2.2a). For the ectomycorrhizal roots, the sealant was placed on the root so that the tracer could only exit through the fungal mantle (Figure 2.2b). This technique allows the permeability of specific root zones to various substances to be tested, and allows the permeability per unit surface area of root to be determined.

PTS and  $^{35}\text{SO}_4^{-2}$  permeability tests were implemented in the same manner using the IPT. For the cork zone, a root segment of 15 mm lacking laterals was held under water and cut from the root system. Three millimeters of one end were then placed in a disposable, 1 ml micropipette tip and fixed in place with sealant, which was also used to cover the end of the segment outside the micropipette (Figure 2.2a). The micropipette was then filled with either 1 ml of 0.1% PTS in de-ionized water or 1 ml of 0.69 mCi/ $\mu\text{l}$   $^{35}\text{SO}_4^{-2}$  in sulphate buffer (1 mM  $\text{Na}_2\text{SO}_4$ , 0.5 mM  $\text{Ca}(\text{NO}_3)_2$  in de-ionized water). This created a tracer column of 53 mm high above the root. The micropipette tip was then placed in a support apparatus so that the coated root tissue and exposed cork surface were submerged in 13 ml de-ionized water (for PTS) or the sulphate buffer (for  $^{35}\text{SO}_4^{-2}$ ) previously described in a small flask. The entire apparatus was placed on an orbital shaker set to approximately 1 revolution per second (to disperse any tracer in the receiver solution), and covered with plastic wrap. The receiver solutions were changed 1, 3, 5, 7 and 24 h after the experiment was initiated (4 replicates).

Two controls were employed for the cork zone roots. In the first (intact control), the pipette was filled with de-ionized water (for the PTS experiment) or sulphate buffer (for



**Figure 2.2 a, b:**        **Sketches of cork zone (a) and ectomycorrhizal roots (b) prepared for the internal perfusion technique (IPT). Apparatus and root segments are shown in longitudinal section.**

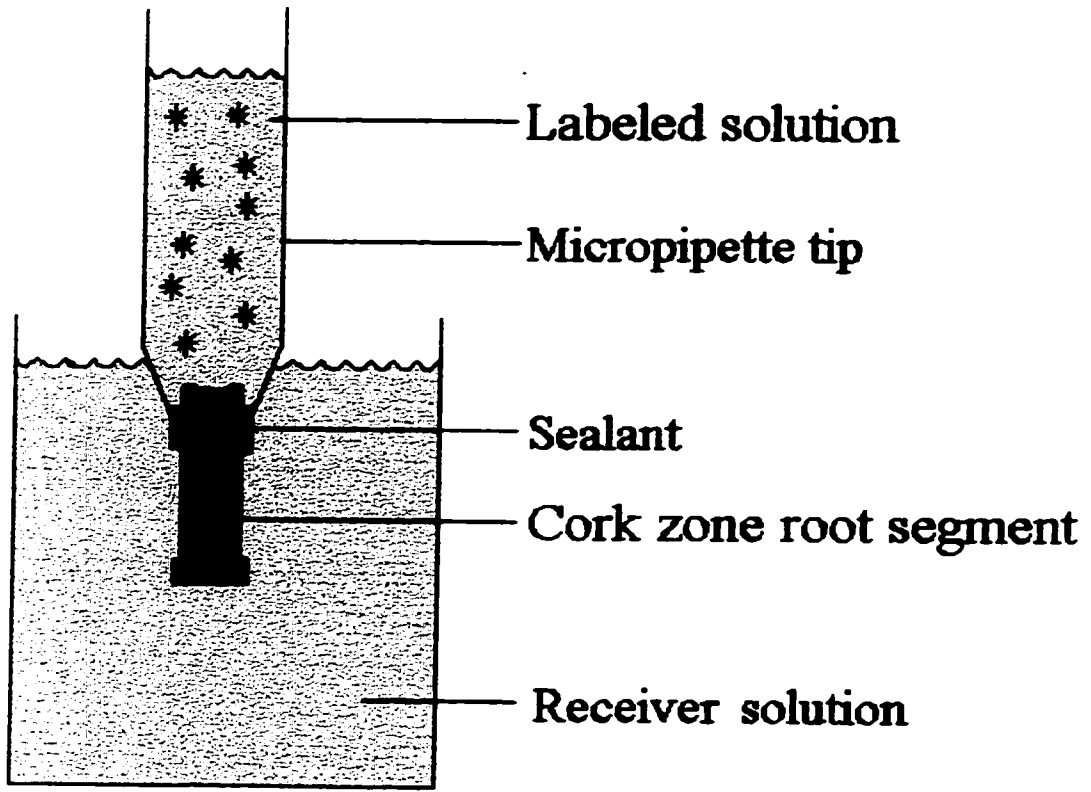


Figure 2.2a

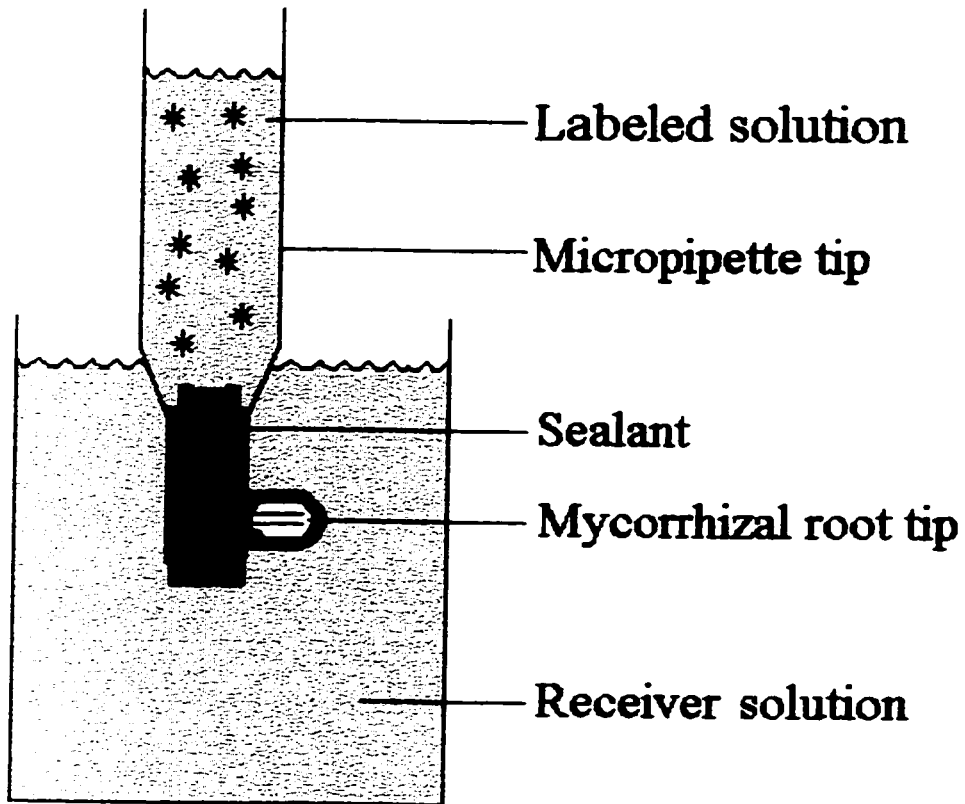


Figure 2.2b

the  $^{35}\text{SO}_4^{-2}$  experiment). The purpose of this was to establish that the root and sealant would not create artifactual results (4 replicates). In the second (cut control), a shallow, longitudinal cut was made to expose the underlying tissue while the root segment was still under water. The damaged phellem was oriented so that it was outside the pipette tip (in the receiver solution) and not sealed. If the tracer solutions could freely access the root tissues within the phellem, this damage should allow the tracer solution entry to the receiver solution (4 replicates). In addition, this second control provided an indication of the rate at which ions could pass through the tissue in the absence of the phellem surface.

To prepare the ectomycorrhizal roots for the IPT, roots possessing an ectomycorrhizal lateral were held under water and cut from the root system. These segments were then placed in a disposable 1 ml micropipette tip so that the ectomycorrhizal lateral was outside the pipette and fixed in place with sealant (Figure 2.2b). The sealant was also used to cover all the root tissue outside the micropipette tip, save for the mantle-covered tip (Figure 2.2b). The same procedure described above was used to test fungal mantle permeability to PTS and  $^{35}\text{SO}_4^{-2}$ . See Table 2.1 for a list of the treatment and receiver solutions for each test and control group.

PTS was measured using a MS III spectrofluorometer (Photon Technology International, Canada), exciting wavelength 405 nm and emission wavelength 510 nm. For  $^{35}\text{SO}_4^{-2}$ , a Searle liquid scintillation counter set to Program 8 (ISO-1) measuring each sample for 10 min was employed. For each sample, 6 ml was mixed with 14 ml of Ecolite (+) liquid scintillation fluid (ICN Pharmaceuticals Inc., Costa Mesa, CA).

Table 2.1: The treatment and receiver solutions for the cork and ectomycorrhizal IPT tests under the three conditions (1 experimental, 2 control) examined with both PTS and radiolabeled sulphate.

Condition	PTS/Sulphate Test	Treatment solution	Receiver solution
Intact	PTS	0.1% PTS in de-ionized water	de-ionized water
	Sulphate	0.69 mCi/ $\mu$ l $^{35}\text{SO}_4^{-2}$ in sulphate buffer (1 mM $\text{Na}_2\text{SO}_4$ , 0.5 mM $\text{Ca}(\text{NO}_3)_2$ in de-ionized water)	sulphate buffer
Intact control	PTS	de-ionized water	de-ionized water
	Sulphate	sulphate buffer	sulphate buffer
Cut surface control	PTS	0.01% PTS in de-ionized water	de-ionized water
	Sulphate	0.69 mCi/ $\mu$ l $^{35}\text{SO}_4^{-2}$ in sulphate buffer	sulphate buffer

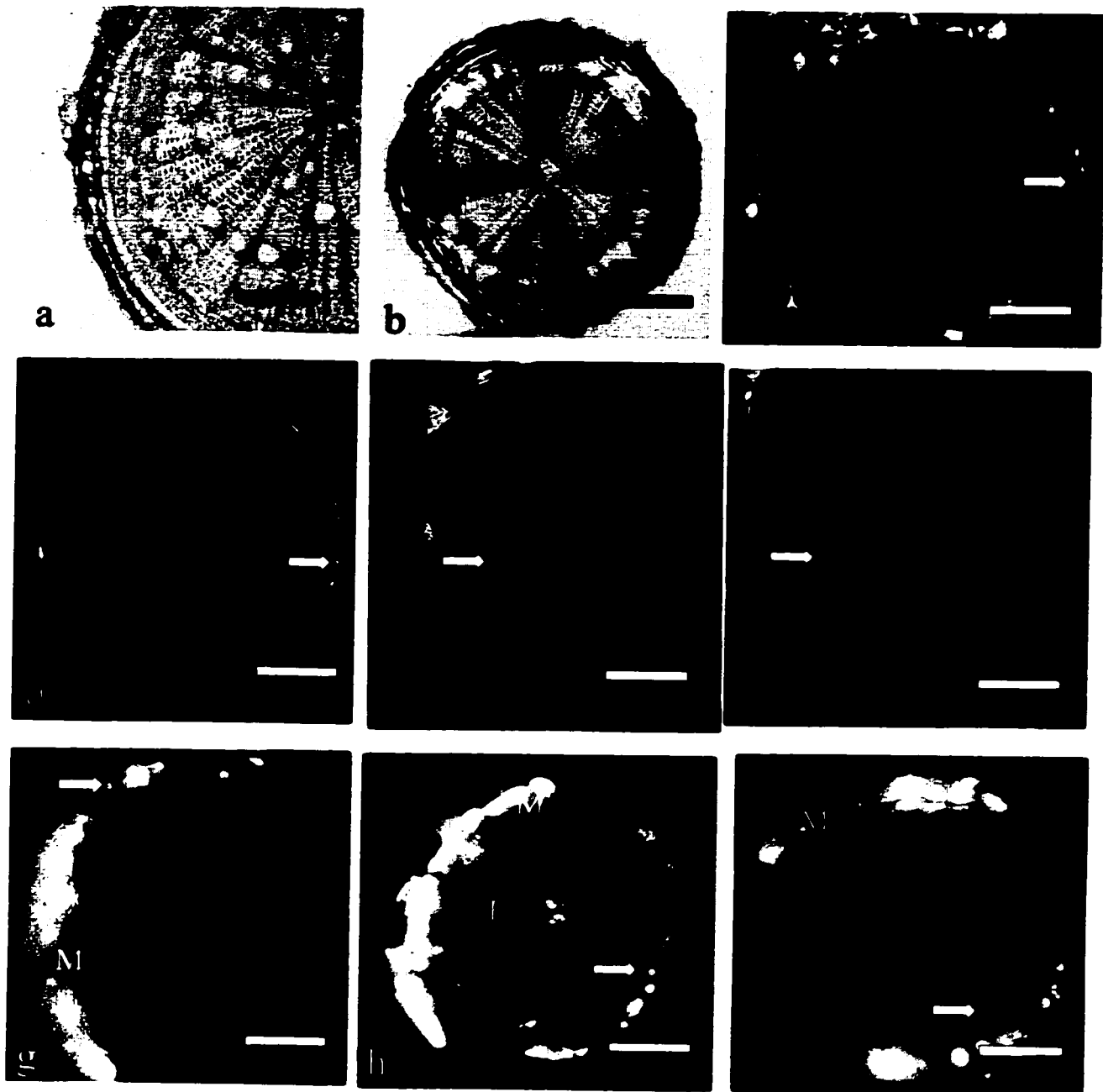
## 2.4 Results

### 2.4.1 Periderm and polyderm

#### 2.4.1.1 Permeability to berberine

Under white light, the control cross-sections (exposed only to phosphate buffer) of *Pinus banksiana* and *Eucalyptus grandis* appeared relatively similar (Figure 2.3a, 2.3b). Both possessed a few layers of phellem with a small amount of degrading tissue on their outer surfaces. The alternating suberized and non-suberized layers of the *E. grandis* polyderm were not often observed, likely due to the young age of the cork zone roots. The bulk of the root interior was made up of secondary xylem. In pine roots, this tissue formed a fairly regular cylinder. Its only conducting elements were tracheids, as determined in a maceration experiment (data not shown). In *E. grandis*, the outline of the xylem was irregular; the tissue contained both tracheids and vessel members (as seen in macerations, data not shown). Between the xylem and the cork were the cells of the pericycle, vascular cambium, phloem, and cork cambium. These cells were all similar in appearance, and they were much less distinct than the thick-walled elements in the xylem. Under UV light, the cross-sections of control *P. banksiana* and *E. grandis* roots were quite striking. Both the xylem and cork tissues emitted a deep blue light. The phloem and cambia were either colorless or gave off a dull, pale blue that may have been a reflection of the light from the xylem and cork. Photographs of these sections are not shown because they were barely visible at the low exposure times appropriate for controls of berberine-treated specimens.

- Figure 2.3a: Cross-section of a cork zone *P. banksiana* root in white light. Bar = 100  $\mu\text{m}$  (P = phellem).
- Figure 2.3b: Cross-section of a cork zone *E. grandis* root in white light. Bar = 200  $\mu\text{m}$  (P = phellem).
- Figure 2.3c: Cross-section of a *P. banksiana* cork zone root following treatment with B/KSCN. Ultraviolet illumination. Bar = 200  $\mu\text{m}$  (arrow = berberine thiocyanate crystal, P = phellem).
- Figure 2.3d: Cross-section of an *E. grandis* cork zone root following treatment with B/KSCN. Ultraviolet illumination. Bar = 200  $\mu\text{m}$  (arrow = berberine thiocyanate crystal, P = phellem).
- Figure 2.3e: Cross-section of a *P. banksiana* cork zone root in which the phellem was severed before treatment with B/KSCN. Ultraviolet illumination. Bar = 100  $\mu\text{m}$  (arrow = berberine thiocyanate crystal, P = phellem).
- Figure 2.3f: Cross-section of an *E. grandis* cork zone root in which the phellem was severed before treatment with B/KSCN. Ultraviolet illumination. Bar = 100  $\mu\text{m}$  (arrow = berberine thiocyanate crystal, P = phellem).
- Figure 2.3g: Cross-section of a *H. cylindrosporum* / *P. banksiana* ectomycorrhizal root following treatment with B/KSCN. Ultraviolet illumination. Bar = 100  $\mu\text{m}$  (arrow = berberine thiocyanate crystal, M = mantle, E = endodermis).
- Figure 2.3h: Cross-section of a *H. cylindrosporum* / *P. banksiana* ectomycorrhizal root in which the mantle surface was severed before treatment with B/KSCN. Ultraviolet illumination. Bar = 100  $\mu\text{m}$  (arrow = berberine thiocyanate crystal, M = mantle, E = endodermis).
- Figure 2.3i: Cross-section of a *H. cylindrosporum* / *P. banksiana* ectomycorrhizal root in which berberine was allowed access to the root tissue basipetal to the mantle. Ultraviolet illumination. Bar = 100  $\mu\text{m}$  (arrow = berberine thiocyanate crystal, M = mantle, E = endodermis).





The brilliant yellow fluorescence of the B/KSCN crystals was a strong contrast to the blue of the cork tissue under UV light. When the phellem was intact, such crystals were observed on the root surface but not within the root (Figures 2.3c, 2.3d). On the other hand, when the phellem was damaged before treatment, B/KSCN crystals were observed in the apoplast of the phloem tissue near the cut (Figures 2.3e, 2.3f). The cells of the xylem near the injury fluoresced brightly, but crystals were not evident there. The absence of crystals in the xylem is common, and is presumed to be a result of the spaces in the lignified wall being too small to allow visible crystals to form (Enstone and Peterson 1992). Together, these results establish that the intact phellem is indeed a barrier to the diffusion of berberine.

#### *2.4.1.2 Permeability to PTS and sulphate ions*

PTS permeability, as measured by the IPT technique, was the same for both species. When the phellem was left intact, 0.7  $\mu\text{l}$  of PTS solution entered the receiver solution (Figure 2.4). This small delivery was not due to a lack of PTS within the root, since damage to the phellem allowed up to 12 times more dye to enter the receiver solution (Figure 2.4), an amount of tracer approximately equivalent to 8  $\mu\text{l}$  (*P. banksiana*) and 3  $\mu\text{l}$  (*E. grandis*) of the 0.01% PTS solution by the end of the 24 h treatment (Figure 2.4). When the control was run with de-ionized water in place of PTS, the receiver solution reading was not significantly different from background. Therefore, the phellem of these species is measurably permeable to PTS.

The results of the  $^{35}\text{SO}_4^{-2}$  permeability work showed general similarity to the PTS results. When the phellem was intact, a quantity approximately equal to 60  $\mu\text{l}$  (for *P. banksiana*) and 110  $\mu\text{l}$  (for *E. grandis*) of  $^{35}\text{SO}_4^{-2}$  solution moved through the phellem to enter the receiver solution (Figure 2.5). When the cork surface was damaged, almost the entire volume of  $^{35}\text{SO}_4^{-2}$  solution in the micropipette tip entered the receiver solution, and the small quantity that remained was likely only prevented from passing through by surface tension (Figure 2.5). In *E. grandis* roots, the flow of  $^{35}\text{SO}_4^{-2}$  solution into the receiver solution slowed dramatically after 10 h (Figure 2.5), which corresponded to the time when roughly 65% of the solution had already passed through. The reason for the drop in the rate of  $^{35}\text{SO}_4^{-2}$  solution flow was likely the reduced height of solution above the root, resulting in less pressure forcing the  $^{35}\text{SO}_4^{-2}$  through the root segment. These results establish that the phellem layers of *P. banksiana* and *E. grandis* are sparingly permeable to sulphate ions. See Table 2.2 for the rate of flow through the intact phellem per unit surface area.

#### 2.4.2 Fungal mantle

##### 2.4.2.1 Permeability to berberine

The unstained *Hebeloma cylindrosporum* / *Pinus banksiana* ectomycorrhiza cross-sections viewed under the microscope using UV light had very characteristic colors. The fungal mantle autofluoresced a dull yellow, while the cortical cell walls were a pale yellow. The endodermis autofluoresced a brilliant blue. Pictures of the autofluorescent ectomycorrhizal

**Figure 2.4:** The average apparent volume ( $\mu\text{l}$ ) of PTS solution ( $\pm$  S.E.) that entered the receiver solution at various times during the IPT experiment for both intact and wounded cork zone roots of *E. grandis* and *P. banksiana* (n=4).

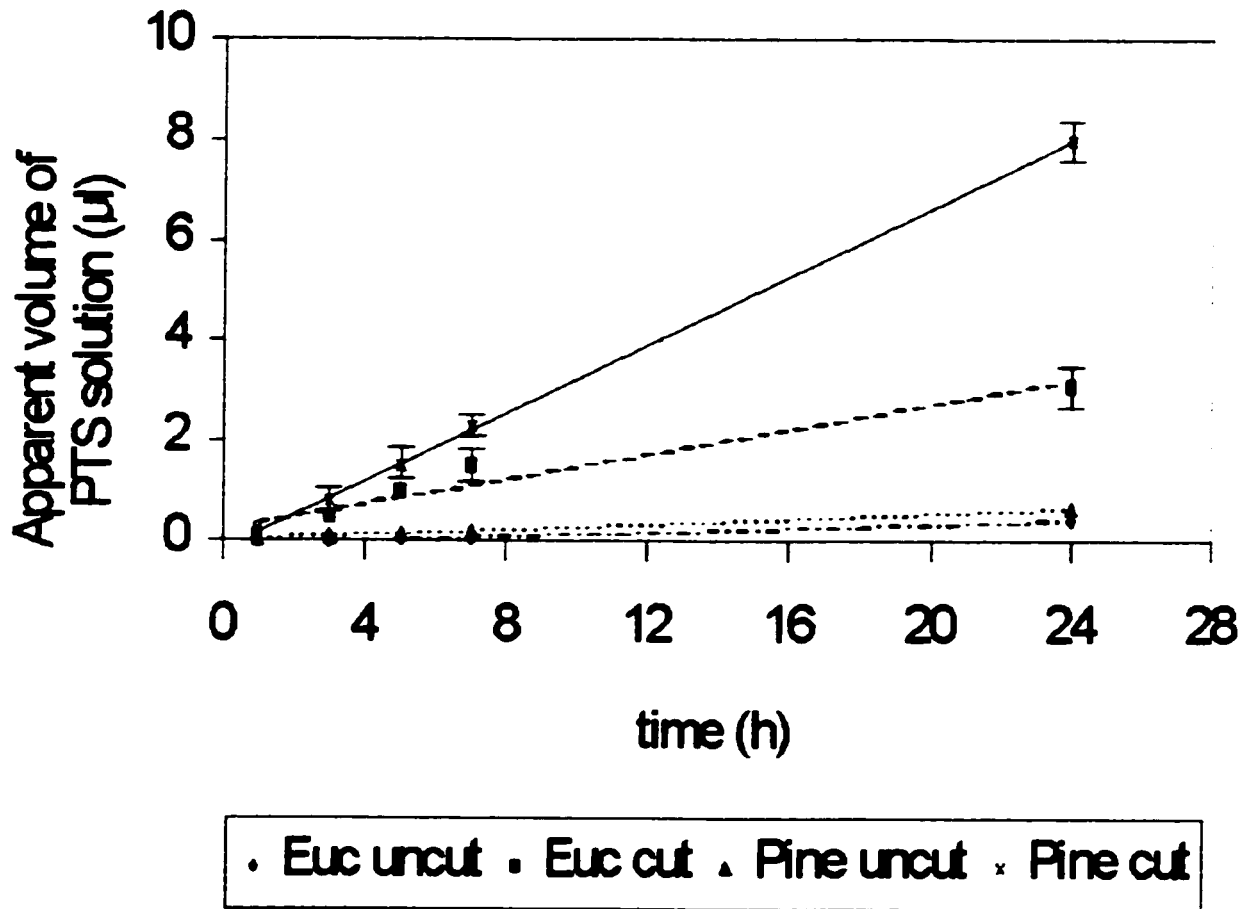


Figure 2.4

**Figure 2.5:** The average apparent volume ( $\mu\text{l}$ ) of  $^{35}\text{SO}_4^{-2}$  solution ( $\pm$  S.E.) that entered the receiver solution at various times during the IPT experiment for both intact and wounded cork zone roots of *E. grandis* and *P. banksiana*.

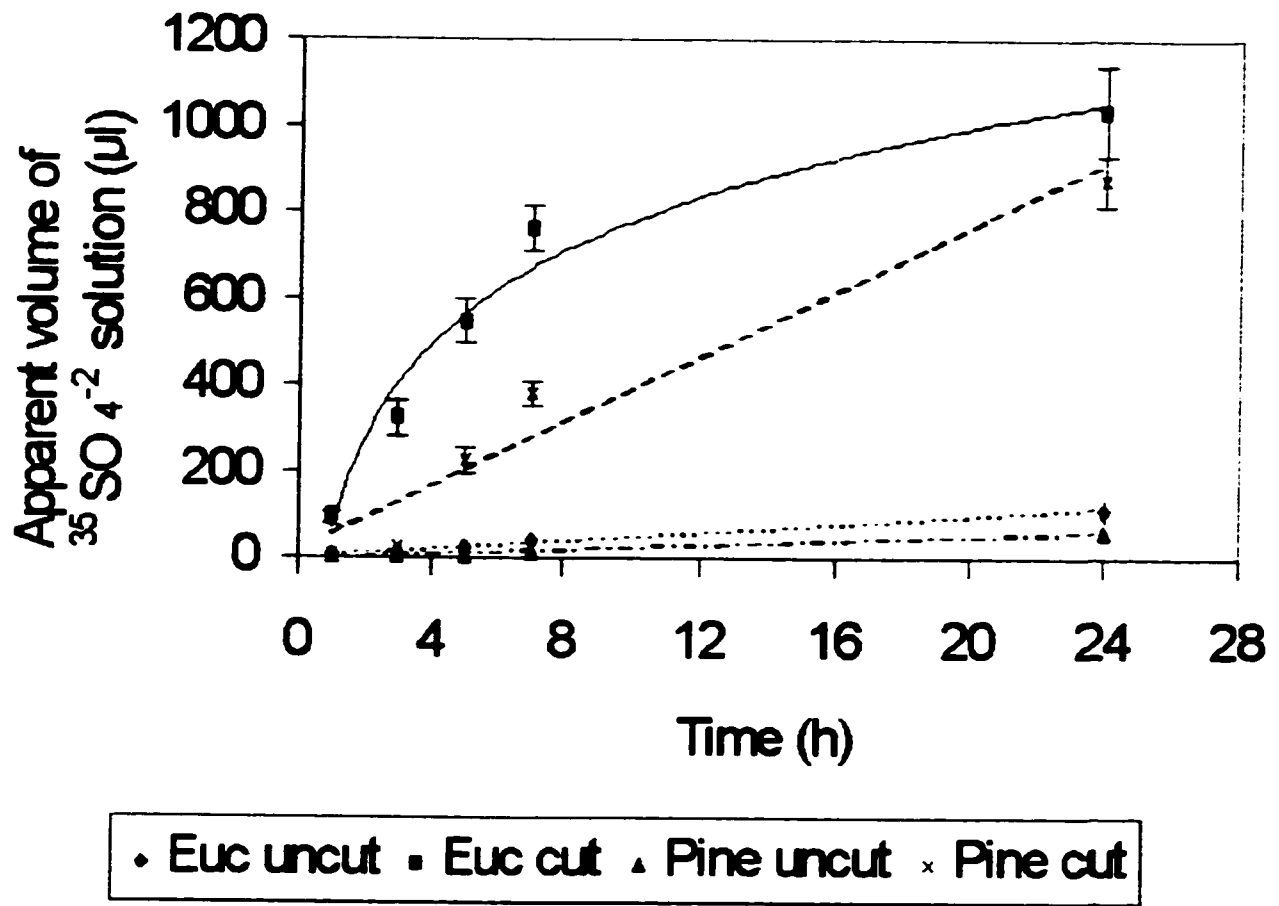


Figure 2.5

roots are not shown as the exposure times required to match them to the B/KSCN-treated roots were too brief. When ectomycorrhizal roots were treated with the B/KSCN technique, the brilliant yellow fluorescent crystals of B/KSCN were restricted to the outer surface of the fungal mantle (Figure 2.3g). The autofluorescence of the hyphae is not visible in the photographs of the berberine-treated samples, because the exposure time necessitated by the tracer is too brief. Note that the brilliant yellow of the berberine was easily distinguished from the dull yellow of the fungal mantle under the microscope. No berberine was evident in the plant or fungal tissues.

Damaging the mantle before exposing the ectomycorrhizal root to berberine gave the tracer access to the underlying root tissues. As shown in Figure 2.3h, the ectomycorrhizal roots of *H. cylindrosporum*/*P. banksiana* have berberine present throughout the cortex, and sometimes in the stele (likely as a result of damaging the endodermis). This indicates that the berberine was, indeed, capable of permeating the cortical apoplast and forming crystals, but was prevented from moving into the stele by the endodermis. When the berberine and thiocyanate were given access to the root tissue immediately basipetal to the fungal mantle (b in Figure 2.1), a general berberine fluorescence and some fluorescent crystals were again observed throughout the cortex, but not in the stele (Figure 2.3i). Therefore, the berberine and thiocyanate were capable of diffusing longitudinally along the apoplast of the cortex within 45 min. The berberine tests established that the intact fungal mantle is impermeable to berberine.

Table 2.2: Average flow of PTS and sulphate through the intact phellem (n=4). The amounts of test substances are expressed as equivalent volumes of the treatment solutions.

Tree species	Tracer	Rate of flow through the phellem surface ( $\mu\text{l} \cdot \text{mm}^{-2} \cdot \text{h}^{-1}$ )
<i>P. banksiana</i>	PTS	0.0093
	$^{35}\text{SO}_4^{-2}$	0.87
<i>E. grandis</i>	PTS	0.0069
	$^{35}\text{SO}_4^{-2}$	1.73



#### 2.4.2.2 Permeability to PTS and sulphate ions

The permeability of *H. cylindrosporum*/*P. banksiana* ectomycorrhizal mantles to PTS and sulphate was tested using the IPT. In both cases, when treatment solutions lacking tracer were used (Table 2.1), no fluorescence (PTS) or radioactivity ( $^{35}\text{SO}_4^{-2}$ ) greater than the blank solutions was observed (data not shown).

When the mantles of the PTS-treated ectomycorrhizae were cut, PTS steadily entered the receiver solution (Figure 2.6) at a steady rate. However, when the mantle was not damaged, PTS was not found in the receiver solution. Likewise, when the mantles of the  $^{35}\text{SO}_4^{-2}$ -treated roots were damaged, sulphate moved into the receiver solution at rate of 25  $\mu\text{l/h}$  (Figure 2.7). As with PTS, intact fungal mantles prevented  $^{35}\text{SO}_4^{-2}$  from diffusing to the receiver solution. These results indicate that the *H. cylindrosporum* / *P. banksiana* fungal mantle is impermeable to PTS and sulphate ions.

### 2.5 Discussion

#### 2.5.1 Permeability of the phellem

In this study, *Pinus banksiana* and *Eucalyptus grandis* cork-clad roots were impermeable to berberine, and sparingly permeable to PTS and sulphate ions (Figures 2.4, 2.5). Given that the ultimate aim of a permeability study is to relate the results to physiological situations (in the case of roots, nutrient ion permeability), the results with sulphate ions are clearly the most useful. Using the same (IPT) technique, PTS predicted the phellem to be 100-fold less permeable than it actually is to physiologically significant ions. The B/KSCN technique proved even less accurate (finding the phellem surface to be impermeable),

**Figure 2.6:** The average apparent volume ( $\mu\text{l}$ ) of PTS solution ( $\pm$  S.E.) that entered the receiver solution at various times during the IPT experiment for both intact and cut ectomycorrhizal *H. cylindrosporum*/*P. banksiana* roots.

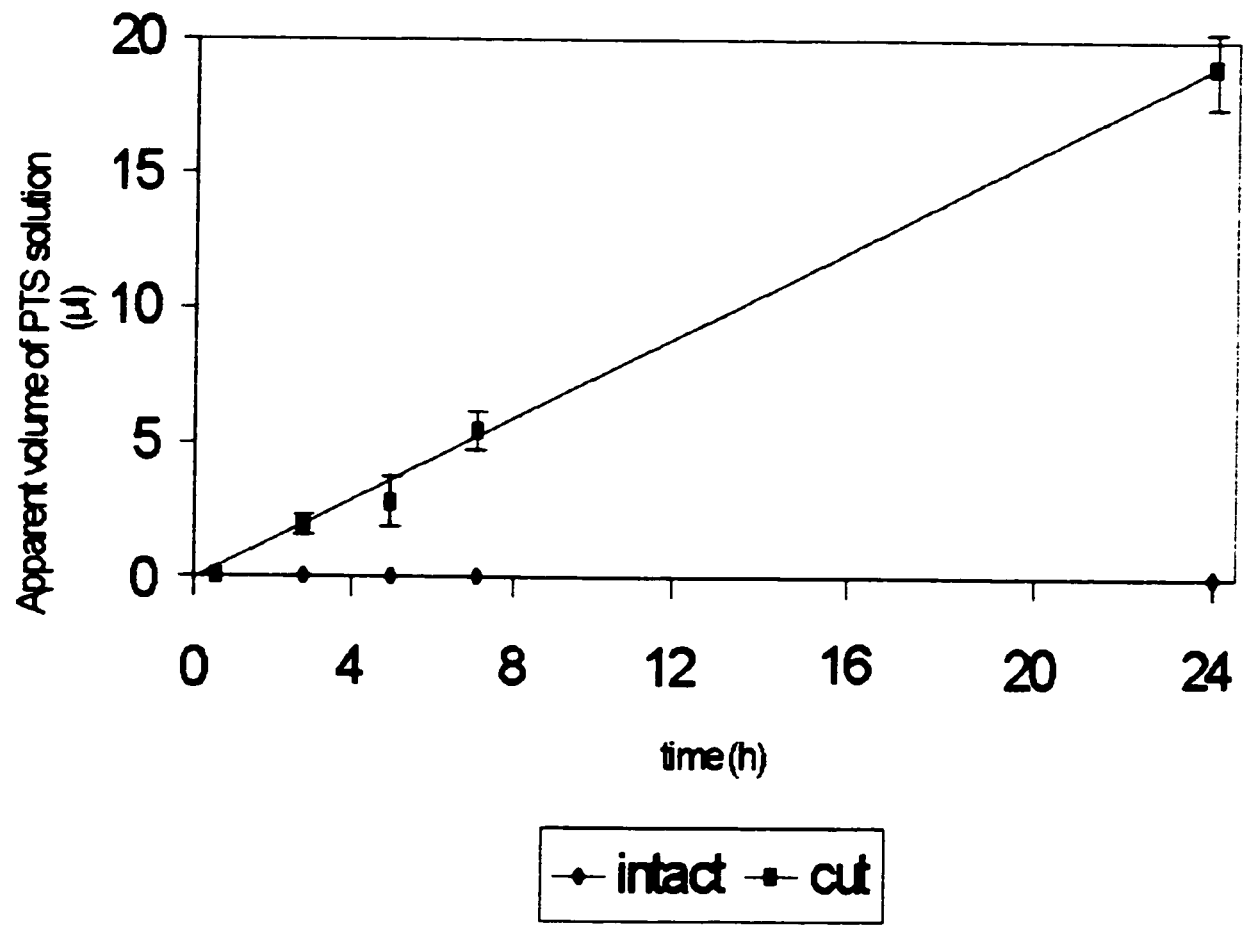


Figure 2.6

**Figure 2.7:** The average apparent volume ( $\mu\text{l}$ ) of  $^{35}\text{SO}_4^{-2}$  solution ( $\pm$  S.E.) that entered the receiver solution at various times during the IPT experiment for both intact and cut ectomycorrhizal *H. cylindrosporum*/*P. banksiana* roots.

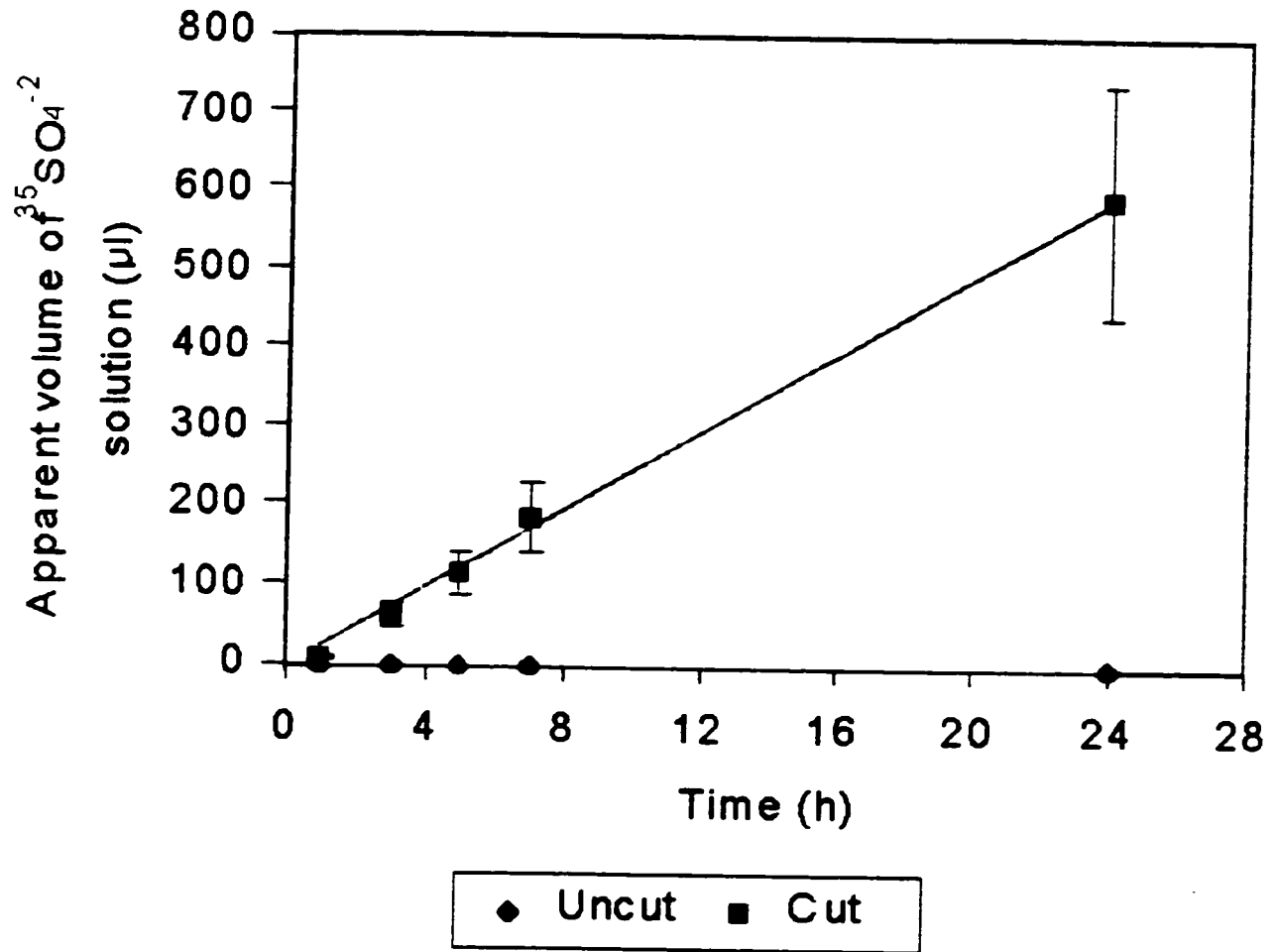


Figure 2.7

probably because it was the least sensitive, requiring a minimum concentration to be form a precipitate (Enstone and Peterson 1992). These results re-emphasize the peril that accompanies attempts to extrapolate to mineral nutrients the results of permeability tests that employ an alternate tracer.

While intact cork zones of *P. banksiana* and *E. grandis* roots have been established as permeable to sulphate, their ability to contribute significantly to nutrient acquisition by the root system is debatable. In the field, the cork root region can represent a small percentage of the total root length. For example, in Chapter 4, the cork zone of field-grown *P. banksiana* was found to contribute less than 15% of the total root length in seedlings, which would present a surface area of approximately 2400 mm<sup>2</sup>. Should the rate of sulphate passage through the phellem observed in this experiment occur in the field, the cork zone would only be able to supply 0.023  $\mu$ mol of sulphate per year. This is due to the low concentration (0.01 mM) of sulphate in typical soil (Kreuzwieser and Rennenberg 1998) relative to the experimental buffer. Even this artificially high value, resulting from the mass of the tracer solution forcing the sulphate through the phellem, would be quite insufficient to meet the needs of the plant (Marschner 1986). The evidence suggests it is unlikely that the cork zone will be a strong region of mineral nutrient acquisition.

To the contrary, both Chung and Kramer (1974) and Van Rees and Comerford (1990) predicted that the cork zone could be an important contributor to nutrient uptake in woody roots. While their results are indeed suggestive, it appears that they included both the cork and condensed tannin zone in their "suberized" or "woody" roots. This is based both on the large fraction of the root system they found to be woody, 58% in Chung and

Kramer (1974) and 90% in Van Rees and Comerford (1990), and the selection criteria by which they differentiated “suberized” or “woody” from roots from the remainder of the root system. Van Rees and Comerford (1990) isolated cork zone roots by macroscopic observation, while Chung and Kramer (1974) employed surface color, neither of which reliably distinguish the cork zone from the condensed tannin zone. The inclusion of the condensed tannin zone, and its passage cells (Peterson and Enstone 1996) could account for a large fraction of the uptake they observed. Therefore, I maintain that the cork zone would not significantly contribute to ion uptake by the root system.

### *2.5.2 Permeability of the fungal mantle*

Through my research, I found the *Hebeloma cylindrosporum/P. banksiana* ectomycorrhizal mantle was impermeable to berberine, PTS, and sulphate ions. These results are important, as they represent the first time that a mycorrhizal fungal mantle has been established as impermeable to an ion of physiological significance.

The fungal mantle of an ectomycorrhizal root ensheathes the white zone, separating the plant cells from the soil solution. As the *Hebeloma cylindrosporum/P. banksiana* mantle is impermeable to (at least one) nutrient ion, the plant tissues underlying the mantle are essentially isolated from the soil solution. A recent study indicates that a considerable portion (up to 85%) of the entire root plasmalemmae surface area potentially capable of ion uptake can be found within the ectomycorrhizal mantle (see Chapter 4) in seedling pines. As a result, a large fraction of the absorptive surface of the root is dependent on the mycorrhizal fungus to supply mineral nutrients. In the case of phosphorus (Melin and Nilsson 1950) and nitrogen (Finlay et al. 1989), the fungus is clearly capable of supplying

the plant with sufficient quantities. However, there is, as yet, no incontrovertible evidence that ectomycorrhizal fungi are capable of passing the other 12 required soil nutrients to the plant partner. If the fungus is incapable of supplying these to the plant, and the mantle is impermeable to these nutrients, the plant partner would be obliged to use the small fraction of root surface capable of absorption outside of the mycorrhizal mantle to acquire these nutrients. Clearly, it is important that the ability of mycorrhizal fungi to supply mineral nutrients other than phosphorus and nitrogen to the root be investigated further.

As noted in the Introduction, there is a great disparity of results regarding the permeability of the fungal mantle to ions. Even if the work of Ashford et al. (1988) and Behrmann and Heyser (1992) is ignored on the basis that both groups employed suspect tracers (dyes), there is still a conflict. Vesik et al. (2000) found that *Pisolithus tinctorius* / *Eucalyptus pilularis* mantles were permeable to lanthanum. However, they exposed root tissue basipetal to the mantle to the tracer, and it is possible that the lanthanum entered the cortex basipetal to the mantle and diffused longitudinally. Kuhn et al. (1999) found *Picea abies* ectomycorrhizal mantles to be permeable to calcium and magnesium. While they also did not seal the basipetal end of the mantle, they did a time series that allowed them to rule out basipetal entry and longitudinal diffusion. This puts their results in direct conflict with mine.

There are a number of explanations that may account for the different results in mantle permeability between our work and that of Kuhn et al. (1999). Both groups employed different tree and fungal species, and grew the ectomycorrhizal roots under different conditions. Any of these factors could influence mantle permeability. Some



mantles are loosely woven, and these would be more likely to be permeable than tightly-woven ones (Chilvers 1968). A second possible reason for mantle permeability variation is a difference in the expression of hydrophobins. These are a class of fungal protein first noted in aerial structures where water conservation was a priority (Wessels 1994). The expression of hydrophobins has since been established in ectomycorrhizae (Tagu et al. 1998), and they are presumed to introduce a high level of impermeability to water in fungal mantles. Should hydrophobins make mantles impermeable to water, it is very likely that this feature would extend to nutrient ions. To test this idea, it is imperative that future researchers examine ectomycorrhizal mantles and their permeability at the molecular level.

### 2.5.3 Conclusions

In the present work, the young cork of *P. banksiana* and *E. grandis* roots was impermeable to berberine, but sparingly permeable to PTS and sulphate ions. While this implies that ion uptake by older roots is feasible, it probably does not occur to a significant extent under typical field conditions. Conversely, the fungal mantle of *H. cylindrosporum*/*P. banksiana* mantle was found to be impermeable to all three tracers. How this affects nutrient uptake in general will be dependent on the permeability of the fungal mantle in various systems, longitudinal diffusion of ions within the cortex, and the ability of the extramatrical hyphae to absorb all 13 essential soil nutrients. These results highlight the importance of employing the correct tracer and technique to study tissue permeability. Additionally, the importance of properly distinguishing the root zones was re-emphasized.

## CHAPTER 3

### **Maturation of the tracheary elements in the roots of *Pinus banksiana* (Lamb.) and *Eucalyptus grandis* (W. Hill ex Maiden).**

#### **3.1 Abstract**

The tracheary elements of the xylem are responsible for the longitudinal (axial) transport of water and ions that have moved radially across the root. These vessel members and/or tracheids mature some distance behind the root tip, and it is generally believed that this distance is directly related to root growth rate. To better test this idea, the distances behind the root tip at which the tracheary elements of *Pinus banksiana* (Lamb.) and *Eucalyptus grandis* (W. Hill ex Maiden) mature were examined. From each species, three root tip types (white, brown, and ectomycorrhizal/short lateral) were assessed. Unlike previous studies of this topic, two different methods of testing tracheary element maturity were employed concurrently. The first was anatomical and involved visualizing the deposition of lignin in the walls of the tracheids or vessel members, while the second was functional and consisted of determining the capability of the tracheary elements to conduct a fluorescent tracer dye. The distance behind the root tip at which the conductive xylem cells mature varied from 1.6 to 0.16 mm and was highly dependent on species and root type. No significant correlation was found between growth rate and proximity of tracheary element maturation to the tip for white roots. The presence of lignin in the tracheary element walls was not a good indicator of the tracheary element's functional maturity.

### 3.2 Introduction

Mature tracheary elements of the xylem are responsible for the longitudinal transport of ions and water taken up by the root to the stem (see Marschner 1986), but there is a zone at the root tip where these elements are immature, leading to the presence of a hydraulically isolated zone (Peterson and Steudle 1993). This zone contributes negligible water or ions to the remainder of the plant. The ontogeny of tracheary elements, which may be vessel members or tracheids, is well known (Esau, 1977). During primary growth, they originate as procambial cells, which are produced from the root apical meristem. A short distance behind the root tip, these cells cease dividing and continue to elongate. This process is usually more exaggerated in tracheids compared to vessel members. A secondary wall is deposited, the pattern of which is variable, depending on the both the species and whether or not the cell has ceased elongating. Next, the secondary wall and its immediately adjacent primary wall are lignified. Finally, the cell dies, leaving a lumen in place of the protoplast. (In the case of vessel members, cell death is preceded by partial removal of the transverse wall.) At this point, the cell is a functional extension of the xylem's longitudinal transport system. The loss of the membranes in the tracheids and vessel members greatly lowers their resistance to the flow of water and ions dissolved therein. In vessel members, the resistance is further decreased due to the loss of some or all of the transverse wall.

The factors that influence the distance behind the root tip at which the tracheary elements become functionally conductive are not well established. It is generally supposed that this distance is directly related to the growth rate of the root (Wilcox, 1962a). However, this view is based on relatively little experimental evidence. The issue is further

confused because there is no consensus with regard to what technique is most effective at determining the distance behind the tip a tracheary element becomes functional. A number of studies have relied on anatomical features such as lignification (Peterson and Lefcourt 1990), vacuolation (Wilcox 1962a), and loss of cytoplasm and end walls (McCully and Canny 1988), only the last of which establishes that the tracheary elements are fully mature and capable of functioning. The only study known in which a functional test was employed (Peterson and Steudle 1993) was performed on a herbaceous species, and the results cannot be extrapolated to more complex woody root systems. For example, in rapidly growing maize roots, the vessel members are functionally mature 21.5 mm from the root tip (Peterson and Steudle 1993). If this were true in the heterorhizic root systems of woody species, some short roots would lack a functional connection to the xylem system.

In the present work, there were two primary goals. The first was to determine the suitability of lignin deposition as a predictor of tracheary element maturity, as this method had been employed in an earlier study (Peterson and Lefcourt 1990). For this, a chlorazol black E (CBE) method, modified by Daryl Enstone (personal communication) from Brundrett et al. (1984), was performed alongside the cellufluor test. The second goal was to assess the distance behind the root tip at which the tracheary elements become mature in woody roots. To do this, the cellufluor method of Peterson and Steudle (1993) was extended to *Pinus banksiana* (Lamb.) and *Eucalyptus grandis* (W. Hill ex Maiden) roots. Experiments were designed to measure the impact of root tip type and root growth rate, in addition to species, on the distance behind the root tip at which the tracheary elements become mature.

### 3.3 Methods

See Chapter 2 for details of plant and fungal culture, and inoculation. Three root types from *P. banksiana* and *E. grandis* were examined. From both, roots that were white and roots that were brown to the tip (2<sup>nd</sup> and 3<sup>rd</sup> order) were studied. For *P. banksiana*, ectomycorrhizal roots were also observed, while in *E. grandis* short lateral roots of determinate length, which typically become mycorrhizal if inoculated were examined. The classification of each root type was easily accomplished by macroscopic observation.

Growth rates of the roots were determined over a two-week period prior to sampling. A mark was made on the surface of the pouch to record the location of each root tip twice a week. The average growth rates from a two-week interval were used.

Lignification of the tracheary element walls was visualized by a modified technique of Brundrett et al. (1984), in which entire roots were first cleared and then stained with chlorazol black E (CBE). Briefly, the roots were fixed overnight in glacial acetic acid:alcohol (1:1), rinsed in several changes of de-ionized water for at least one h (hereafter referred to only as 'rinsed'), autoclaved (121°C) for 20 min in 10% KOH (w/v) to clear the tissue, and then rinsed. To continue the clearing process, roots were soaked overnight in 3% H<sub>2</sub>O<sub>2</sub> (w/v) with a few drops of 10% KOH, and rinsed. Finally, the roots were autoclaved in 0.3% (w/v) CBE for 15 min, and mounted in 70% glycerol (v/v) for viewing under the microscope.

To assess how far behind the tip the tracheary elements were functionally conductive, a modification of the method of Peterson and Steudle (1993) was used. In this technique, cellufluor is drawn through the conductive tracheary elements from a cut end by

water loss from the root surface, much as transpiration draws the xylem sap up the stem. Initial tests established that cellufluor could travel a maximum of 27 mm through mature, conductive xylem of both *P. banksiana* and *E. grandis* roots. Root tips approximately 27 mm were cut under water on an extremely oblique angle (to increase the effective size of the tracheary element openings), and orientated so that the cut end was near one end of a microscope slide. While keeping the cut end under water, the apical segment was blotted, and a line of petroleum jelly perpendicular to the root was applied a few millimeters above the cut end. The slide was then transferred to a beaker containing 0.01% cellufluor so that the cut end of the root was immersed in the solution but the line of grease was above it. The opening of the beaker was then loosely covered with aluminum foil. The roots were left for 2 h, after which a dry razor blade was used to cut the root just above the grease lines. The apical end of the whole root was then mounted in 70% glycerol and viewed under the epifluorescence microscope using UV light. The cellufluor was easily visible, as it fluoresced brilliant blue. To perform this technique on the very short ectomycorrhizal/short lateral roots, a parent root containing many ectomycorrhizal/short lateral roots was isolated from the root system and treated as described above. The cellufluor would flow into the short laterals from the parent root.

All specimens were viewed using a Zeiss Axiophot microscope (Carl Zeiss Canada, Don Mills, ON) equipped with an Osram HBO 100W mercury lamp and epifluorescence optics. For the CBE-stained roots, white light was used. For the cellufluor method, UV light was used, exciting wavelengths 365 nm (dichroitic mirror FT 395, barrier filter LP

420 nm). Images were recorded on Kodak Ektachrome Elite II 100 film and developed into slides. The plate was made in Corel Draw 7.0.

### **3.4 Results and Discussion**

The methods used to study xylem maturation gave different results. CBE consistently picked up tracheary elements closer to the root tip than did the cellufluor technique (Figure 3.1, see Figure 3.2a-h for cellufluor- and CBE-stained roots). This difference was most pronounced in *E. grandis*, but was observed in *P. banksiana* as well (Figure 3.1). The obvious reason for this discrepancy is that the secondary walls of the tracheids and vessel members are deposited and lignified before the cells die and become functional (Esau 1977, St. Aubin et al. 1986). While this was expected, it was encouraging that these relatively simple tests were sensitive enough to differentiate between secondary wall deposition and complete maturity. The extent of the difference between the CBE and cellufluor tests was highly variable. For all *E. grandis* root types, the tracheary elements were stained by CBE almost twice as close to the tip as the cellufluor indicated that the xylem was functional (maximum distance 0.74 mm), while the difference was substantially less in the *P. banksiana* roots (maximum distance 0.4 mm; Figure 3.1). Clearly, anatomical tests for lignin underestimate the distance from the root tip at which the tracheary elements become functional. Further, there is no regular correlation between these results and those of a direct test for functionality in different species.

Although the cellufluor results are likely to be indicative of the point at which the tracheary elements became functional, there may be a number of negative aspects to this test. One complication involves the flow of solutions into terminal veins (Carol Peterson,

Figure 3.1: The average growth rates (solid bar), and distances from the tip at which CBE (diagonal line bar) and cellufluor (wavy line bar) detected tracheary elements in *Pinus banksiana* and *Eucalyptus grandis* roots. The root categories and number of each type sampled are as follows: Euc. W = *E. grandis* white roots (CBE n = 14, cellufluor n = 12), Pine W = *P. banksiana* white root (CBE n = 15, cellufluor n = 12), Euc. B = *E. grandis* brown roots (CBE n = 14, cellufluor n = 8), Pine B = *P. banksiana* brown roots (CBE n = 15, cellufluor n = 10), Euc. SL = *E. grandis* short lateral roots (CBE n = 14, cellufluor n = 11), and Pine Myc = *P. banksiana* ectomycorrhizal roots (CBE n = 17, cellufluor n = 10). Error bars represent standard deviations.



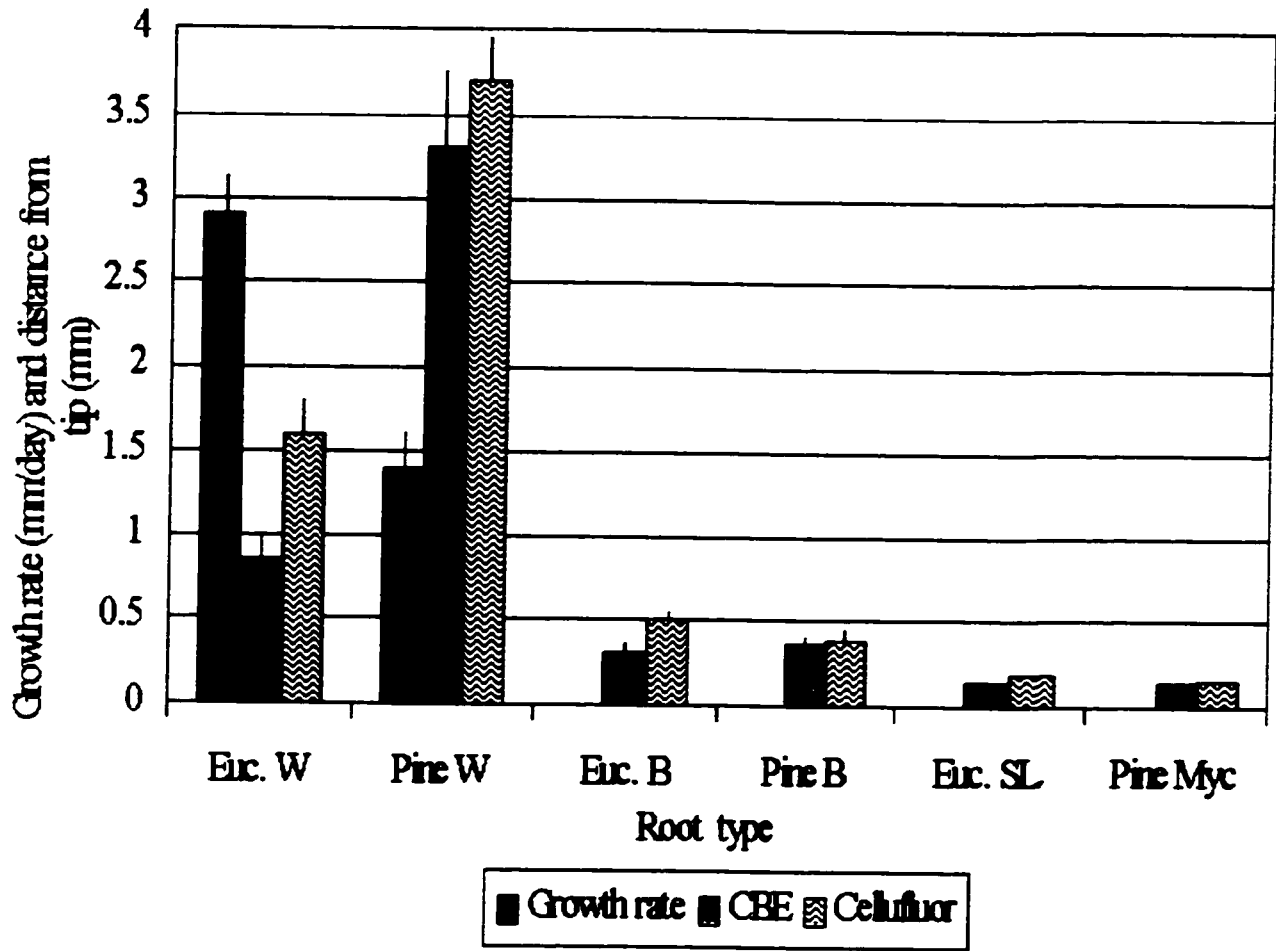
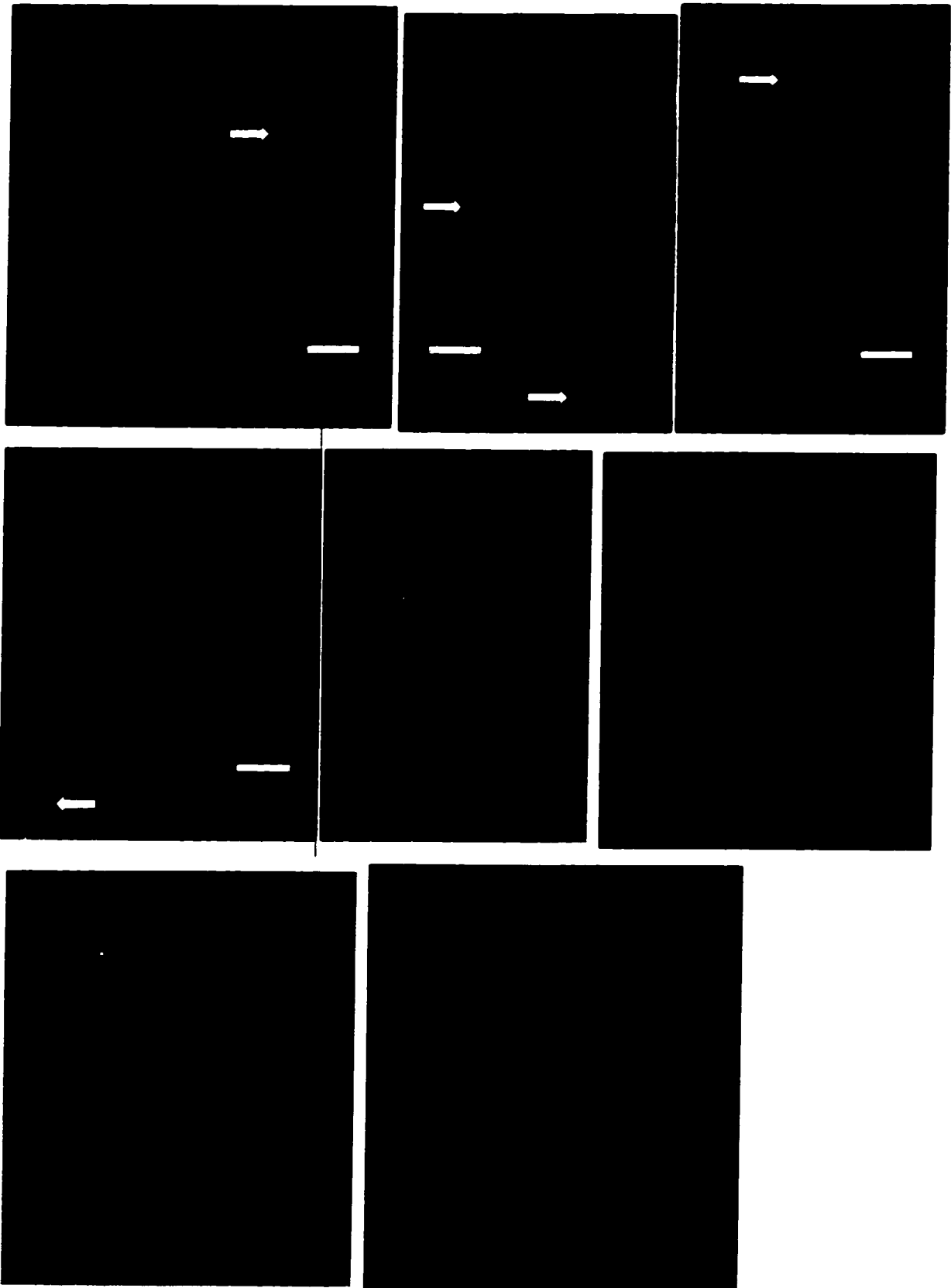


Figure 3.1

personal communication). As solutions are drawn towards the end of the vessel, the speed at which they travel is reduced, essentially reaching zero at the end of the ultimate tracheary element. Since the present study involved feeding tracheary elements of roots in the reverse (towards the distal tip), this phenomenon would also occur. Therefore, the predictions of the cellufluor test as to the distance from the tip that the tracheary elements become functional may be slight overestimates. However, unimpeded diffusion of the cellufluor in the near static solution at the end of the tracheids/vessel members may overcome this effect to some extent. Cellufluor never diffused radially out of the tracheary elements in detectable amounts. Part of this may be the result of the more rapid movement longitudinally than radially due to the low resistance of the lumen pathway. However, it is also possible that the cellufluor reduced the apoplastic spaces of the tracheids/vessel members, and therefore was unable to exit these tubes (Carpita et al. 1979). Despite these complications, I feel the results of the cellufluor test are essentially accurate and that this test represents a simple yet powerful tool in examining tracheary element maturation.

As judged from the cellufluor test, tracheary elements matured much further behind the root tip in the white roots of both species relative to the other root types. In *E. grandis*, the tracheary elements of the white zone proved functional roughly 1.6 mm behind the root tip (Figures 3.1, 3.2a), substantially further than either the brown roots (0.50 mm; Figures 3.2b), or the short lateral roots (0.20 mm). *P. banksiana* was even more extreme, where the tracheary elements matured about 3.7 mm behind the white root tip (Figures 3.1, 3.2c), compared to 0.39 and 0.16 mm for the brown and ectomycorrhizal (Figures 3.2d) roots, respectively.

- Figure 3.2a: *E. grandis* white root tip treated with cellufluor, bar = 1000  $\mu\text{m}$ . (T = root tip, arrow = end of tracheary element).
- Figure 3.2b: *E. grandis* brown root tip treated with cellufluor, bar = 1000  $\mu\text{m}$ . (T = root tip, arrows = ends of tracheary elements).
- Figure 3.2c: *P. banksiana* white root tip treated with cellufluor, bar = 1000  $\mu\text{m}$ . (T = root tip, arrow = end of tracheary element).
- Figure 3.2d: *P. banksiana* ectomycorrhizal root tip treated with cellufluor, bar = 400  $\mu\text{m}$ . (T = root tip, arrow = end of tracheary element).
- Figure 3.2e: *E. grandis* short lateral root tip treated with CBE, bar = 200  $\mu\text{m}$ . (arrowhead = end of tracheary element).
- Figure 3.2f: *E. grandis* brown root tip treated with CBE, bar = 200  $\mu\text{m}$ . (arrowhead = end of tracheary element).
- Figure 3.2g: *P. banksiana* ectomycorrhizal root tip treated with CBE, bar = 100  $\mu\text{m}$ . (arrowhead = end of tracheary element).
- Figure 3.2h: *P. banksiana* brown root tip treated with CBE, bar = 100  $\mu\text{m}$ . (arrowhead = end of tracheary element).



Evidently, root type has a strong influence on the distance behind the tip at which the tracheids or vessel members become functional.

Root growth rate, either within or between species, had little influence on the distance behind the tip at which the tracheids or vessel members became conductive. While the white roots of *E. grandis* grew at roughly twice the rate of those of *P. banksiana*, the tracheary elements matured twice as close to the tip in the former as in the latter (Figure 3.1). Likewise, no correlation was found between the growth rate and distance behind the tip of xylem element maturation among individual white roots in *P. banksiana* or *E. grandis* (Figure 3.3). Therefore, the correlation between root growth rate and tracheary element maturation seen by Wilcox (1962a) for *Libocedrus decurrens* is not universal. The discrepancy in results may be due to a difference between species or, perhaps, the conditions under which the experiments were conducted. For example, Wilcox (1962a) used soil-grown roots, which encounter much more mechanical resistance than do the pouch-grown roots used in this study.

Tracheary element maturation in non-white roots showed little difference between species. However, these elements matured closer to the tip in the ectomycorrhizal/short lateral roots than in the brown roots (Figures 3.1, 3.2c, d-h). While the reasons for this are not clear, it would seem to be beneficial to the ectomycorrhizal association. Having the conductive cells of the xylem mature close to the tip in ectomycorrhizal (and *E. grandis* short lateral roots which would form ectomycorrhizal associations in nature) makes these roots especially well-suited to transport the ions provided by the fungi to the remainder of

**Figure 3.3: Relationship between the distance from the root tip the tracheids/vessel members mature and the growth rate of the white root for *Pinus banksiana* and *Eucalyptus grandis* ( $R^2$  value determined in Microsoft Excel).**

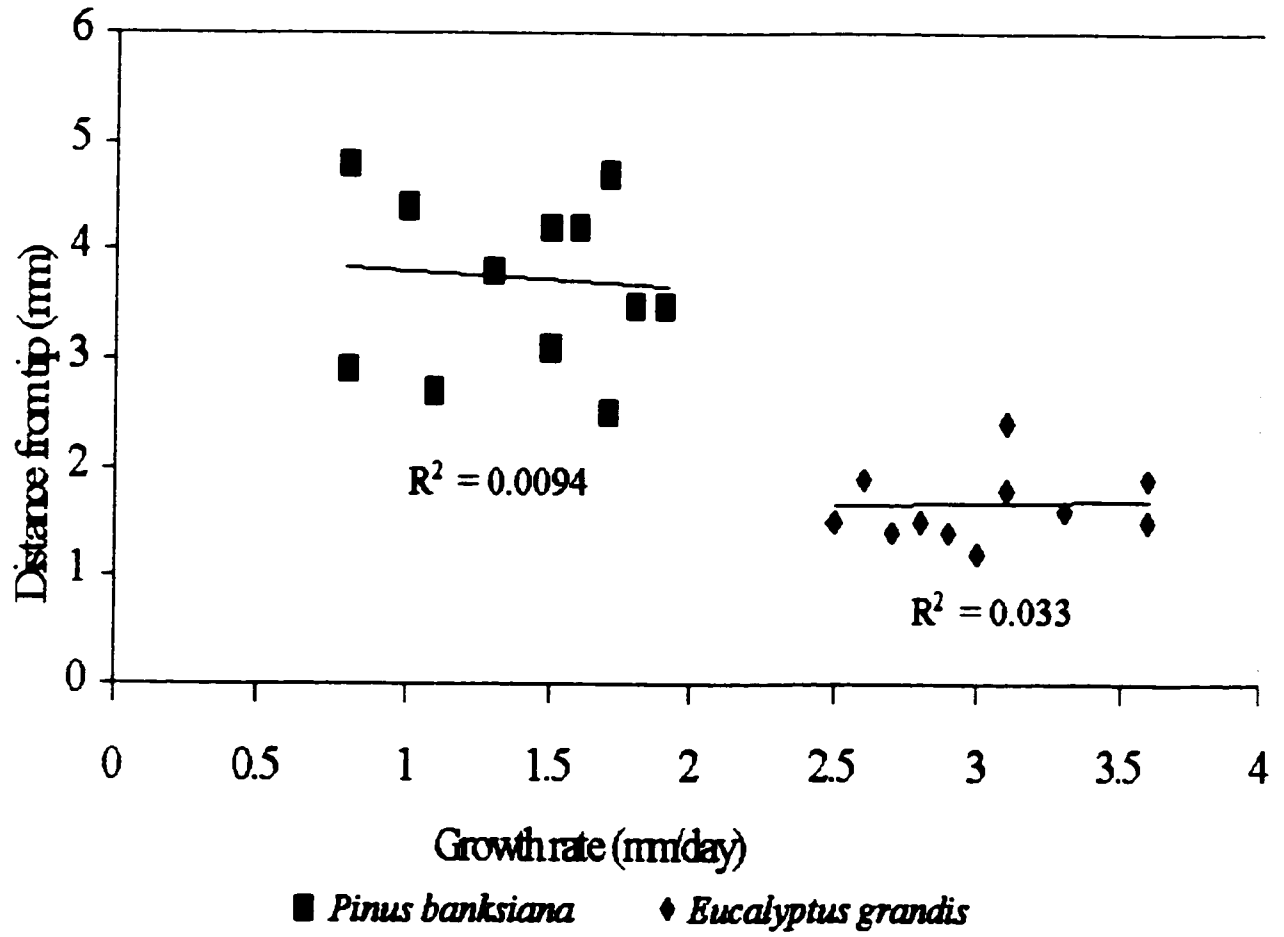


Figure 3.3

the plant. The similar results between ectomycorrhizal roots and roots that commonly become ectomycorrhizal under natural conditions supports the idea that these roots are designed for the express purpose of forming mycorrhizal associations (see Smith and Read 1997).

To conclude, species and root tip type greatly influence the distance behind the root tip at which the tracheary elements become functional in woody root systems. Conversely, root growth rate had little impact. It is important that further studies be carried out on other species and field-grown roots, and that these studies employ functional tests of tracheid/vessel member maturation.



## CHAPTER 4

### **Morphometric analysis of *Pinus banksiana* (Lamb.) root anatomy during a three-month field study.**

#### **4.1 Abstract**

Tree roots are variable in their growth rates, alternating between periods of elongation and dormancy. This variability may have a strong influence on root anatomy. In the present study, field-grown *Pinus banksiana* Lamb. roots were divided into four distinct anatomical regions (i.e., white without mycorrhizae, white with mycorrhizae, condensed tannin, and cork). Changes in root growth, the proportions of the root system occupied by the various regions, and cortical plasmalemma surface area (CPSA) were determined for ectomycorrhizal *P. banksiana* 6- to 9-month old seedlings during a three-month period (August through October) in northern Ontario. The region in which the greatest change in length occurred was the condensed tannin zone, which was also the dominant contributor to root length (up to 74% of total). The roots of seedlings grown under artificial conditions had the same zones but in different proportions compared to roots in the field. A correlation was noted between increased root growth, low metacutization, and high soil water availability. The CPSA data were assumed to be a factor influencing ion uptake capacity in a positive manner. Interestingly, increases in CPSA were not directly correlated with changes in root length for field-grown seedlings. The primary contributor to CPSA in the field-grown roots was the ectomycorrhizal zone (approximately 80%). In comparison, the bulk (85%) of the CPSA in the chamber-grown roots was found in the white root region.

The conditions under which the seedlings were grown strongly influenced the anatomy of their roots.

#### **4.2 Introduction**

Roots of pouch-grown *Pinus banksiana* (Lamb.) were previously divided into three distinct anatomical regions, i.e. the white, tannin, and cork zones (McKenzie and Peterson 1995a,b; Figure 1.1). The white zone has viable central cortical cells and passage cells (endodermal cells without suberin lamellae) in its more mature regions. Unlike the white zone, the cortex of the condensed tannin zone (change in term discussed in Peterson et al. 1999) is dead but the passage cells remain. The cork zone, which is superficially similar to the condensed tannin zone, is characterized by a continuous layer of dead, suberized phellem cells. A number of tree root studies published before the work of McKenzie and Peterson (1995a,b), such as that of Kramer and Bullock (1966), defined roots as either suberized (brown) or non-suberized (white), failing to distinguish between the condensed tannin and cork zones, both of which are brown. For an excellent discussion of root zone terminology, see Richards and Considine (1981).

Ion uptake should vary substantially amongst the root zones identified by McKenzie and Peterson (1995a,b). For a cell to be even potentially capable of taking ions into the symplast, it must be alive and have access to the soil solution. Within the root, access is limited by Casparian bands in the anticlinal walls of the endodermis (Baker 1971; Robards and Robb 1974). Thus, in the white zone, the plasmalemmae accessible to the soil solution are those of the cortex, including the outer membrane of the endodermal passage cells (Peterson and Enstone 1996). In the condensed tannin zone, the relevant plasmalemma

would be reduced to the outer tangential faces of the passage cells, and in the cork zone would be reduced to zero. *Pinus banksiana* roots do not have a coherent epidermis (Wilcox 1954), and the cork zone is so sparingly permeable to ions (Chapter 2) that it was treated as impermeable.

In the field, roots commonly undergo changes that influence their anatomy and function. Ectomycorrhizae are a prevalent symbiosis between tree roots and fungi (see Smith and Read 1997). The fungal partner in an ectomycorrhizal symbiosis consists of three components, i.e. the Hartig net, the fungal mantle that ensheathes the white root tip distal to the condensed tannin zone, and the extramatrical (or extraradical) hyphae and rhizomorphs (see Piché et al. 1983). In mycorrhizal associations, especially in infertile soils, the fungus supplies some fraction of certain essential ions to the plant by absorbing them with its extramatrical hyphae and eventually passing the ions to the plant at the Hartig net-cortical cell interface. There is convincing evidence that phosphorus (Melin and Nilsson 1950) and nitrogen (Finlay et al. 1989) are delivered in this manner by ectomycorrhizal fungi. Since these ions are delivered to the cortical apoplast, the cortical plasmalemmae surface area (CPSA) is a factor which will influence the plant's capacity for ion uptake from the fungus. It is not as yet clear how the remaining essential mineral elements (i.e., potassium, calcium, magnesium, sulfur, chlorine, boron, iron, manganese, zinc, copper, nickel, and molybdenum) are supplied to plants. Some of these show increased uptake in ectomycorrhizal roots, but the mechanism by which absorption takes place is uncertain. These ions may be taken up by plant cells without the active involvement of the fungus. In an ectomycorrhizal root, the possibility for such ion uptake

depends, at least in part, on the ion passage through the fungal mantle. At present, there is no consensus regarding the permeability of this structure (Ashford et al. 1988, Behrmann and Heyser 1992).

Another anatomical change roots undergo is metacutization (also referred to as metacutinization), a temporary state in which a layer of cells ensheathing the root apical meristem and connecting to the endodermis deposits suberin in its walls (Wilcox 1954). It is generally accepted that a root with a metacutized tip is non-growing. As the root resumes growth, it will burst through the modified cell layer (Wilcox 1954). Although the metacutis has long been recognized (Müller 1906; Mager 1913; Plaut 1918), it has received little attention recently.

The growth of tree roots is known to vary over the course of a year. In temperate climatic zones, roots commonly cease growing in summer and winter, with flushes of growth occurring in spring and fall (Wilcox 1962b). The causes of this hiatus are believed to be drought in the summer, and the combination of low water availability and low temperatures in the winter (Wilcox 1968). One impact of lack of root growth is that further soil exploration by roots is prohibited. It is unclear if the extramatrical hyphae continue to grow.

In the present work, we examined changes in the anatomy of 6- to 9- month old, field-grown *Pinus banksiana* roots during the late summer and autumn in northern Ontario. The observations of McKenzie and Peterson (1995a,b) were extended from soil-free pouches (consisting of a paper backing on which the nutrient solution was held within a flat, plastic pouch [Piché et al. 1983]) to pot-grown and field-grown roots that were in a

more natural environment. At each time of sampling, several measurements were made, including the total root length and the length of each root region, as well as the total number of root tips and the number of each type of root tip (growing or metacutized). In addition, dimensions and numbers of cortical cells were determined for each root zone. From these measures, the CPSAs for each root zone and the total root were determined. Growth chamber-grown seedlings were analyzed in the same manner to compare the development of seedlings grown under different conditions. Growing seedlings in pots allowed the introduction of soil as a growth medium while retaining growth-chamber conditions. Through this study, we were able to show the contribution of each root zone to mycorrhizal root systems characteristic of soil-grown roots, and how the root growth rate and CPSA changed over the specified time period.

### **4.3 Materials and methods**

#### *4.3.1 Plant material*

##### *4.3.1.1 Growth chamber*

In early January of 1997, *Pinus banksiana* Lamb. seeds were stratified in cold water for 48 h, rinsed, and planted in 0.175-m-deep by 0.0375-m-diameter containers filled with 70% peat moss and 30% medium, horticultural grade vermiculite. The containers were held in a growth chamber at Mikro-Tek (36 Emerald St., P.O. Box 2120, Timmins, Ontario, P4N 7X8, Canada) with day conditions (25 °C, 35% humidity, light intensity 150-250  $\mu\text{mol}/\text{m}^2/\text{s}$ , 18 h), and night conditions (18 °C, 90% humidity). Seedlings were watered to saturation twice weekly with tap water. Two weeks post-planting, they were inoculated by drenching the soil mix with a concentrated slurry of *Hebeloma cylindrosporum*

(Romagnesi) prepared from solid agar culture plates. Ten weeks later, the seedlings were removed from the containers and the root systems gently rinsed free from soil with a spray of water. The shoot was then removed and the roots were used immediately for the viability, permeability and histochemical tests. Other roots were preserved in a mixture of alcohols (85% ethanol, 15% methanol) until they were analyzed for root zone lengths, root tip type and number, and cellular dimensions.

#### *4.3.1.2 Field*

Seeds of *P. banksiana* were germinated in Mini-Jiffy pouches (mesh cylinders 18 mm in diameter by 83 mm in height packed with finely sifted peat, Jiffy Products Ltd. P.O. Box 360, Shippagan, N.B., E0B 2P0, Canada) in early February of 1997 at LaFleur Nursery (R.R. #2, Airport Rd., Timmins, ON, Canada). The seedlings were misted with river water every other day and fertilized (20-20-20 Plant Products Ltd., 314 Orenda Rd. Brampton, ON, L6T 1G1, Canada) once a week through a boom apparatus. A liquid inoculum of *H. cylindrosporum* was applied through the boom on March 18. On June 10, 60 seedlings were transferred to the Kamiskotia Lake flats east of Mt. Rob on a site previously occupied by *P. banksiana*. Once in the field, the roots rapidly penetrated the Mini-Jiffy pouches and entered the surrounding soil. Soil conditions were very sandy, and competition from surrounding plants was minimal.

Soil temperature and moisture were measured every 2 to 4 weeks from the time of planting to the end of the sampling period. Temperatures were measured at roughly 10 AM, approximately 0.15 m below the surface by insertion thermometers, at 4 randomly chosen sites within the plot. Soil moisture was determined gravimetrically, using four 100 to 150-

g-replicate samples from approximately 0.15 m below the surface. The soil was dried to a constant weight at 95 °C in a convection oven.

#### *4.3.2 Root sampling*

On the first sampling date, five seedlings were taken back to the lab and used for the viability, permeability and histochemical tests, as in the chamber-grown roots. For the first and remaining sampling dates, 10 seedlings were randomly selected. After first removing a large quantity of soil to ensure that no roots were severed, the root system was gently shaken to remove excess soil. The seedlings and adhering soil were placed in plastic bags and transported to the laboratory. Within 90 min, the root systems were washed free of soil using a spray of water, the shoots removed, and the roots stored in the alcohol mixture.

#### *4.3.3 Root structure*

The anatomy of soil-grown *P. banksiana* was investigated as in the previous study of McKenzie and Peterson (1995a,b). Tests included permeability, vitality and histochemical analyses. On the basis of the results obtained, soil-grown roots could be divided into four zones, i.e. white without mycorrhizae, white with mycorrhizae, condensed tannin, and cork.

The total number of root tips was counted in each of the ten sampled root systems. During this procedure, tips were categorized as brown, white or mycorrhizal with the aid of a dissecting microscope (Olympus S061). Samples of each root tip type were assessed for metacutization by staining longitudinal sections with Sudan red 7B (Brundrett et al. 1991). The red-stained, metacutized layer was visible under a microscope (Nikon Labophot) using white light.

#### *4.3.4 Root measurements*

Total root length was calculated for both the growth chamber- and field-grown trees by the gridline-intersect method (Tennant 1975) with a 40 by 40 mm grid. The length of the white root zones was determined using a ruler. The length of the mycorrhizal zone was determined by first averaging the lengths of 20 fungal mantles and then multiplying this value by the total number of mycorrhizal root tips. Condensed tannin and cork zone lengths were more difficult to establish. For the latter, cross-sections were made basipetally from the distal end of the condensed tannin zone on each root and viewed under a Nikon Labophot microscope with blue light (exciter filter 485-540, barrier filter 515W, dichroic mirror 400). Autofluorescent cork cells were obvious, when present, as a continuous ring internally adjacent to the endodermis. The cork zone was considered to begin from the first appearance of autofluorescent cork tissue. The total length of the remaining root was measured using a ruler, and the length of the condensed tannin zone was determined by subtracting the mycorrhizal, white, and cork root zone lengths from the total root length.

The CPSA of each root zone was determined by calculating the total plasmalemma surface area of the cells that were alive with access to the soil solution. For the white zone, it was necessary to determine the CPSA contribution for cortical cells including the endodermal passage cells. To determine the plasmalemma surface area of the former, the average diameter and length of the cortical cells external to the endodermis was determined. Each cell was assumed to be a regular cylinder with flat ends, and the plasmalemma surface area was assumed to be equal to the cell surface area. The CPSA contribution of an average cell was then multiplied by the average number of cells in a



cross-section. Using the cell length data, the contribution of cortical cells per millimeter of white root length could be determined. The passage cell contribution was determined by multiplying the average width of the outer tangential face of a passage cell in cross-section by the average number of passage cells. This value was multiplied by 1 mm to determine the contribution per millimeter of root length. Refer to Kamula et al. (1994) for more details on these calculations. The mycorrhizal zone CPSA was calculated as in the white zone. Within the condensed tannin zone, only the passage cells could contribute to the CPSA. The cork zone was assumed not to contribute to the CPSA of the root system.

#### *4.3.5 Calculations of CPSA*

##### *4.3.5.1 Cortical cells*

In the white and mycorrhizal zones, the central cortical cells contributed to the CPSA. The contribution of the cortical cells was calculated as follows.

The tangential and radial plasmalemma surface area for all cortical cells in a 1 mm length of root,  $S_1$  ( $\text{mm}^2$ ), was determined by equation 1. Each cell was treated as if it were 1 mm long (to allow the heights of the “stacked” cells to be combined), and the slight overestimation this introduces (by ignoring the transverse walls of each cell) was disregarded.

$$1) \quad S_1 = n(h * 2\pi r_c)$$

Where  $h = 1$  mm (assumed cell height),  $r_c =$  average radius of a cortical cell in cross-section (mm) and  $n =$  the average number of cortical cells in a cross-section.

The transverse plasmalemmae surface area contribution for a 1 mm length of root,  $S_2$  ( $\text{mm}^2$ ), was determined by equation 2.

$$2) \quad S_2 = n(\pi r_c^2) * 2h * h_c^{-1}$$

Where  $h_c$  = average cortical cell height (mm), and the remainder of the abbreviations were as in equation 1. Note that the 2 accounts for the two membranes at the ends of the cell.

Finally, the total contribution of the central cortical cells, was determined by adding  $S_1$  to  $S_2$ .

#### *4.3.5.2 Passage cells*

The contribution to CPSA of the passage cells per 1 mm of root length,  $P$  ( $\text{mm}^2$ ), was determined by equation 3.

$$3) \quad P = n_p * w_p * h$$

Where  $n_p$  = the average number of passage cells in cross-section,  $w_p$  = the average width of the outer tangential face of a passage cell, and  $h = 1$  mm.

## **4.4 Results**

### *4.4.1 Field conditions*

Soil moisture fluctuated from being very dry (2.8% to 6.5%) in June, July, and August to wetter in September and October with a maximum of 15% (Figure 4.1). It should be noted that northern Ontario experienced a dry summer and fall in 1997, so that soil moisture levels may have been lower than average. Soil temperature declined rather steadily over the measured period, from 19.5 °C on June 10 to 7.1 °C on October 17 (Figure 4.2).

### *4.4.2 Root anatomy*

The three anatomical zones previously described by McKenzie and Peterson (1995a,b) were also present in field-grown roots (data not presented), along with ectomycorrhizal white roots that were not present in their study. Histochemical tests confirmed the presence

**Figure 4.1: Percent moisture ( $\pm$  SD) of the soil 0.15 m below the surface at the Kamiskotia Lake site over the time course of the experiment (June 10 to October 17); (n=4).**

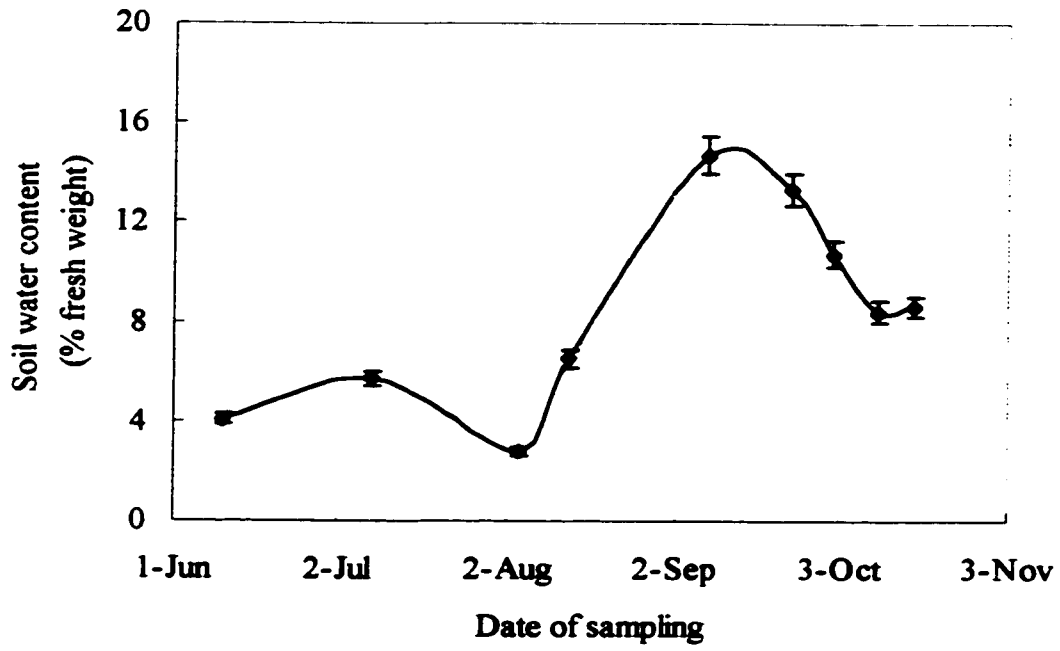


Figure 4.1

**Figure 4.2: Soil temperature ( $\pm$  SD) 0.15 m below the surface from the Kamiskotia Lake site over the time course of the experiment (n=4).**

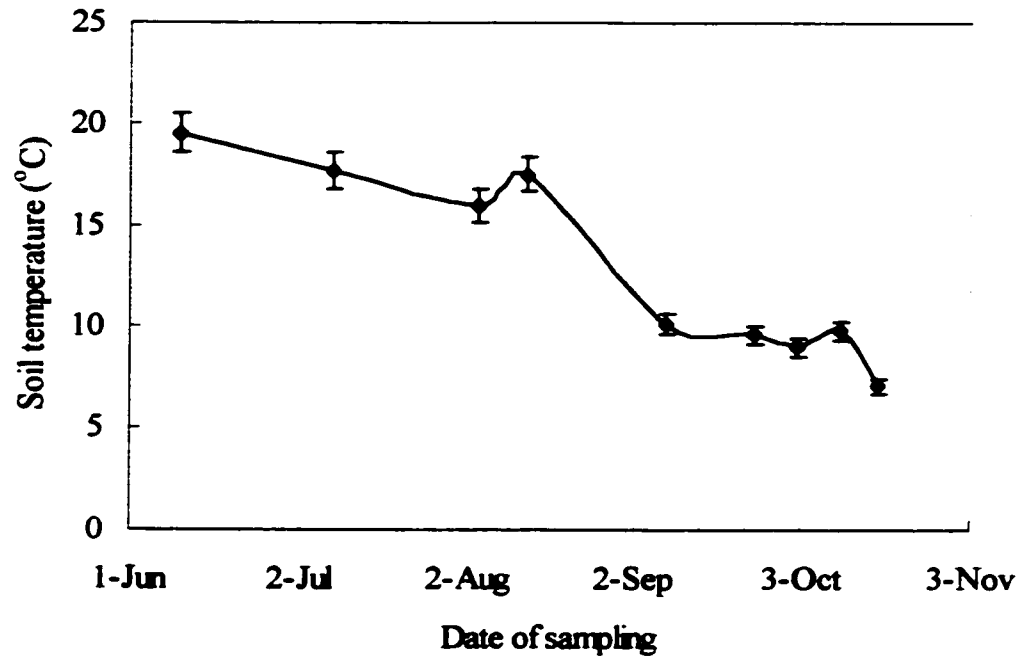


Figure 4.2

of condensed tannins in the cortex of the condensed tannin zone. Likewise, brown root tips were found to have condensed tannins in their cortex. Thus, in brown root tips, the condensed tannin zone occupied the root region that was previously white. The white and condensed tannin zones were permeable to berberine (an apoplastic dye) up to the endodermis, while the cork zone was impermeable at its outer surface (data not shown). The only viable cells exposed to the soil solution by the apoplastic continuum were the cortical cells (including the endodermal passage cells) of the white zone and the passage cells of the white and condensed tannin zones.

#### *4.4.3 Contributions of the anatomical zones to total root length*

Root growth over the observed time period was variable (Figure 4.3). The average total root length per tree on the first date measured (August 4) was 3.6 m, and it had increased less than 0.5 m by September 8. However, from September 8 to October 2 a substantial increase in average root length (more than 2 m) was observed. There was little change in the overall root length between October 2 and October 17.

At all ages, most of the root length consisted of condensed tannin zone, ranging from 72% to 74%. This zone increased substantially in length during the September 8 to October 2 interval. The mycorrhizal zone consistently occupied a lesser fraction of total root length (about 16%), as did the cork zone (about 10%). The white zone represented a very small fraction of the total root length (about 2%).

The total and zonal lengths of the growth-chamber pines differed markedly from those of the field-grown trees (Figure 4.3). Despite being considerably younger than the

field-grown trees (12 weeks compared to 6 months), the root systems of growth-chamber trees were over 1.5 m longer than their field-grown counterparts. This may have been a result of the small pouches in which the field-grown trees were initially held, as the roots tended not to leave the pouch until they were placed in the field, but were more likely due to the suboptimal environment for tree growth encountered in the field. By the first sampling date, the root system had extended beyond the volume of the Mini-Jiffy pouch. A second striking difference between the field- and chamber-grown pines was that the white zone of the latter roots contributed over 10% of the total root length.

#### *4.4.4 Root tip frequency and structure*

The most striking result from an analysis of the field-grown tree root tips is that a very small fraction (less than 10%) of them were white (Figure 4.4). The majority (at least 75% of the total) were mycorrhizal. In fact, it was an increase in the number of mycorrhizal root tips that was responsible for the increase in the number of root tips between September 8 and October 2. This increase was so great largely due to the dichotomous and coralloid pattern of development common in pine mycorrhizae, leading to the production of many tips (see Le Page et al. 1997). The remainder of the root tips were brown and had cortical anatomical features of the condensed tannin zone.

In the growth chamber, there were twice as many root tips as in field-grown seedlings (Figure 4.4). The difference was primarily a result of the large number of brown tips on the chamber-grown seedlings.



**Figure 4.3: Lengths of cork, condensed tannin, white, and mycorrhizal root zones in roots of field- and chamber-grown seedlings. The uncapped lines show the standard deviations of the lengths of the root zones, while the capped line shows the standard deviation of the total root length. There is no standard deviation line shown for the white zone of the field-grown roots as it was too small to be visible (n=10).**

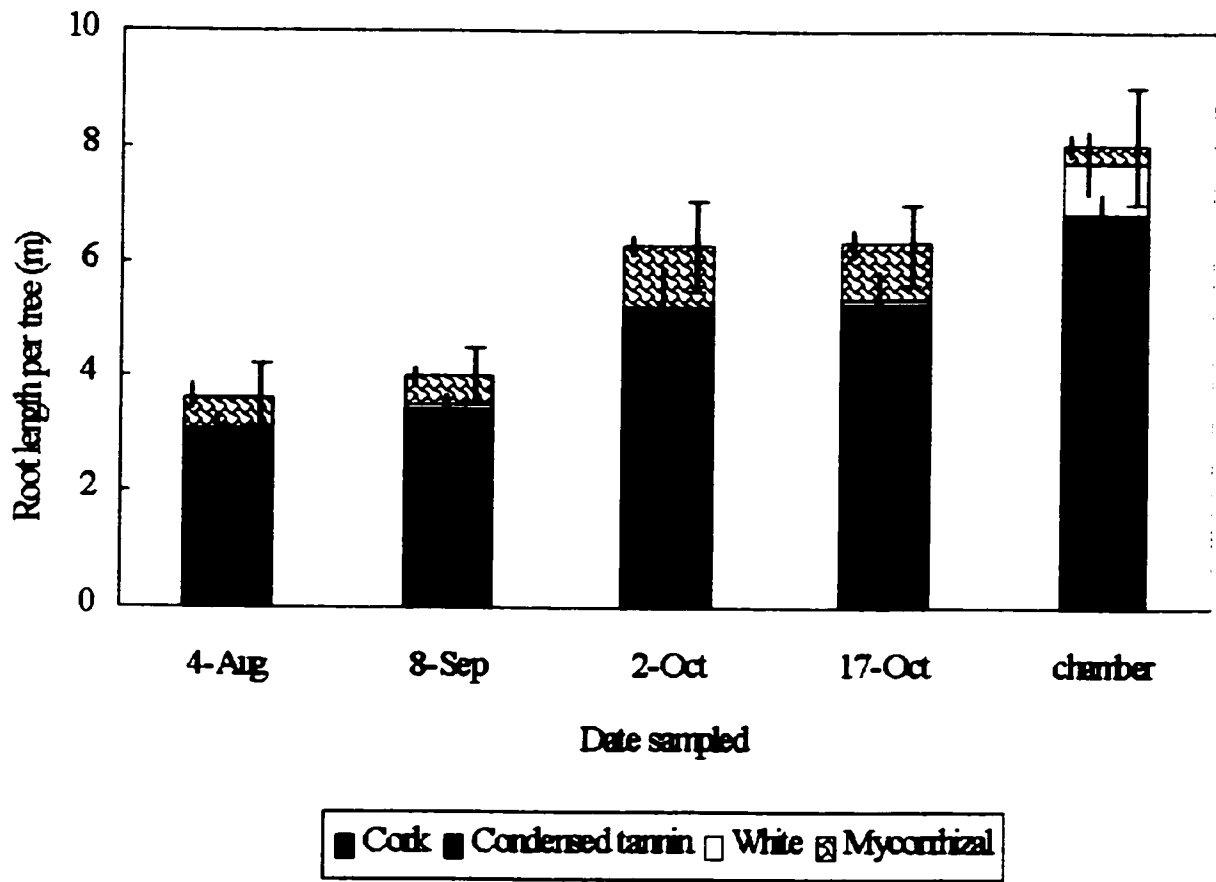


Figure 4.3

The proportion of root tips that were metacutized was lowest (roughly 30%) between September and October (Figure 4.5), around the time period of maximal root growth (Figure 4.3). Between October 2 and October 17, the percentage of metacutized tips increased (Figure 4.5), indicating a rapid onset of root dormancy or quiescence after the period of elevated root growth, and corresponding with a period of minimal growth (Figure 4.3).

The fraction of metacutized tips varied considerably among the three tip types identified macroscopically (white, brown and mycorrhizal). Brown roots were almost always metacutized (Figure 4.6). White roots showed considerably more variability, possessing high numbers of metacutized tips in August and October, and substantially fewer in September. Some mycorrhizal tips were also metacutized (about 25%), increasing to almost 50% by October 17.

#### *4.4.5 CPSA*

The contribution per unit length of each root zone to CPSA was highly variable (Table 4.1). The white zone always possessed the greatest CPSA per millimeter, primarily because of its large number of cortical cells. The mycorrhizal zone possessed substantially fewer cortical cells so that its CPSA was 33 to 50% of the non-mycorrhizal white zone CPSA. The contribution of the condensed tannin zone was very small (0.068 to 0.21% of the non-mycorrhizal white zone), as only the outer membranes of the passage cells of this zone were included.

**Figure 4.4:** Numbers of brown, white, and mycorrhizal root tips in field- and chamber-grown seedlings. The uncapped lines show the standard deviations of the number for root tip types, while the capped line indicates the standard deviation of the total root tip number. There is no standard deviation line shown for the white tips of the field-grown roots as it was too small to be visible (n=10).

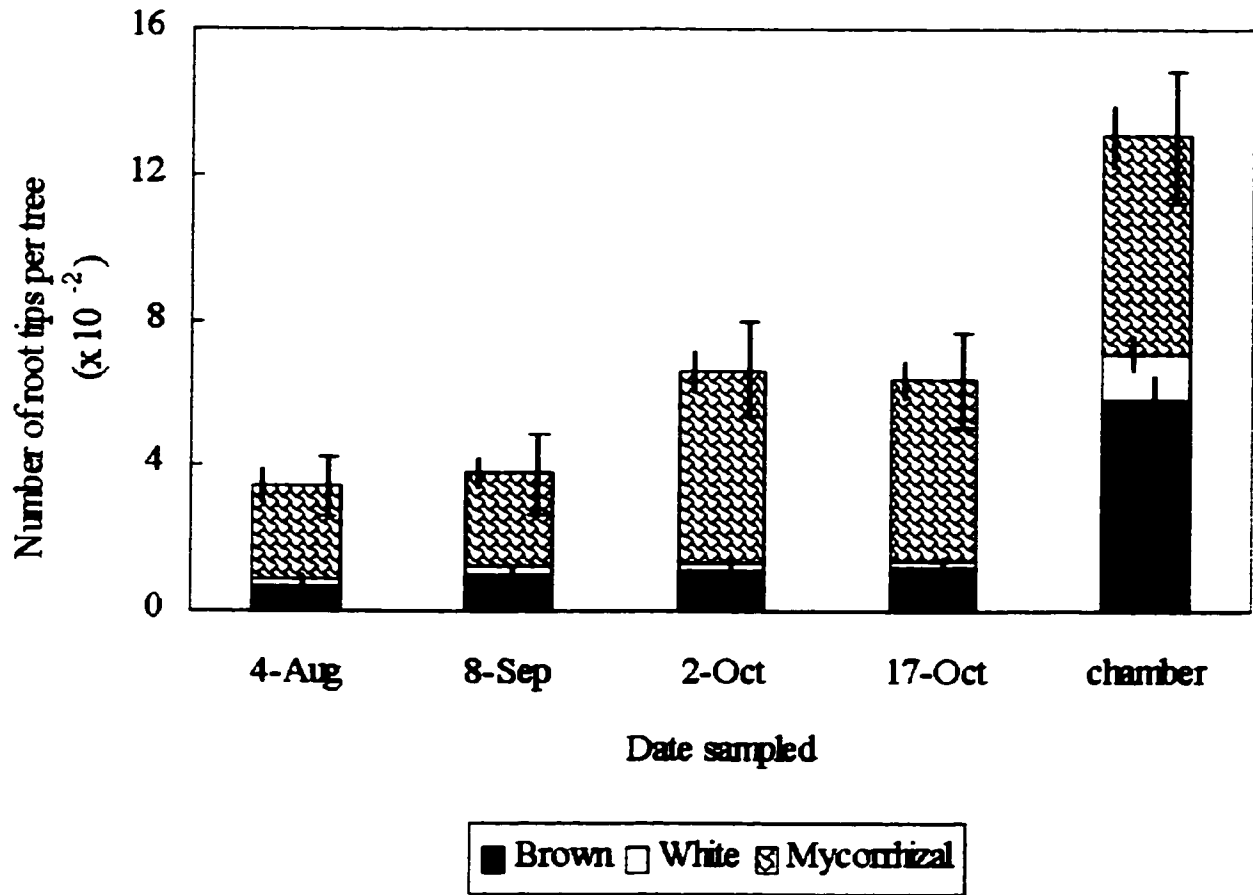


Figure 4.4

**Figure 4.5: The percent of metacutized root tips in field-grown seedlings.**

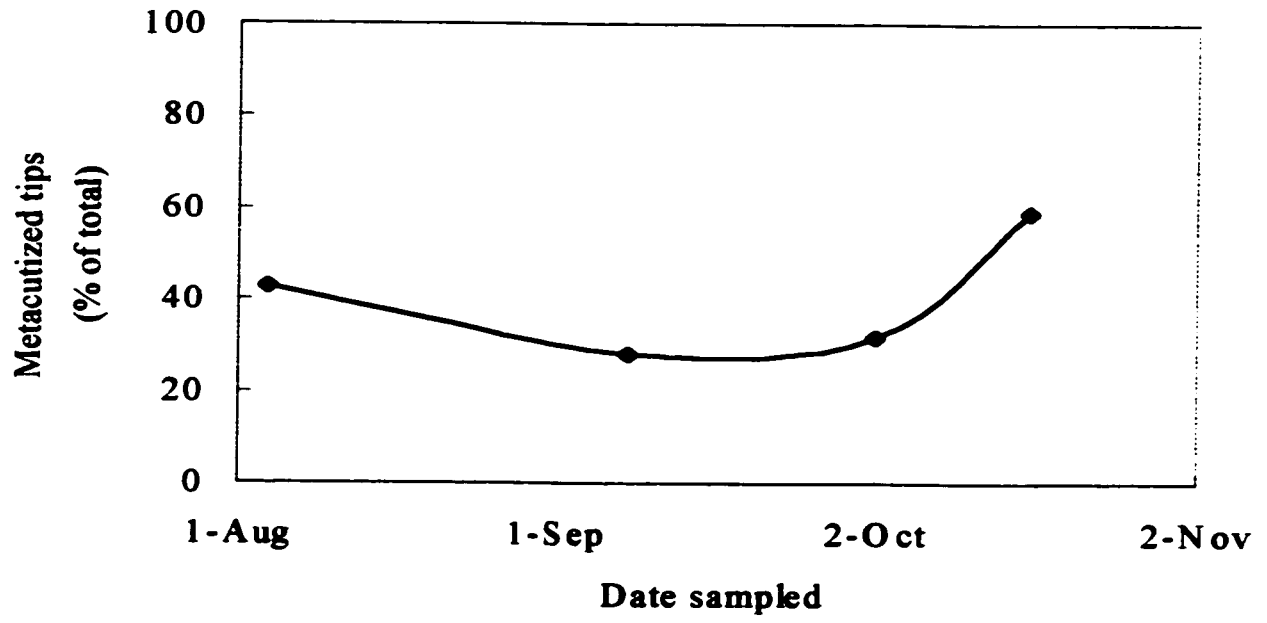


Figure 4.5

**Figure 4.6: The percent of metacutized root tips among the three root tip types (white, brown, and mycorrhizal) in field-grown seedlings.**



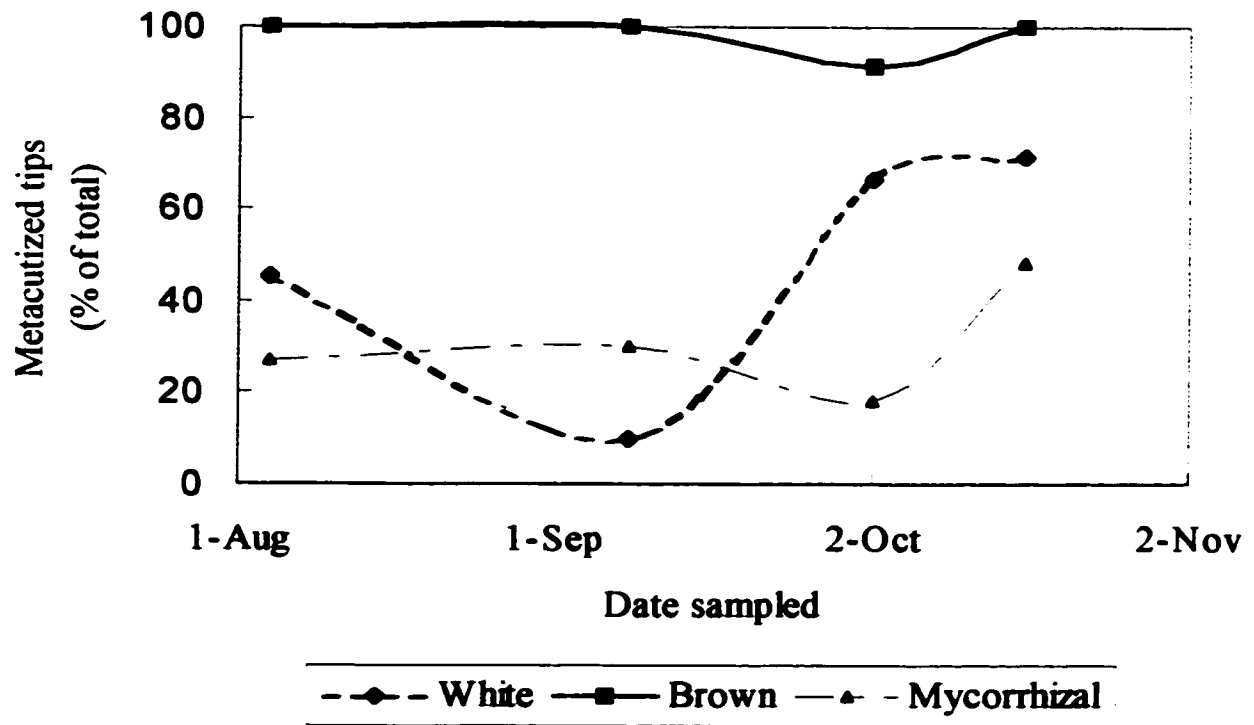


Figure 4.6

Table 4.1: Average dimensions and numbers (#) of living cortical cells (CC), passage cells (PC), and average calculated CPSA per millimeter root length for each root zone. Standard deviations (SD) and numbers of values (n) are included.

Sample date	Root zone	Width CC (mm) ±SD (n)	Length CC (mm) ±SD (n)	# CC ±SD (n)	Width PC (mm) ±SD (n)	#PC ±SD (n)	CPSA (mm <sup>2</sup> ) per mm root length
4-Aug	white	0.035 ±0.011 (165)	0.099 ±0.027 (34)	186 ±46 (24)	0.029 ±0.0064 (78)	3.5 ±1.8 (24)	24
	mycorrhizal	0.040 ±0.014 (76)	0.059 ±0.017 (34)	49.1 ±10 (17)	0.036 ±0.0074 (13)	0.77 ±0.75 (17)	8.3
	c. tannin	...	...	...	0.037 ±0.0095 (19)	0.63 ±0.81 (30)	0.023
8-Sep	white	0.034 ±0.012 (162)	0.106 ±0.028 (33)	212 ±73 (19)	0.037 ±0.014 (59)	3.0 ±1.3 (19)	26
	mycorrhizal	0.039 ±0.011 (133)	0.064 ±0.017 (37)	51.4 ±12 (19)	0.038 ±0.0098 (20)	1.3 ±0.95 (19)	8.3
	c. tannin	...	...	...	0.034 ±0.0071 (13)	0.52 ±0.59 (25)	0.018
2-Oct	white	0.036 ±0.012 (90)	0.156 ±0.045 (38)	153.8 ±42 (12)	0.035 ±0.012 (42)	3.6 ±1.4 (12)	20
	mycorrhizal	0.033 ±0.013 (125)	0.056 ±0.019 (34)	66.8 ±38 (12)	0.035 ±0.015 (16)	1.3 ±1.4 (12)	9.0
	c. tannin	...	...	...	0.035 ±0.013 (24)	1.7 ±1.3 (14)	0.060
17-Oct	white	0.034 ±0.013 (124)	0.16 ±0.033 (35)	148 ±39 (22)	0.032 ±0.0058 (83)	3.2 ±1.5 (22)	17
	mycorrhizal	0.033 ±0.011 (105)	0.061 ±0.017 (35)	70.1 ±16 (21)	0.035 ±0.0093 (15)	1.0 ±0.84 (21)	9.0
	c. tannin	...	...	...	0.031 ±0.0063 (20)	1.2 ±1.2 (25)	0.036
Chamber	white	0.022 ±0.0072 (151)	0.088 ±0.017 (32)	137 ±23 (29)	0.029 ±0.0058 (77)	5.1 ±1.4 (15)	11
	mycorrhizal	0.026 ±0.0095 (98)	0.058 ±0.015 (32)	38.5 ±8.4 (21)	0.030 ±0.0031 (23)	1.5 ±0.83 (15)	3.9
	c. tannin	...	...	...	0.026 ±0.0080 (17)	1.1 ±0.99 (15)	0.023

By August 4, the average root system of one field-grown seedling possessed 0.57 m<sup>2</sup> of CPSA (Figure 4.7). The CPSA more than doubled from August 4 to October 2 (increasing to 1.39 m<sup>2</sup>) and had declined somewhat by October 17 (Figure 4.7). The largest contributor to CPSA at any time was the root tissue encased in the fungal mantle. In fact, changes in the CPSA contribution by the mycorrhizal roots were primarily responsible for changes in the CPSA of the entire root system. If the mantle is permeable, then the total CPSA would be as presented in Figure 4.7. However, if the mantle is impermeable, independent ion uptake by the plant would be impeded for over 81% of the root CPSA, and the total root CPSA would remain relatively constant over the time period observed. In the latter case, the greatest proportion of the CPSA would be contributed by the white zone. The condensed tannin zone, despite its major contribution to total root length (Figure 4.3), actually contributed little to CPSA.

In seedlings raised in the growth chamber, by far the largest fraction of CPSA was contributed by the white zone (85%; Figure 4.7). Roots ensheathed by mantles contributed significantly less CPSA compared to field-grown plants.

## **4.5 Discussion**

### *4.5.1 Anatomy*

The cork, condensed tannin and white zones described by McKenzie and Peterson (1995a,b) in roots of pouch-grown *P. banksiana* were also found in the ectomycorrhizal, pine seedlings grown in soil both in pots and the field. Earlier anatomical analyses lumped

**Figure 4.7:** The average total CPSA (cortical plasmalemma surface area) per seedling root system and the contribution of three root regions (condensed tannin, white, and mycorrhizal) in field- and chamber-grown seedlings.

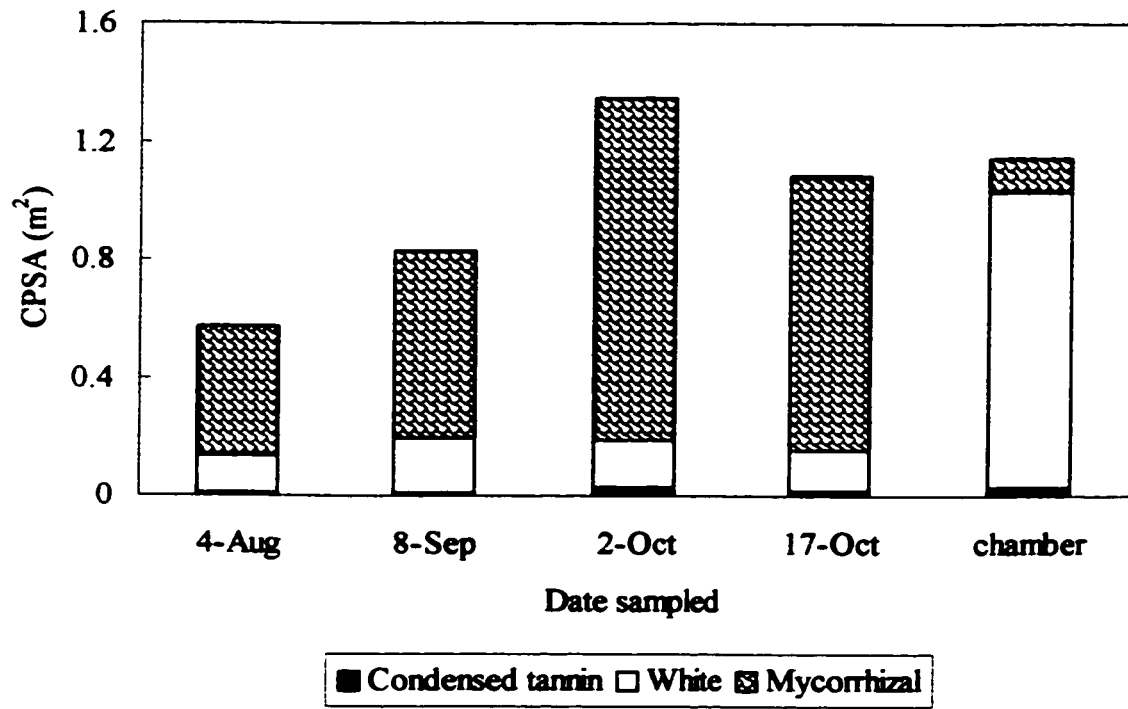


Figure 4.7

the condensed tannin and cork zones together as “suberized roots” based on their external brown coloration (e.g., Kramer and Bullock 1966; Chung and Kramer 1974). In the present study, the condensed tannin zone constituted the majority of the root length in both mycorrhizal field- and growth chamber-grown pines.

It is important to note that changes in root system CPSA did not correlate with changes in root length because the cork, condensed tannin, white, and mycorrhizal zones all contributed very different CPSAs based on their anatomy. In this research, the longest root region (the condensed tannin zone) actually contributed very little to the root system CPSA. The only root zone that contributed less was the cork zone, which was considered to be zero in the present work. The region that contributed most to the total root CPSA and was responsible for the change in root CPSA as the season progressed was the mycorrhizal region, and the field-grown trees were heavily mycorrhizal. This occurred despite the fact that the mycorrhizal zone contained relatively few cortical cells (on average, 34% as many cells as the non-mycorrhizal white zone). Both the lengths of the white and condensed tannin zones remained rather constant over the three-month period investigated. Consequently, the change in CPSA of these zones was minimal (Figure 4.2).

#### *4.5.2 Root composition and growth*

Growth chamber seedlings differed from those grown in the field in several respects. The growth chamber pines had over 80% of their CPSA in the white zone, with the mycorrhizal region making up the bulk of the rest. This occurred despite a high number of mycorrhizal tips, because the length of the average mycorrhizal region on an individual root tip was

considerably shorter than in the field (data not shown) and the white zones were considerably longer.

Some of the differences in proportional root anatomy between chamber- and field-grown trees were probably related to growth rates. The chamber-grown roots were longer and possessed more root tips than the field-grown seedlings, despite being much younger. Faster root growth by the chamber-grown seedlings undoubtedly reflected better conditions compared to those of the field. Wilcox (1962a) found that with faster growth, maturation of metaxylem and other structures occurred farther from the root tip. Thus, faster growing roots would be expected to have long white zones. In fact, even the growth of our field-trees may have been exceptionally fast as they were initiated under artificial conditions.

The field-grown seedlings exhibited uneven rates of root growth, as described in the earlier literature (Wilcox 1962b). The time periods in which root growth was most rapid, both in regard to new root tips and overall root length, correlated with the times of high soil moisture and not with temperature. The increases in length were primarily due to increases in the condensed tannin zones. These data show that even when the roots were growing relatively quickly in the soil, the condensed tannin zones were maturing shortly behind the tips but the maturation of the cork zone was not similarly accelerated. The majority of the increases in the number of root tips were provided by the mycorrhizal roots. This likely relates to the dichotomous and coralloid growth pattern of mycorrhizal roots in pine.

#### *4.5.3 Metacutization*

At all times, a substantial number of root tips were metacutized. As expected, the fraction of metacutized tips correlated inversely with root growth rate. Roots that were brown to the

tip were almost always metacutized (Figure 4.6). It is possible that metacutized white and mycorrhizal root tips represent an early stage, and that the cortex of these roots would eventually die. Comparing Figure 4.5 to the percent moisture of the soil (Figure 4.1) reveals that the time (approximately September 12) during which a lower fraction of root tips are metacutized coincides with the time of greater water availability. Further, the time interval of maximal increase in root length and tip number corresponded to the time of the lowest fraction of metacutized root tips. The latter correlation supports the earlier conclusion of Wilcox (1968) that metacutization is a feature of non-growing roots.

The function of the metacutized layer is unclear. Originally, it was believed to impede water movement and could, therefore, protect the underlying tissue from drying during drought (Mager 1913). However, Leshem (1970) disproved this idea by establishing that metacutized roots were more permeable to water than white roots. The onset of metacutization seems to be related to both environmental conditions and a natural cycle, neither of which can completely overcome the other (Leshem 1970). We propose that the metacutized layer could protect the underlying viable tissue from attack by microorganisms. Clearly this phenomenon warrants further study.

#### *4.5.4 Ion uptake capacity*

The CPSA measured in the present study represented the plasmalemma of living cells which could be contacted by the soil solution. Because ions must access membranes before they can be absorbed into the symplast, the CPSA contributes to the root's potential for ion uptake, along with the activities of transporters on the membranes themselves. The CPSA contribution of the white and condensed tannin zones changed little during the course of the



field study (Figure 4.7). Instead, the mycorrhizal zone was the dominant contributor both to overall CPSA and changes in CPSA. Conversely, in the chamber-grown trees, the mycorrhizal zone contributed much less than the white zone to their CPSA. The difference between the field- and chamber-grown trees may relate to the field trees being much older, differences in soil structure, fungal inoculation, or the more idyllic growth conditions found in the growth chamber.

The large quantity of the root system occupied by the condensed tannin zone could be significant, despite its low contribution to root CPSA. The absorption of water and ions by “suberized roots”, was not understood in earlier studies (Crider 1933; Kramer and Bullock 1966; Sougnez-Remy et al. 1993; Van Praag et al. 1993). This may have been a result of not distinguishing between the condensed tannin zones, which have living endodermal passage cells (Enstone, personal communication), and the cork zones. Similarly, dormant metacutized roots were bordered by a condensed tannin zone with passage cells, which may allow the root to retain some nutrient-acquiring abilities.

The question of ectomycorrhizal mantle permeability is critical for an understanding of the pathway of ion uptake for heavily mycorrhizal trees, as the cortical cells of the mycorrhizal zone are separated from the soil solution by the mantle. In this study, the largest amount of root CPSA was located in the mycorrhizal region. While this large CPSA is conducive to enhanced uptake of ions that are delivered by ectomycorrhizae (Smith and Smith 1990), the fungal sheath’s permeability to nutrient ions will greatly influence the pathway by which other ions are taken up by the root. If the mantle is permeable to nutrient ions, the CPSA of the root systems would be as shown in Figure 4.7. In this case, a

minimum of 75% of the root system CPSA is found within the fungal mantle. However, if the fungal mantle is impermeable to nutrient ions, then the underlying root tissue would be more isolated from the soil solution, and most importantly, from those ions that the fungus is not able to absorb and deliver to the root. Based on the present work, elimination of the total mycorrhizal CPSA would reduce the overall CPSA by as much as 85% in the field-grown trees. As well, if the mycorrhizal zone does not contribute to the CPSA for ions not absorbed by ectomycorrhizae, then the change in CPSA for those ions over the course of this study was very small. Clearly the absorptive capabilities of extramatrical hyphae regarding other mineral nutrients and the permeability of the mantle must be clarified.

In summary, this work has established that distinct anatomical zones exist in field-grown seedlings, the anatomy of which should strongly influence ion uptake potential. Among field-grown pines, the majority of the CPSA is located within the ectomycorrhizal mantle and may be somewhat isolated from the soil solution. A significant fraction of root tips were metacutized and contributed little to the root CPSA. It would be interesting to extend this investigation to mature trees. This anatomical analysis stresses the importance of revisiting some basic questions of tree root physiology. Is the cork zone impermeable to nutrient ions and/or water as assumed in this study? Are membrane transporters equally distributed amongst the living cells, or is their prevalence dependent on the location of the cell? What is the purpose of metacutization in root dormancy? These queries will not be easily answered, but must be addressed for a rudimentary understanding of tree root function.

## CHAPTER 5

### **Morphometric study of ectomycorrhizal *Eucalyptus grandis* (W. Hill ex Maiden) seedling roots.**

#### **5.1 Abstract**

Eucalypt roots present a complex anatomy, being woody, exodermal, and forming ectomycorrhizal associations. There is little information available on the structure and morphology of entire eucalypt root systems. In the present study, the anatomy and ion uptake potential was investigated for pot-grown seedlings of 9-week-old *Eucalyptus grandis* (W. Hill ex Maiden) inoculated with the ectomycorrhizal fungus *Pisolithus tinctorius* (Coker & Couch). It was revealed that, in addition to possessing four root zones (white, condensed tannin, cork, and ectomycorrhizal), *E. grandis* roots also have four distinct root types (main/tap, side, fine, and ectomycorrhizal). Additionally, the white root zone is divided into three distinct regions (non-exodermal, Casparian bands only and mature). The majority of the potentially absorptive plasmalemmae surface area was attributed to the super-numerous fine roots, which were almost entirely occupied by the white zone. The impact of these results on eucalypt root function is discussed.

#### **5.2 Introduction**

Eucalypt roots have a remarkable structure. First, they are woody roots, which differentiates them from herbaceous roots. Woody roots have three distinct regions (Figure 1.2), namely the white, condensed tannin, and cork zones (McKenzie and Peterson, 1995a,b). In the white zone, which is the youngest region located at the root tip, the cells of

the cortex and epidermis are alive. Basipetal to the white zone is the condensed tannin zone, in which the epidermal cells and the majority of the cortical cells are dead. The only cortical cells in this zone which may be alive are those of the endodermis, although concrete evidence for this is lacking (McKenzie and Peterson 1995a). The most mature region is the cork zone, which is characterized by at least one layer of dead, suberized phellem cells. The periderm of eucalypts is deposited in alternating suberized and non-suberized cell layers, and thus is defined as a polyderm (Tippett and O'Brien 1976).

Second, eucalypt roots possess an exodermis (Tippett and O'Brien 1976). This is a hypodermis that develops Casparian bands and suberin lamellae much like the endodermis (Peterson and Perumalla 1990). As a result, the radial inward apoplastic diffusion of ions is halted at the outer tangential face of the exodermis, and the symplastic uptake of mineral nutrients must occur in the epidermis or exodermal passage cells (Peterson and Enstone 1996). While the exodermis is by no means unique to eucalypt roots (Perumalla et al. 1990, Peterson and Perumalla 1990), it is still an interesting and influential aspect of the root structure in these trees.

Third, eucalypt roots form a symbiotic association with soil-borne fungi, resulting in the formation of an ectomycorrhiza (see Smith and Read 1997). The root portion of the ectomycorrhiza is similar to a typical white zone root, except that the epidermal cells become radially elongated following fungal inoculation (Chilvers and Pryor 1965, Massicotte et al. 1986). The fungal portion of an ectomycorrhizal root can be divided into three regions. Innermost are the Hartig net hyphae which penetrate between the cells of the epidermis. In a non-exodermal root (i.e., *Pinus* sp.), the Hartig net hyphae would penetrate

between the epidermal and cortical cells radially until the endodermis was encountered. The exodermis of eucalypts, however, prevents the Hartig net from entering the cortex. Ensheathing the root tip is the fungal mantle, which is made of densely weft hyphae packed in an extrahyphal matrix. The mantle is continuous over the tip and ends where the condensed tannin zone begins. Radiating out from the mantle into the soil solution are the extramatrical (or extraradical) hyphae, which are known to absorb mineral nutrients from the soil solution.

For a root cell to be even potentially capable of ion uptake, it must be alive and have its plasmalemma exposed to the soil solution by a permeable apoplast. The potential for ion uptake will be influenced by the potentially absorptive plasmalemmae surface area (APSA) exposed to the soil. As a result of the very different anatomy of the root zones, the contribution of each to ion uptake potential should be significantly different. The condensed tannin and cork zones should contribute nothing to ion uptake. In the condensed tannin zone, the apoplastic radial diffusion of dyes is halted at the exodermis (McKenzie and Peterson (1995 a,b) and thus only dead tissues are encountered. If these results can be extrapolated to nutrient ions, they would not be taken up symplastically to pass the exodermis and would not be absorbed. In the cork zone, the phellem greatly limits ions from accessing any of the underlying, living cells, thus strongly inhibiting the ions from being absorbed (see Chapter 3).

For this research, it was assumed that the white zone possessed three distinct regions. These regions were differentiated by distinct differences in plasmalemma surface exposed to the soil solution (Figure 1.2). In the very young white zone, before the

exodermis had developed Casparian bands, the epidermal and all cortical cells up to the outer tangential face of the endodermis are available for ion uptake (Region 1). It should be noted that the endodermis does not extend to the root tip, but the portion of the root in which the endodermis did not possess Casparian bands was never observed, and was thus assumed to be small enough to be ignored. Behind this region, the Casparian bands developed in the exodermis (Region 2). Therefore, the soil nutrients may only access the epidermis and the outer tangential face of the exodermis by apoplastic diffusion. In the most mature white regions, the majority of the exodermal cells had deposited suberin lamellae (Region 3). As a result, only the epidermal cells and the outer tangential face of the exodermal passage cells would be apoplastically exposed to the soil solution (McKenzie and Peterson 1995a). All three regions of the white root zone possess root hairs, which contribute considerably to APSA (Peterson and Farquhar 1996).

In the present study, the anatomy of *Eucalyptus grandis* (W. Hill ex Maiden) seedling roots which had been inoculated with the ectomycorrhizal fungus *Pisolithus tinctorius* (Coker & Couch) was studied in detail. In addition to determining what fraction of the total each root region occupied, the contribution of each root region to potential for ion uptake was assessed by determining the available plasmalemmae surface area (APSA) for each.

## **5.3 Methods**

### *5.3.1 Plant material*

Seeds of *Eucalyptus grandis* (W. Hill ex Maiden) were soaked in cold tap water for 48 h, rinsed, and then planted in a peat moss:vermiculite (70:30) mixture in pots (0.04-m-

diameter, 0.15-m-deep) in early July of 1997 at MikroTek (36 Emerald St., Timmins, ON, P4N 7X8). The seedlings were maintained in a growth chamber with day conditions 25 °C, 35% humidity, light intensity 150-250  $\mu\text{mol}/\text{m}^2/\text{s}$ , 18 h, and night conditions 18 °C, 90% humidity. Twice weekly, the seedlings were watered to saturation with tap water. Two weeks post-planting, they were inoculated by drenching the soil mix with a concentrated slurry of *Pisolithus tinctorius* prepared from solid agar culture plates.

### 5.3.2 Root sampling

On September 7, 1997, the seedlings were removed from the containers and the root systems gently rinsed free from soil with a spray of water. Those roots used for the viability, permeability, and histochemical tests were held in water and used immediately. Other roots were preserved in a mixture of alcohols (85% ethanol, 15% methanol) until they were analyzed for root zone lengths, root tip type and number, and cellular dimensions.

### 5.3.3 Root structure

The anatomy of roots of *E. grandis* was investigated as in the previous study of McKenzie and Peterson (1995a,b). Tests of permeability, vitality, and histochemistry were included. On the basis of the results obtained, the roots could be divided into four zones, i.e. white without mycorrhizae, white with mycorrhizae, condensed tannin, and cork.

In addition to the four root zones, the roots were also divided into four root types based on superficial differences. The first type was the main or tap root, which was much larger than any other root observed. The second type was termed the side root, as these roots always branched off the tap root, and were approximately half its diameter. The third

root type was the fine roots. These roots grew off the main or side roots, were very fine (roughly 1 mm in diameter), and were typically only 10 mm long. The fourth root type was the ectomycorrhizal roots, which were distinguished by the presence of a fungal mantle.

#### *5.3.4 Root measurements*

The total number of root tips was counted in each of ten root systems. During this procedure, roots were categorized as tap, side, fine, or ectomycorrhizal with the aid of a dissecting microscope (Olympus S061).

The total root length was calculated using the gridline-intersect method of Tennant (1975) with a 40 by 40 mm grid. The length of the white zones was determined using a ruler. It was also necessary to determine the length of each region of the white zone (i.e., Regions 1, 2, and 3, Figure 1.2) for each root type (except for ectomycorrhizal roots, which were in Region 3 along their entire length as revealed by a preliminary study). To estimate the length of each white root region, freehand serial sections were made every 2 mm basipetally from the tip (generally, three sections were obtained from the 2 mm length). This was repeated on 15 randomly selected roots of each root type, performed three at a time by holding the three roots between pieces of Parafilm (American National Can, Menasha, WI) and collecting the resulting sections. The sections were stained with Sudan Red 7B (Brundrett et al. 1991) and viewed under a Nikon Labophot microscope with white light. Both the Casparian bands and suberin lamellae appeared red following this procedure, and, therefore, the beginning of each of these regions of the white zone was determined. The average length of each of the three white root regions for each of the three measured root types was determined and applied to all roots of that type. Similarly, the



total length of the ectomycorrhizal zone was determined by first averaging the lengths of 20 fungal mantles and then multiplying this value by the total number of ectomycorrhizal roots.

To determine the length of the cork zone, cross-sections were made basipetally from the distal end of the condensed tannin zone on both the tap and side roots. (Neither ectomycorrhizal nor fine roots developed to cork zone stage.) Sections were viewed under a Nikon Labophot microscope with blue light (exciter filter 485-540, barrier filter 515W, dichroic mirror 400). The cork cells were easily visible as soon as they became suberized as a result of their autofluorescence. The cork zone was considered to begin at the point where a continuous ring of cork cells was present. The length of the condensed tannin zone was determined by subtracting the lengths of the ectomycorrhizal, white, and cork zone lengths from the total root length.

The APSA of each root zone was determined by calculating the total plasmalemma surface area of the cells that were alive with access to the soil solution. For the white zone, it was necessary to determine the APSA contribution for each of the three regions separately. For all three white root zones, the epidermal cells were treated as regular cylinders, and the plasmalemma surface area was assumed to be equal to the cell surface area. The average diameter and length of the cells were determined in longitudinal sections ( $n = 40$ ). Cross-sections were used to determine the average number of epidermal cells around the root ( $n = 10$ ). For Region 1, the contribution of the cortical cells was determined in the same manner as the epidermal cells. Using the cell surface area data, the contribution of epidermal (and cortical in Region 1) per millimeter of white root region

could be determined. The root hairs were treated as cylinders capped with hemispheres. The contribution of the root hairs was determined by using their average length and width to calculate the average ASPA contribution per root hair, and then multiplying this by the average number of root hairs in a 1 mm-thick cross-section. In Region 2, the contribution of the exodermis was determined by multiplying the average width of the outer tangential face of an exodermal cell by the total number of exodermal cells. For Region 3, the contribution of the passage cells in the exodermis was determined by multiplying the average width of the outer tangential face of a passage cell in cross-section by the average number of passage cells. This same method was used to determine the contribution of the endodermal cells in Region 1. For all the passage cells, the contribution per millimeter root length was determined by multiplying by 1. All calculations were made separately for the white roots regions of tap, side and fine roots. Refer to Kamula et al. (1994) for more details on these calculations. The mycorrhizal zone APSA was calculated as in the white zone Region 3, possible only because the extreme radial extension of the epidermal cells previously noted in ectomycorrhizal eucalypt roots (Chilvers and Pryor 1965, Massicotte et al. 1986) was not observed in this study. The condensed tannin and cork zones were assumed not to contribute to the APSA of the root system.

### *5.3.5 Calculations of APSA*

#### *5.3.5.1 Epidermal and cortical cells*

In the white and ectomycorrhizal zones, the cortical (white zone Region 1 only) and epidermal cells contributed to the APSA. Note that the epidermal and cortical cells were

calculated separately in Region 1. The contribution of the epidermal and cortical cells was calculated as follows.

The tangential and radial plasmalemma surface area for all epidermal and cortical (in non-exodermal white roots only) in a 1 mm length of root,  $A_1$  ( $\text{mm}^2$ ), was determined by equation 1. Each cell was treated as if it were 1 mm long, and the minor overestimation this introduces (by ignoring the transverse walls of each cell) was disregarded.

$$1) \quad A_1 = nh * 2\pi r_c$$

Where  $h = 1$  mm (assumed cell height),  $r_c =$  average radius of a cortical cell in cross-section (mm) and  $n =$  the average number of epidermal or cortical cells in a cross-section.

The transverse plasmalemmae surface area contribution for a 1 mm length of root from the epidermal and cortical cells (calculated separately),  $A_2$  ( $\text{mm}^2$ ), was determined by equation 2.

$$2) \quad A_2 = n\pi r_c^2 * 2h * h_c^{-1}$$

Where  $h_c =$  average epidermal or cortical cell height (mm), and the remainder of the abbreviations are as in equation 1. Note that the 2 accounts for the two membranes at the ends of each cell.

Finally, the total contribution of the epidermal and cortical cells was determined by adding  $A_1$  to  $A_2$ .

#### *5.3.5.2 Root hairs*

The contribution to APSA of the root hairs per 1 mm of white root length,  $H$  ( $\text{mm}^2$ ), calculated separately for tap, side, and fine roots, was determined by equation 3.

$$3) \quad H = n_h \pi l_h w_h + \frac{2}{3} \pi r^2$$

Where  $n_h$  = the average number of root hairs in a 1 mm length of root,  $l_h$  = the average length of a root hair,  $r$  = the average radius of a root hair and  $w_h$  = the average width of a root hair.

#### 5.3.5.3 Passage cells

The contribution to APSA of the passage cells (exodermal or endodermal) per 1 mm of root length,  $P$  ( $\text{mm}^2$ ), was determined by equation 4.

$$4) \quad P = n_p * w_p * h$$

Where  $n_p$  = the average number of passage cells in cross-section,  $w_p$  = the average width of the outer tangential face of a passage cell, and  $h = 1$  mm.

## 5.4 Results

### 5.4.1 Root anatomy

The white, condensed tannin, and cork zones illustrated by McKenzie and Peterson (1995a,b) were also found in the *Eucalyptus grandis* roots grown in the soil mix. In addition, ectomycorrhizal roots were present, which were not observed in their studies. Also as in the McKenzie and Peterson (1995a,b) study, histochemical tests revealed the presence of condensed tannins in the epidermis and cortex of condensed tannin zone roots. Cells that were both alive and accessible to the soil solution by a permeable apoplast are presented in Table 5.1.

The majority of the roots were of the fine and the second most numerous were the ectomycorrhizal type (Figure 5.1). These two categories made up nearly 98% of the root

Table 5.1: Living cell plasmalemma surfaces accessibility by the soil solution in ectomycorrhizal eucalypt roots. The membranes are shown as available to the soil solution (+), not available (-), or unclear ( $\pm$ ). exodermis = exo, endodermis = endo, passage cell = PC, central cortex = CC.

Root zone	Cells accessed by the soil solution			
	epidermal	exo PC	CC	endo PC
White				
<u>Region</u>				
1	+	+	+	+
2	+	+	-	-
3	+	+	-	-
Condensed tannin	-	-	-	-
Cork	-	-	-	-
Mycorrhizal	$\pm$	$\pm$	-	-

Figure 5.1: The average number of roots of each type ( $\pm$ S.D.) observed on an *E. grandis* seedling (n = 10).

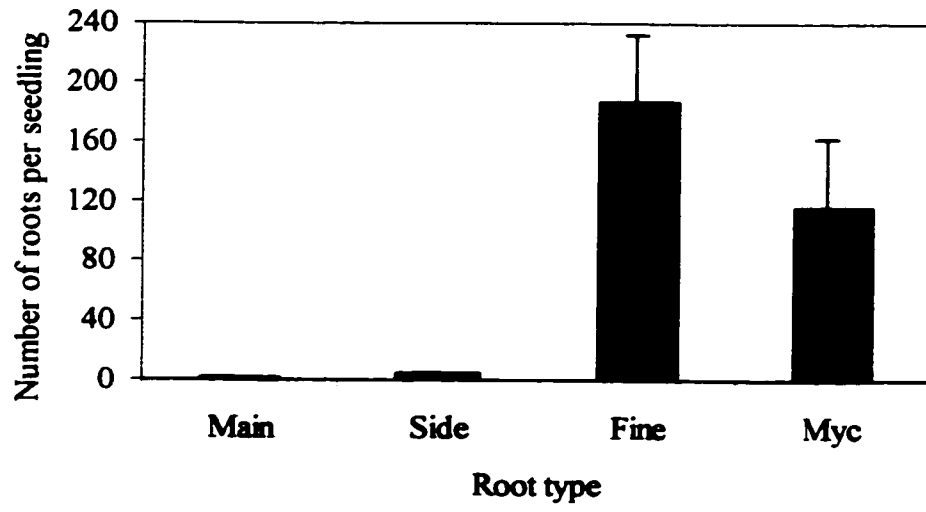


Figure 5.1

types observed. Of course, there was only one main/tap root, and never more than five side roots. As a result of the fine roots being almost all white, approximately 80% of the root system (by length) was occupied by white roots (Figure 5.2). The condensed tannin, cork, and ectomycorrhizal zones equally occupied the remaining 20% of the total root length.

#### *5.4.2 APSA*

The APSA per millimeter was directly related to root thickness among the three root types with white regions (Figure 5.3). The main/tap root was the thickest, and it possessed the greatest APSA per millimeter root length. Conversely, the very thin, fine roots had the smallest APSA per millimeter root length. The same relationship held true when regions within the white zone were examined (Figure 5.3), with the regions in the thicker roots having a greater APSA per millimeter than those in thinner roots. Within each root type, Region 1 was the greatest contributor to APSA per millimeter, which is not surprising given that its cortical cells are exposed to the soil solution. The smallest contributing region to APSA per millimeter was from Region 3. The ectomycorrhizal roots possessed a very low APSA per millimeter, which was expected since it consists entirely of mature region white root and lacks root hairs. It should be noted that the mantles were assumed to be permeable to nutrient ions, though some earlier studies disagree with this (Ashford et al. 1988). Should the mantle indeed be impermeable to nutrient ions, the APSA of the ectomycorrhizal roots would be zero.

The fine roots, which were entirely white, provided over 90% of the total root system APSA (Figure 5.4). This overwhelming value is primarily due to the tremendous number of fine roots in the eucalypt root system. Within the fine roots, Region 1 (with an



**Figure 5.2:** The average length of each root region ( $\pm$ S.D.) in an *E. grandis* seedling root system (n = 10).

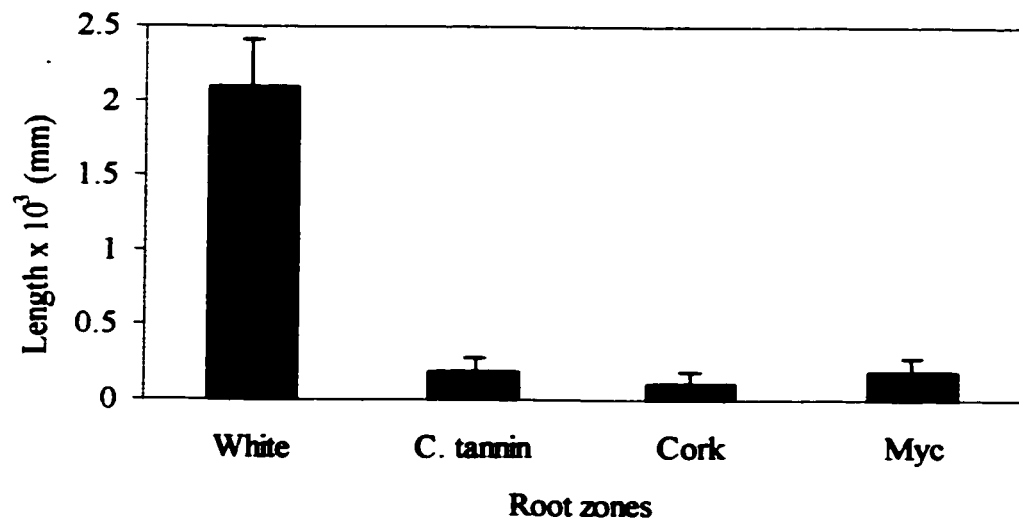


Figure 5.2

**Figure 5.3:** The average APSA ( $\text{mm}^2$ ) per millimeter root length for each white root region of the main/tap, side, fine roots, and the ectomycorrhizal roots of the *E. grandis* seedlings. See Figure 1.2 for an explanation of these three regions.

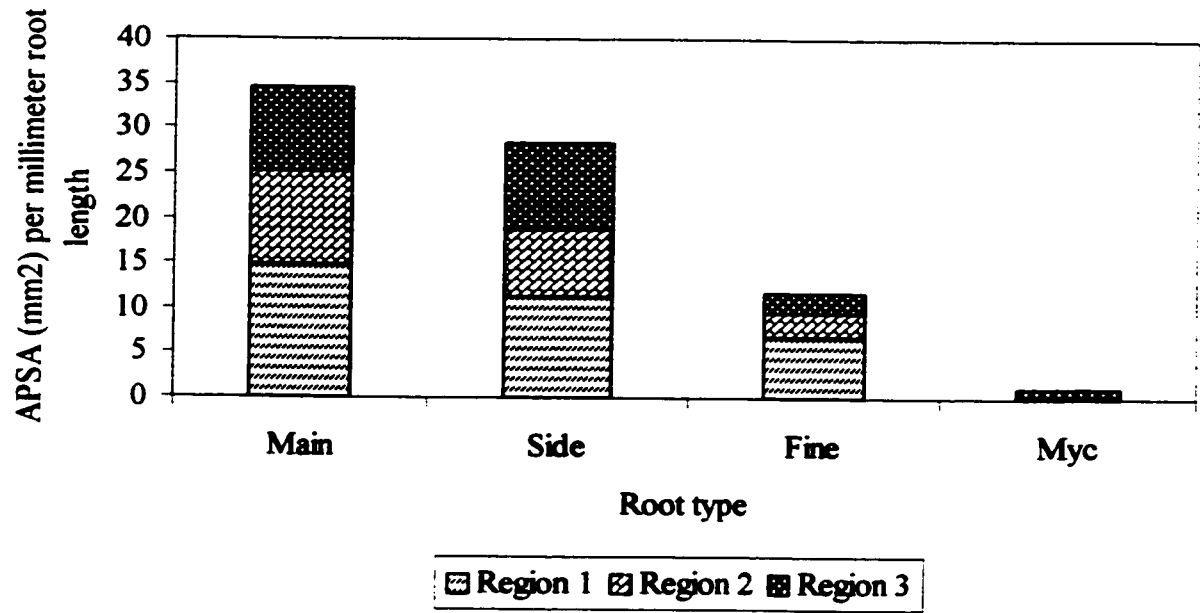


Figure 5.3

**Figure 5.4:** The average total APSA ( $\text{mm}^2$ ) for each white root region of the main/tap, side and fine roots, and the ectomycorrhizal roots of an *E. grandis* seedling. See Figure 1.2 for an explanation of these three regions.

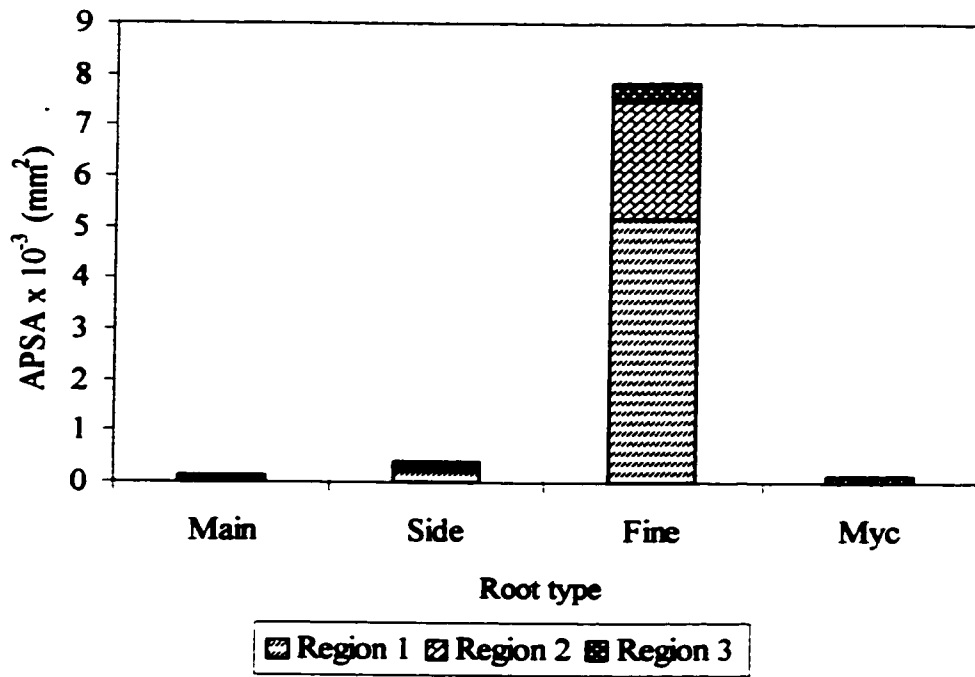


Figure 5.4

immature exodermis) and Region 2 (with an exodermis with Casparian bands but no suberin lamellae) were the primary contributors. Among the other root types, the side roots were the main providers of APSA, but their contribution was almost insignificant relative to that of the fine roots.

### **5.5 Discussion**

This study basically supported the anatomical work of McKenzie and Peterson (1995a,b). Even when grown in a soil mix, the same three root zones (white, condensed tannin, and cork), and the same characteristics of each were present, along with an ectomycorrhizal zone as a result of fungal inoculation. However, by expanding this study to all roots, as opposed to focusing on the main/tap root, the impact of each root zone could be assessed for the entire root system. The condensed tannin, cork, and ectomycorrhizal zones made up a very small fraction of the total root length, while the white root zone occupied the vast majority of the root system. This result was not surprising, given the very numerous fine roots which were almost entirely white. The cork and condensed tannin zones, first differentiated by McKenzie and Peterson (1995a,b), were only significant on the main/tap and side roots. These results are quite different from those for pine (see Chapter 4), where the condensed tannin zone of the field-grown roots occupied the largest portion of the total root length. It is noteworthy that the condensed tannin zone increased while the white zone was smaller in the pine roots grown in the field compared to those grown in the more idyllic growth-chamber environment (see Chapter 4). It is possible that the condensed tannin zone of eucalypt roots would occupy a larger portion of the root zone if grown under less ideal conditions. It was also noted that growth-pouch-grown *E. grandis* produced

many fine roots which were almost entirely brown (data not shown), while none were noted on the pot-grown seedlings of this study. It is possible that these roots were lost in the washing stage, despite efforts to prevent this, and that a greater fraction of condensed tannin zone roots were actually present.

In this study, the white zone of the fine roots contributed the overwhelming bulk of the APSA of the root system. Therefore, one would predict that these fine roots are responsible for the majority of the ion uptake. This prediction is not without practical merit, as these roots are numerous, fine (of low metabolic expense), and act to extend the root system radially into the soil solution. It also appears that the main/tap and side roots act primarily as a scaffolding for the fine roots, as the main/tap and side roots contribute little APSA. It is possible that the fine roots serve a function much like proteoid roots, being transiently produced in regions of nutrient density and then lost. However, further work is required to validate this idea. In comparison to pine roots (Chapter 4), the eucalypt roots have a very low fraction of their APSA in the ectomycorrhizal root category. It is possible that, as in the pines, the proportion of APSA in the white roots would be reduced and the fraction in the ectomycorrhizal roots increased if the seedlings were grown in the field. Another factor is that the ectomycorrhizal roots of eucalypts do not undergo the dichotomous or coralloid branching of ectomycorrhizal pine roots, which will reduce the number of ectomycorrhizal roots in eucalypts. Even with these considerations, it appears that the eucalypt roots possess a larger fraction of their APSA outside the ectomycorrhizal roots than pine, and, therefore, the eucalypt roots may be less dependent on ectomycorrhizae for nutrient acquisition.



As with any introductory study, this investigation of eucalypt root anatomy and APSA has produced as many questions as answers. A significant question involves our use of living plasmalemma surfaces exposed to the soil solution to predict ion uptake capacity. This simplification requires a number of assumptions (i.e. that nutrient transporters are equally present on all these membranes) that are not established and likely not true. Further work is necessary (possibly *in situ* hybridizations) to locate the membrane transport proteins. Another question involves our choice of mycorrhizal fungus. We chose *Pisolithus tinctorius*, which is known to have a broad "host" range. However, recent work has revealed that *P. tinctorius* is actually a number of different fungal species (see Smith and Read 1997), and our particular isolate may have been less than ideal for *E. grandis* (Malajczuk et al. 1989). Perhaps the most important question is how the eucalypt root morphology will change both if the roots are grown under field conditions and as the plant ages. Despite these caveats, this study was the first to present a detailed analysis of the anatomical basis of ion uptake capacity for a woody, exodermal, mycorrhizal root system.

## CHAPTER 6

### **Viability and wall permeability of the extramatrical hyphae of the ectomycorrhizal fungus *Hebeloma cylindrosporum* (Romagnesi)**

#### **6.1 Abstract**

The extramatrical hyphae of ectomycorrhizae are known to absorb ions from the soil for the symbiotic association, but the fraction of hyphae involved in this activity has not been studied. For hyphae to potentially absorb ions, they must have permeable walls and be viable. In the present study, the proportion of living, extramatrical (or extraradical) hyphae of *Hebeloma cylindrosporum* (Romagnesi) was measured by a grid-intersect method after staining with fluorescein diacetate, disodium fluorescein, or ethidium bromide. Results with ethidium bromide indicated that 89% of the hyphae were alive when the association was 2 weeks old and that this value declined to 76% at 26 weeks. In contrast, both fluorescein treatments resulted in staining of only 25% of the hyphae at 2 weeks and 7% at 26 weeks. The difference in measured viability was ascribed to wall permeability. Ethidium bromide was applied following an ethanol pretreatment, which apparently increased the permeability of the hyphal wall as well as that of its membranes. Our results indicate that only a fraction of hyphae are likely involved in ion uptake (as indicated by the fluorescein tests), a fraction that declines as the association ages. Further, parts of the hyphal mass are alive but incased in impermeable walls; these parts may act as conduits for the ions which were absorbed by the younger regions.

#### **6.2 Introduction**

Ectomycorrhizae are a predominant feature on the root tips of many woody plant species.

As a result of this symbiotic association with a fungus, the plant receives an increased concentration of ions, particularly phosphate (see Harley and Smith 1983). Ectomycorrhizae are typically characterized by a mantle which coats the root tip, a Hartig net which extends into the root cortex, and extramatrical hyphae which radiate out from the mantle into the surrounding soil. The work of Rhodes and Gerdemann (1975), Finlay et al. (1989) and Burkert and Robson (1994) has established that the extramatrical hyphae can take up nutrient ions from the soil and transfer them, through the mantle and Hartig net, to the plant partner. It has generally been assumed that the entire surface of the extramatrical hyphae is potentially involved in ion uptake (e.g., Read and Boyd 1985). However, Schubert et al. (1987) showed that soil hyphae in a vesicular-arbuscular mycorrhizal system lose viability, as tested with fluorescein diacetate (FDA), with age. If this is generally true, then only a fraction of the symbiont hyphae would be capable of absorbing ions.

The three fluorochromes used in the present investigation, FDA, disodium fluorescein (DF) and ethidium bromide (EB) test a variety of cellular attributes. FDA treatment results in the accumulation of fluorescein in hyphae which have a permeable wall, an intact outer membrane, active esterases in the cytoplasm, and a non-acidic cytoplasmic pH. FDA has been used previously (Söderström, 1977, Ritter et al. 1986, Barak and Chet 1986, Schubert et al. 1987) as a test of fungal viability. This fluorochrome stains the Hartig net, mantle and extramatrical hyphae of ectomycorrhizal fungi (Ritter et al. 1986). DF treatment also results in an accumulation of fluorescein in the cytoplasm. The primary difference between DF and FDA tests is that cytoplasmic esterases are not required for DF trapping by the cytoplasm. EB stains intact DNA when employed in the method of

Roser (1980) which includes an ethanol pretreatment. Assuming that intact nuclear material is indicative of a living (or recently living) cell, EB may be employed as a viability treatment (Roser et al. 1982).

In the present study, age-related changes in the viability of the extramatrical hyphae of the ectomycorrhizal fungus *Hebeloma cylindrosporum* (associated with *Pinus banksiana*) were followed. Accumulation of fluorescein in the cytoplasm following application of either disodium fluorescein or fluorescein diacetate was taken as an indicator of viability. However, the absence of fluorescein accumulation in the cytoplasm could not be taken to indicate cell death, because it could also have been due to hyphal wall impermeability. The question of wall permeability was resolved with ethidium bromide (which stains DNA) applied after two different treatments, one of which made both the wall and the membrane permeable and the other only the membrane.

### **6.3 Methods**

#### *6.3.1 Organisms and cultural conditions*

Seeds of *Pinus banksiana* (Lamb.) were supplied by Mikro-Tek (36 Emerald St., PO Box 2120, Timmins, Ontario, Canada). The seeds were stratified in 4°C water for two days, sterilized in 33% hydrogen peroxide with a drop of Tween 80 for 30 min and then germinated on 1.5% Bactoagar. When the seedlings were 20 mm long (with roots and shoots being about equal length) they were transferred to sterile growth pouches (Fortin et al. 1980) which forced the root system to develop in a two-dimensional manner. Water and nutrient solutions were held on a paper insert within the pouch, and the system was aerated by a vertically orientated pipette. The pouches were maintained in a growth chamber where

temperatures were maintained at 25/23° C (day/night), daylength 16 h, photosynthetic photon flux density 300  $\mu\text{mol m}^{-2} \text{s}^{-1}$  and relative humidity 75-85%. Seedlings were watered twice weekly with 5 ml of sterile, distilled water; every fourth watering was with 1/4-strength Knop's solution (Loomis and Shull 1937).

The ectomycorrhizal fungus *Hebeloma cylindrosporum* (Romagnesi), also obtained from Mikro-Tek, was maintained on plates of modified Melin-Norkrans medium (MMN) at 22 °C. Cultures were allowed to grow to a diameter of 60 mm. To inoculate the plants, three agar cuttings of five mm<sup>2</sup> were taken from the periphery of the fungal cultures and placed closer than five mm to white roots. Hyphal contact with the root generally occurred less than three days following inoculation. Ectomycorrhizal establishment was considered complete at the time the mantle was mature. This occurred less than ten weeks following inoculation.

### 6.3.2 Reagents and techniques

Fluorescein diacetate (FDA) stain was prepared by adding 5 mg FDA (JT Baker, Phillipsburg, N.J.) to 1 ml acetone, then diluting with 0.15 M phosphate buffer (PB), pH 7.4, to a final concentration of 50.0  $\mu\text{g ml}^{-1}$ . Disodium fluorescein (DF) was prepared in the same fashion, with the exception that the pH was 5.4. Ethidium bromide (EB, diamino-10-ethyl-9-phenylphenanthridinium bromide supplied by BDH Chemicals Ltd., Poole, England) stain was produced by dissolving EB in 0.15 M PB, pH 7.4, to yield 50.0  $\mu\text{g EB ml}^{-1}$ . All stains were stored in the dark at 4°C.

Extramatrix hyphae grow along the surface of the paper within the growth pouch. To obtain hyphae for staining, the plastic face of the pouch was removed, allowing access

to the mycorrhizal root system. To remove a sample of extramatrical hyphae, a mycorrhizal root tip was cut from the root system. Using fine tweezers, the mycorrhizal root tip was used to lift the surrounding network of extramatrical hyphae. With care, almost the entire system of extramatrical hyphae could be removed. Each sample was then placed in a small staining chamber with a nylon mesh base (Brundrett et al. 1988) sitting in a Petri dish containing PB holding solution (0.15 M, pH 7.4).

Extramatrical hyphae were assayed with three viability stains. 1. Staining cups were moved to a dish containing FDA for 5 min at 22°C in the dark. Hyphae were rinsed with a small volume of PB, mounted in PB on a slide, and viewed immediately using a Zeiss Axiophot microscope equipped with an Osram HBO 100W mercury lamp and epifluorescence optics (blue filter set: exciter filter BP 395-440, chromatic beam splitter FT460, barrier filter LP470). The field of view could then be photographed under blue or white light using Kodak Elite II, ISO 200 film. 2. The DF procedure was identical to that with FDA, but because of the fluorescence of extracellular DF, a more thorough rinse was necessary. 3. Ethidium bromide was employed as described by Roser et al. (1982). The hyphae to be stained were first fixed in 95% ethanol for two min, rinsed in PB for two min, stained with EB for five min, rinsed with PB and mounted in the same buffer. Stained hyphae were viewed under both white and green light (epifluorescence microscope as described above but using exciter filter BP546, chromatic beam splitter FT580, barrier filter LP490). Regions of hyphae with red-fluorescing nuclei were scored as stained, while extended lengths of hyphae lacking stained nuclei were scored as unstained.

For all stains, a gridline-intersect method (Abbott et al. 1984) was used to determine the relative length of stained hyphae to the length of total hyphae. Note that this study was not designed to determine the total length of hyphae present, only the relative lengths of the stained and unstained hyphae.

### *6.3.3 Influence of the age of the ectomycorrhizal association*

Mycorrhizal associations were examined 2, 9, 12 and 26 weeks following inoculation. The staining procedures described above were performed on three different root systems for each of the association ages. For every stain performed on each root system, 50 fields of view were examined since Abbott et al. (1984) found the mean and standard deviation were established with this number of observations. For each field of view, the number of times hyphae crossed a gridline under white light were tallied first; then the same field of view was viewed with blue light or green light and the number of fluorescing hyphae crossing a gridline was counted. The fraction of the total hyphae that took the stain was thus established for each sample.

### *6.3.4 Wall permeability of the extramatrical hyphae*

A series of experiments were undertaken to establish whether the ethanol pretreatment used in the normal EB staining made hyphal walls as well as membranes permeable to the stain. Extramatrical hyphae from four-week-old associations were used. One group of hyphae was pretreated with ethanol, and another by heating to 60°C in PB for five min. The heat treatment would render the membranes permeable, but should not affect the wall or DNA (see Daniell et al. 1969, Szybalski 1967). A control group was held in PB at room temperature for 5 min, and then stained with EB. Fractions of stained hyphae were

determined as described above. To test the effect of a heat treatment on nuclear staining, non-mycorrhizal *P. banksiana* white root tips known to be alive were also stained with EB using the same three pretreatments described above. Following staining, the hyphae and whole mounted, intact root tips from each treatment were mounted in PB and viewed microscopically under both green and white light.

#### **6.4 Results**

Portions of hyphae stained with FDA fluoresced a much brighter yellow-green than those which remained unstained (Figure 6.1). Unstained hyphae were usually not seen on film at the exposure times utilized, unless they were illuminated by nearby fluorescing hyphae. Often stained and unstained regions were adjacent parts of a continuous hypha (Figure 6.1). Absence of background fluorescence from the FDA treatment solution allowed these specimens to be easily photographed. Hyphae stained with DF were similar in appearance to those stained with FDA but the background fluorescence, due to incomplete rinsing of the fluorescent staining solution, made them difficult to photograph (data not shown). The autofluorescence of hyphae not treated with FDA or DF was too faint to capture on film at the exposure times used for stained specimens (data not shown).

Autofluorescence controls for EB (viewed with green light) were bright red (Figure 6.2). Fixing the tissue in ethanol prior to treatment with EB resulted in stained nuclei which appeared as brightly fluorescing spots at regular intervals in the hyphae (Figure 6.3).



Figures 6.1-8: Whole mounts of *Hebeloma cylindrosporum* extramatrical hyphae (Figures 6.1-5) and *Pinus banksiana* white roots (Figures 6.6-8). F, fluorescein-stained hyphae; U, unstained hyphae; N, nuclei. Scale bars = 100  $\mu$ m.

Figure 6.1: Extramatrical hyphae stained with fluorescein diacetate showing stained and unstained regions. Blue light illumination.

Figure 6.2: Unstained extramatrical hyphae. Green light illumination.

Figure 6.3-5: Extramatrical hyphae stained with ethidium bromide. Green light illumination.

Figure 6.3: Concentrated ethanol pretreatment, showing fluorescing nuclei.

Figure 6.4: Heat pretreatment.

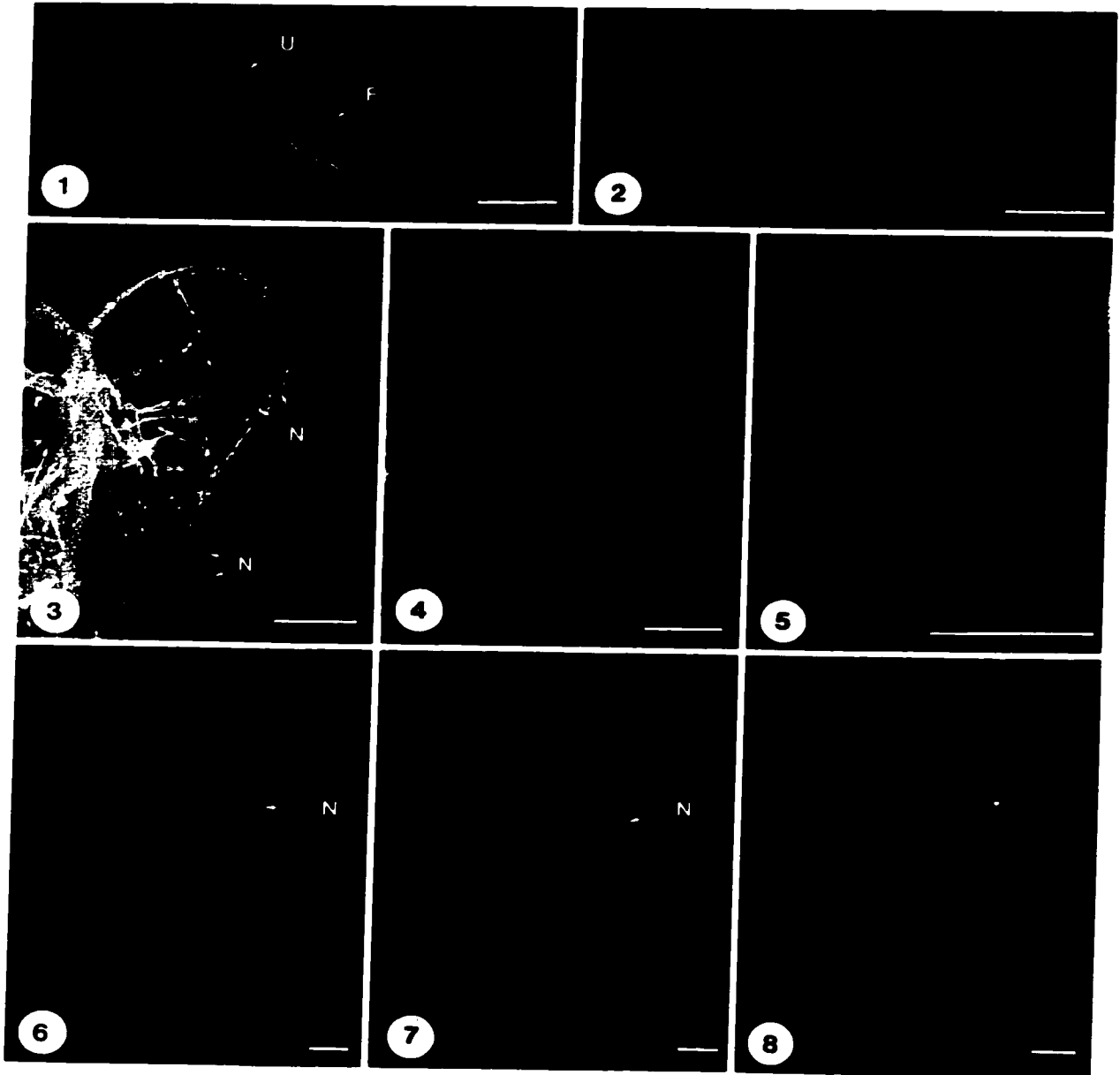
Figure 6.5: Control (no pretreatment).

Figures 6.6-8: Roots stained with ethidium bromide. Green light illumination.

Figure 6.6: Ethanol pretreatment, fluorescing nuclei.

Figure 6.7: Heat pretreatment, fluorescing nuclei.

Figure 6.8: No pretreatment. Few fluorescing nuclei were present.



Fewer nuclei were stained when a heat pretreatment was substituted for the ethanol treatment (Figure 6.4). Similarly, when hyphae were treated directly with EB (no pretreatment), few nuclei were stained (Figure 6.5). In the case of plant root cells, pretreatment with ethanol led to virtually all nuclei being stained by EB (Figure 6.6). However, unlike the results with the fungal hyphae, virtually all the plant nuclei were also stained after the heat pretreatment (Figure 6.7). With no pretreatment, EB stained few plant nuclei (Figure 6.8).

When the mycorrhizal association was two weeks old, fluorescein was concentrated in 25% of the hyphae following treatment with FDA and DF (Figure 6.9). At this time, EB (with the ethanol pretreatment) stained 89% of the hyphae (Figure 6.9). As the age of the association increased from 2 to 26 weeks, the fraction of stained hyphae decreased to 6-7% in the case of FDA and DF compared to 76% with EB (Figure 6.9). The results with FDA and DF were essentially the same, but in all stages of the association sampled, EB stained a much greater proportion of hyphae than did fluorescein.

Pretreatment with ethanol gave the EB access to nearly 13 nuclei per millimetre of hyphae (Figure 6.10). The heat pretreatment allowed EB to stain one or two nuclei for each millimetre of hyphae (Figure 6.10). EB applied in the absence of a pretreatment stained approximately one nucleus per mm of hyphae (Figure 6.10).

### **6.5 Discussion**

A major function of extramatrical hyphae in the ectomycorrhizal association is to absorb ions from the soil for transfer to the remainder of the fungus and the plant. To perform this function, a hypha must have a wall permeable enough for ions to gain access to the

**Figure 6.9: Fraction of hyphae showing the fluorescence of the vitality stains ethidium bromide (EB), disodium fluorescein (DF) and fluorescein diacetate (FDA) at various ages of association. Standard errors were determined with n=3.**

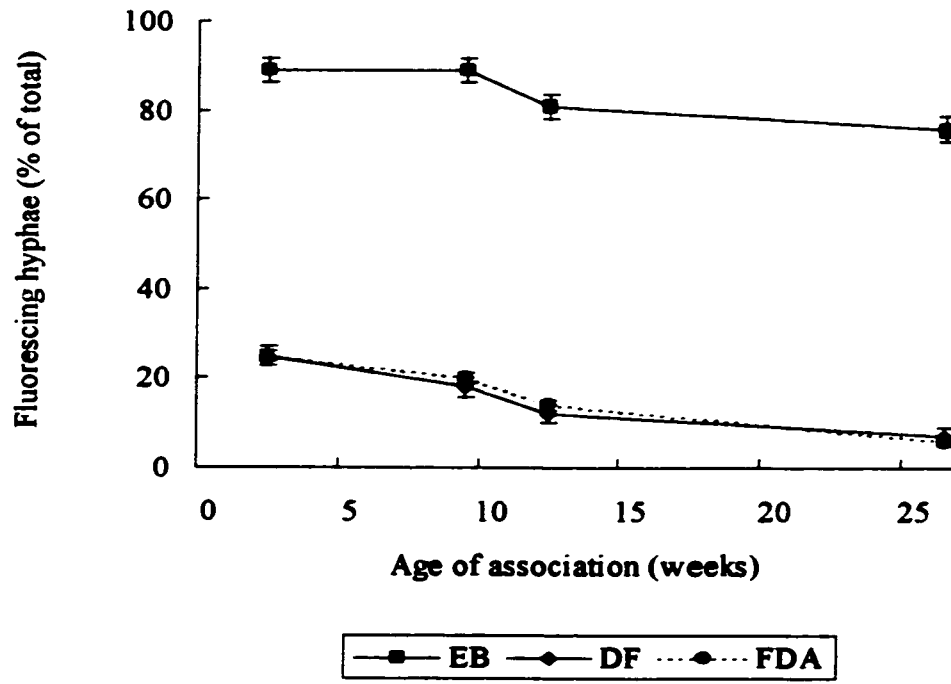


Figure 6.9

**Figure 6-10: The number of fluorescing (ethidium bromide-stained) nuclei observed per millimeter of hyphae, following three pretreatments for extramatrical hyphae of a four week old association. For details of the pretreatments, see 6.1 Methods. Standard errors were determined using n=3.**

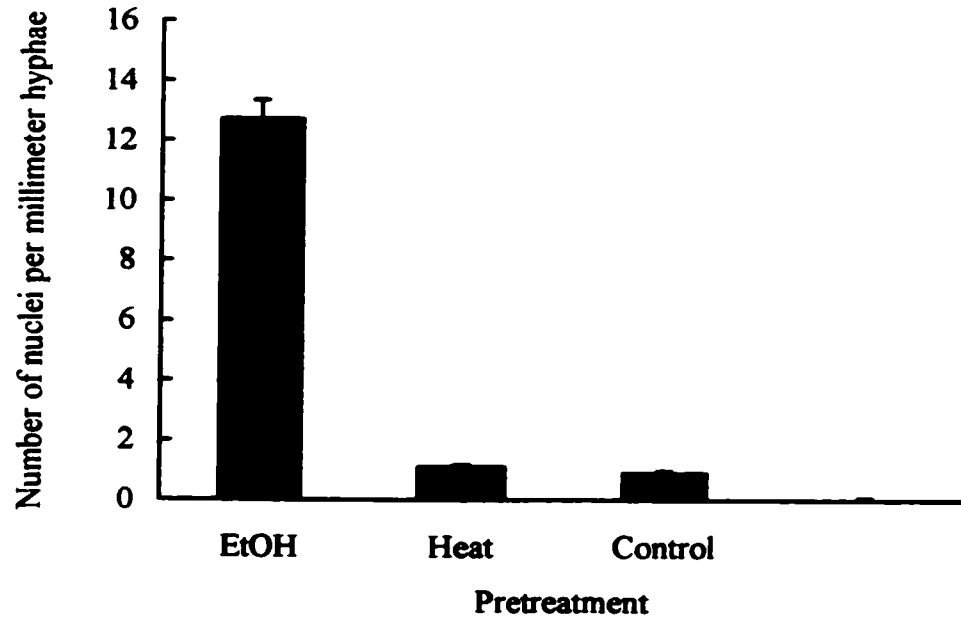


Figure 6.10

plasmalemma and also carriers or porins in the membrane that allow movement of the ion into the protoplast of the living cell. A study of the specific carriers in the membranes was outside the scope of the present work. However, it proved possible to test viability and wall permeability of the hyphae and thus to measure the proportion of the hyphal mass with the potential to absorb ions.

In the present work, FDA stained a fraction of hyphae that declined steadily from 25% two weeks after inoculation to less than 10% twenty-five weeks after inoculation; the proportions of hyphae stained with DF were essentially the same. Fractions of hyphae with EB-stained nuclei also declined steadily with increasing age of the mycorrhizal association, but EB consistently stained a much larger fraction of hyphae (e.g., 89% at 2 weeks after inoculation and 76% at 26 weeks after inoculation) than did the fluoresceins. Could these apparent differences in hyphal viability be due to the wall impermeability of some hyphae? Söderström (1977), for example, found that resting cells such as spores (which have modified walls) could not accumulate fluorescein following FDA treatment.

Although it was not possible to test hyphal wall permeability directly, indirect evidence indicates that the reduced staining with FDA and DF was due to wall impermeability. First, the increased apparent viability of the hyphae with EB occurred following the ethanol pretreatment (used in the procedure of Roser et al. 1982) but not following a hot water pretreatment. (A parallel experiment with root tips verified that the hot water treatment increased the permeability of membranes but did not interfere with nuclear staining.) The nature of the change in the hyphal wall during ethanol treatment is unknown. The results of the present study indicate that EB is superior to FDA or DF for



testing the viability of *Hebeloma cylindrosporum* extramatrical hyphae. Further, much of the mycelium is alive but has walls with reduced permeability.

Currently available information on hyphal wall permeability is scattered. According to Money (1990), the pore size in young hyphae of *Achlya bisexualis* is 2-3 nm (a dimension sufficient to allow the passage of nutrient ions and viability stains). Young fungal hyphae secrete large molecular weight proteins into the media (Chang and Trevithick 1974), indicating the presence of relatively large pores in their walls. However, older hyphal walls can be modified and their permeability reduced (see Burnett 1979, Wessels 1990, Rayner 1991, Ruiz-Herrera 1992, Rayner et al. 1994, Unestam and Sum 1995). Hydrophobins are small proteins found in walls of aerial hyphae (Wessels 1994). cDNAs that encode for hydrophobins have been found in the ectomycorrhizal fungus *Pisolithus tinctorius*; the genes are expressed when the fungus is in a mycorrhizal association but not in plate culture (Tagu et al. 1996). It has been proposed that these proteins are involved in the development of impermeable walls (Wessels 1994). It is probable that the reduced wall permeability noted in the present study occurs in older hyphae, so that the highly branched extramatrical system has young, absorptive areas attached to the mantle by nonabsorbing conduits. Mycorrhizae show the greatest benefit in absorbing ions with low mobility in soil (e.g., phosphate). After the growing hyphal tip has mined the nutrient ions from its microenvironment, there is little need for absorptive hyphae in this area.

How the results of this study relate to mycorrhizae growing in soil is a matter of speculation. In the present study, pouch-grown material was used to minimize damage to

the hyphae, and to avoid contamination by other soil fungi. The stresses of growing in the soil may well reduce the proportion of viable and/or absorptive hyphae.

The results of this viability and permeability study on the extramatrical hyphae of ectomycorrhizal *H. cylindrosporum* have both practical and physiological ramifications. A much higher fraction of the hyphae are alive than was previously estimated by the use of fluorescein stains (Schubert et al. 1987). Conversely, the potential absorbing surface area of the hyphae is significantly smaller than was often assumed previously so that the absorbing regions are more efficient than previously realised. Further work is definitely needed in the areas of hyphal development and nutrient acquisition, particularly for mycorrhizal systems.

## **CHAPTER 7**

### **Conclusions**

The papers included in this thesis presented studies on a plethora of topics involving woody root anatomy, physiology, and potential impacts on mineral nutrient acquisition. General aspects of the research as a whole will be presented in three parts. The first will deal with the novel techniques or applications of existing methods that were developed to perform the experiments. The focus will not be on the actual methodology, which was detailed in the papers, but on the importance of the technique and its potential application in future studies. The second part will bring together the results of the papers in an attempt to create a clearer picture of woody root structure and function. Naturally, there will be a great deal of supposition and speculation in this, and it will be duly noted when made. However, the results of the research will serve as a solid framework on which a model will be developed. The third and final aspect of the conclusion will be to summarize those questions regarding woody root anatomy and physiology that have been exposed or accentuated by the studies of this thesis. It is hoped that these will inspire future research in this field.

#### **7.1 Novel developments**

In performing the research of this thesis, a number of techniques were modified or combined in attempt to answer the questions that were posed. Two of these are especially significant. The first involved the use of vitality stains to examine the extramatrical hyphae of an ectomycorrhizal association. While no novel techniques were employed, the results pointed out relevant considerations and new applications for commonly used vitality tests. The second was the development of a new method, the internal perfusion technique, to

measure the permeability of tissue surfaces. This rapid, simple technique was invaluable in answering important questions of this thesis, and should find widespread use in the future. In this section of the conclusions, I will discuss the significance and future application of these developments.

### *7.1.1 Fungal vitality tests*

In the study of extramatrical hyphal vitality presented in this thesis (see Chapter 6), two classes of vitality stain were employed. The first type was fluorescein stains, which rely on contact with the plasma membrane and entry into the cytoplasm to function. The second was ethidium bromide, which depends on a heat pretreatment to damage the membranes in order to access and stain the double-stranded DNA of the nucleus. Both these vitality tests had been used previously in separate studies (Roser et al. 1982, Söderström, 1977). However, the difference in their results had never been documented. In Chapter 6, it was noted that the ethidium bromide method predicted a much larger fraction of the extramatrical hyphae to be alive than did the fluorescein-based tests. It was reasoned that the ethanol pretreatment, prescribed to make the membranes permeable to the ethidium bromide, was making the mature fungal walls permeable to the stain as well. Conversely, the fluorescein stains, which do not require and would not function with a ethanol pretreatment, were unable to pass the mature fungal walls.

Clearly, the two vitality stains were representing different proportions of hyphae. The ethidium bromide was identifying the fraction of hyphae that were alive, while the fluorescein was expressing the portion of hyphae that were alive but not encased in mature, impermeable (to fluorescein) walls. If this impermeability can be extrapolated to

physiologically significant ions, then those lengths of hyphae encased in mature walls would also be unable to contribute to ion uptake. Therefore, allowing the same assumption, the fluorescein test revealed the fraction of hyphae that was potentially capable of absorbing ions. This is an incredibly important finding, as no other current test is capable of this. As well, these results highlight the importance of carefully choosing vitality tests for the sample at hand, using more than one vitality test, and thoughtfully analyzing the results.

A number of future applications exist that are well-suited for the ethidium bromide/fluorescein tests. From the perspective of the root physiologist, extending the tests to other extramatrical and extraradical (for vesicular-arbuscular mycorrhizae) hyphae, in particular those grown under natural conditions, is logical. With some modification, the tests may also prove useful for analyzing those hyphae within the root. The information gathered from such studies would be useful in assessing where nutrient exchange occurs between the two symbionts in a mycorrhizal association. Of course, the tests could also be applied to any type of fungus where there was an interest in determining vitality and/or potential for nutrient acquisition.

#### *7.1.2 Tissue surface permeability*

In the course of this thesis project, it was important to assess the permeability of the outer surface of the ectomycorrhizal mantle and cork zone roots. Previously, it was unclear if these surfaces were permeable to ions or not, and the result would have great ramifications on the potential pathways of nutrient absorption in woody root systems. While there were a number of tracer dyes that were suitable for such tests, the molecules of these dyes are

much larger than the ions of interest. As a result, tracer dye conclusions cannot be extrapolated to nutrient ions with much confidence. Therefore, it was necessary to test the permeability of the ectomycorrhizal mantle and cork zone roots surfaces to ions.

There are a number of ways to test tissue permeabilities to ions. However, all have respective flaws. Freeze-substitution followed exposure to a photographic plate is feasible and does produce a visual image of the results. Unfortunately, it is a very technically demanding and lengthy procedure. Compartmental elutions are technically similar, but produce unclear results when working with very small tissues such as those in this study (unpublished data). Modern techniques, such as laser micro mass analysis (LAMMA) are very accurate and reasonably simple, but prohibitively expensive. As no existing method was suitable, the internal perfusion technique (IPT) was developed.

The IPT has many positive attributes. It is rapid, so that testing and result analysis can be completed in less than two days. It is not labour intensive, requiring only sporadic involvement following initial set up. Little tissue is required; a single seedling is capable of providing more than enough material. The IPT is amenable to tracer dyes or most ions. As well, it is relatively inexpensive. Finally, the method allows a permeability per surface area to be determined from the results, making quantification possible.

The technique has only two drawbacks. First, it requires the use of radiolabeled ions (unless a less effective dye is chosen). However, any ion may be employed and it is easy to choose a weak emitter which represents a low health risk. Secondly, it is only practical for determining the permeability of the outermost tissue layer. Despite these limitations, the technique could still be used for a large number of applications.

In the present work, the IPT was used to determine the permeability of the ectomycorrhizal mantle to sulphate ions. It would be simple to test the permeability to other ions as well. It would also be prudent to establish the permeability of the mantle in other plant-fungal species combinations, especially in light of the controversy surrounding this topic (Kuhn et al. 1999, Vesik et al. 2000). It would also be possible to extend the study of cork zone roots to older cork zones in roots and stems. A further extension would be to examine the permeability of above ground organs that are ensheathed in a cuticle (i.e. leaves), as a cuticle represents a (relatively) impermeable coating on the outer surface. It may also be feasible to utilize the IPT to examine the permeability of organ surfaces to water, provided the water was labeled in some manner. This could be especially interesting for leaves, in which permeability to water is extremely relevant. Clearly this innovative method could be useful in a vast range of research studies.

## **7.2 A model of woody root structure and function**

In the course of this thesis, a wide variety of topics pertaining to woody roots were studied. However, most of these studies are united by the common theme of ion uptake potential. In this section, the results of each study will be briefly summarized, and then joined together to create a coherent picture of the potential pathways of ion acquisition in woody root systems. Only the pine data will be presented here, as certain experiments were not performed on the eucalypts.

One of the most important experiments in this thesis was the study of pine root anatomy of field-grown seedlings (Chapter 4). This work had not been done before at the resolution with which it was performed in this study. It was found that while the majority

of the root length was in the condensed tannin zone, the bulk of the cortical absorbing plasmalemma surface area (CPSA) was in the ectomycorrhizal zone. From this, it was concluded that the ectomycorrhizal roots are the primary zone of ion absorption in woody root systems. A subsequent study further supported this concept, as the xylem was found to be functional much closer to the tip of ectomycorrhizal roots than in the other root tip types (Chapter 3), suggesting that ectomycorrhizal roots were well-suited for the translocation of nutrient ions. The purpose of the condensed tannin zone is unclear, but it may serve only to connect the nutrient absorbing ectomycorrhizal root tips to the above ground portion of the plant.

The pathway of ion uptake into the ectomycorrhizal roots however is still unclear. The permeability of the ectomycorrhizal mantle to physiologically significant ions (namely  $\text{SO}_4^{-2}$ ) was investigated, and the fungal mantle was found to be impermeable to this ion. Assuming that this impermeability extends to other nutrient ions, essential mineral elements would be unable to diffuse through the ectomycorrhizal mantle and, therefore, must be absorbed by the extramatrical hyphae.

At this point, an accidental discovery proved fortuitous. Early in the course of this study, experiments were undertaken to determine the fraction of the extramatrical hyphae which were alive (Chapter 6). A collection of vitality tests were employed, and quite conflicting results were obtained. Following careful analysis, it was realized that the fluorescein-based tests were actually presenting the fraction of extramatrical hyphae that were potentially capable of absorbing mineral ions. Unexpectedly, a much lower fraction



of these hyphae were found to be potentially capable of ion uptake than were found to be alive.

With this collection of data, a model of ion uptake in woody roots was constructed. To begin, the vast majority of the root length contributes very little to ion acquisition, as the cork zone is nearly impermeable at its outer surface (Chapter 2) and the condensed tannin zone possesses a very small CPSA. While the white zone may play a role in ion uptake at low levels of fungal association, it is likely overshadowed by the contribution of the ectomycorrhizae. However, the ectomycorrhizal roots are incapable of absorbing ions independent of the fungal partner, as the mantle is impermeable to ions (barring the unlikely distal diffusion of ions through the cortex following entry from the condensed tannin zone cortex basipetal to the mantle). Therefore, the majority of the ions absorbed by a woody root system are first absorbed by the extramatrical hyphae. This may seem unusual, given the small fraction of the extramatrical hyphae found to be potentially capable of absorbing ions, but the substantial length (Marx et al. 1976), and ability to proliferate in regions of nutrient density (Bending and Read 1995) of these hyphae must be considered.

In summary, the vast majority of the woody root system (cork and condensed tannin zones) acts as a scaffolding, and a conduit connecting the absorbing ectomycorrhizae to the shoot. It appears that the majority of the mineral nutrients entering the woody root system are first absorbed by the small fraction of the extramatrical hyphae capable of uptake, stressing the significance of the fungal symbiont. This model contains elements that are substantially different from many commonly accepted ideas about woody root physiology,

such as declaring the majority of the root system length to be a minor contributor to ion uptake. These findings stress the importance of studying topics in which answers have been produced from insufficient evidence.

### **7.3 Pertinent questions raised by this thesis**

The hallmark of any good study is that its results should serve as a base from which further research may be carried forward. This thesis amply meets these criteria, offering a wide array of questions concerning woody root structure and function. In this section, three broad questions will be highlighted and briefly explored.

In this study, a combination of time restraints, space limitations, and other practical considerations necessitated the use of seedlings instead of mature trees. This was unfortunate, as it is unclear how the anatomy of a seedling relates to that of a mature tree. Likewise, growth pouches were employed because they permitted relatively sterile conditions, and facile access to the roots. However, a growth pouch is quite artificial, and the results found here may be considerably different for roots grown in their native environment. It is important that the results of this study be re-explored using more mature trees grown under natural conditions.

A second question raised by this thesis involves the interpretation of ion uptake capacity. In this work, all plasmalemma surface areas (both plant and fungal) exposed to the soil solution by a permeable apoplast were treated as equally capable of absorbing ions. This assumption is almost assuredly incorrect, as it would require all plasmalemma transport proteins to be evenly distributed among all these plasma membrane surfaces. There are two possible ways to solve this conundrum. The first would be to assess the

capability of the various membranes to absorb specific mineral nutrients. While this would be difficult with roots, given the problems inherent in isolating very different membrane surface areas found in close proximity, it would be relatively easy with the extramatrical hyphae. Such a study with the hyphae is long overdue, as extramatrical hyphae have only been confirmed capable of absorbing phosphorus (Skinner and Bowen 1974) and nitrogen (Finlay et al. 1989). The second method would be to determine the presence of the various uptake proteins in the membranes, possibly through *in situ* hybridizations. Such a project would be a monumental undertaking, but would be invaluable to the study of ion uptake in woody roots.

A final question that will be discussed here is how representative our conclusions are to woody roots in general. The significant differences noted between our pine and eucalypt results suggest that extrapolating our results to all woody roots may not be appropriate. Similarly, our characterization of the ectomycorrhizal fungus *Hebeloma cylindrosporum* is not likely representative of all ectomycorrhizal fungi. Clearly, the choice of species is important, and it is imperative that future studies involve a diverse range. Similarly, it is important to examine roots under the plethora of conditions that they endure in the field, to assess the impact of environment on woody root physiology. With a respectable base of knowledge and technique, and so many questions unanswered, it is a wonderful time to be involved in the field of woody root physiology.

#### 7.4 Summary

Several aspects of woody root structure and function were examined in this thesis. In the process, new methods were developed and novel applications of existing techniques were

employed. The most significant contribution of this thesis is a model of woody roots based on anatomy that allows predictions of ion acquisition sites to be made. The model did rely on some assumptions, and these demand investigation in the future. Through this, the model of woody root function designed in this thesis may become more accurate.

**REFERENCES**

Abbott L, Robson AD, De Boer G (1984) The effect of phosphorus on the formation of hyphae in soil by the vesicular-arbuscular mycorrhizal fungus, *Glomus fasciculatum*. *New Phytol.* 97: 437 – 446.

Ashford AE, Peterson CA, Carpenter JL, Cairney JWG, Allaway WG (1988) Structure and permeability of the fungal sheath in *Pisonia* mycorrhiza. *Protoplasma* 147: 149 – 161.

Baker DA (1971) Barriers to the radial diffusion of ions in maize roots. *Planta* 98: 285 - 293.

Barak R, Chet I (1986) Determination, by fluorescein diacetate staining, of fungal viability during mycoparasitism. *Soil Biol. Biochem.* 18: 315 – 318.

Behrmann P, Heyser W (1992) Apoplastic transport through the fungal sheath of *Pinus sylvestris* / *Suillus bovinus* ectomycorrhizae. *Bot. Acta* 105: 427 – 434.

Bending GD, Read DJ (1995) The structure and function of the vegetative mycelium of ectomycorrhizal plants. V. The foraging behaviour of ectomycorrhizal mycelium and the translocation of nutrients from exploited organic matter. *New Phytol.* 130: 401 – 409.

Brundrett MC, Piché Y, Peterson RL (1984) A new method for observing the morphology of vesicular-arbuscular mycorrhizae. *Can. J. Bot.* 62: 2128 – 2131.

Brundrett MC, Enstone DE, Peterson CA (1988) A berberine-aniline blue fluorescent staining procedure for suberin, lignin and callose in plant tissue. *Protoplasma* 146: 133 – 142.

Brundrett MC, Kendrick B, Peterson CA (1991) Efficient lipid staining in plant material with Sudan red 7B or fluorol yellow 088 in polyethylene glycol-glycerol. *Biotech. Histochem.* 66: 111 – 116.

Burkert B, Robson A (1994)  $^{65}\text{Zn}$  uptake in subterranean clover (*Trifolium subterraneum* L.) by three vesicular-arbuscular mycorrhizal fungi in a root-free sandy soil. *Soil Biol. Biochem.* 26: 1117 – 1124.

Burnett JH (1979) Aspects of the structure and growth of hyphal walls. In JH Burnett, APJ Trinci (eds.) *Fungal walls and hyphal growth*. Cambridge University Press, Cambridge, England. pp. 1 – 25.

Carpita N, Subulase O, Mottezinis D, Delmer DP (1979) Determination of the pore size of cell walls of living plants. *Science* 105: 1144 – 1147.

Chang LY, Trevithick JR (1974) How important is secretion of exoenzymes through apical cell walls of fungi? *Arch. Microbiol.* 101: 281 – 293.

Chilvers GA (1968) Some distinctive types of eucalypt mycorrhiza. *Aust. J. Bot.* 26: 49 – 70.

Chilvers GA, Pryor LD (1965) The structure of eucalypt mycorrhizas. *Aust. J. Bot.* 13: 245 – 259.

Chung H, Kramer PJ (1974) Absorption of water and  $^{32}\text{P}$  through suberized and unsuberized roots of Loblolly pine. *Can. J. For. Res.* 5: 229 – 235.

Crider FJ (1933) Selective absorption of ions not confined to young rootlets. *Science* 78: 169.

Cruz RT, Jordon WR, Drew MC (1992) Structural changes and associated reduction of hydraulic conductance of *Sorghum bicolor* L. following exposure to water deficit. *Plant Physiol.* 99: 203 – 212.

Daniell JW, Chappell WE, Couch HB (1969) Effect of sublethal and lethal temperatures on plant cells. *Plant Physiol.* 44: 1684 – 1689.

Enstone DE, Peterson CA (1992) The apoplastic permeability of root apices. *Can. J. Bot.* 70: 1502 – 1512.

Esau K (1977) *Anatomy of Seed Plants, Second Edition.* John Wiley and Sons, New York.

Finlay RD, Ek H, Odham G, Söderström B (1989) Uptake, translocation and assimilation of nitrogen from  $^{15}\text{N}$ -labeled ammonium by *Pinus sylvestris* plants infected with four different ectomycorrhizal fungi. *New Phytol.* 110: 58 – 66.

Fortin JA, Piché Y, Lalonde M (1980) Technique for the observation of early morphological changes during ectomycorrhiza formation. *Can. J. Bot.* 58: 361 – 365.

Harley JL, Smith SE (1983) *Mycorrhizal Symbiosis.* Academic Press, London, England.

Kamula SA, Peterson CA, Mayfield CI (1994) The plasmalemma surface area exposed to the soil solution is markedly reduced by maturation of the exodermis and death of the epidermis in onion roots. *Plant Cell Env.* 17: 1183 – 1193.

Kramer PJ (1946) Absorption of water through suberized roots of trees. *Plant Physiol.* 21: 37 – 41.



Kramer PJ, Bullock HC (1966) Seasonal variations in the proportions of suberized and unsuberized roots of trees in relation to the absorption of water. *Amer. J. Bot.* 53: 200 - 204.

Kreuzwieser J, Rennenberg H (1998) Sulphate uptake and xylem loading of mycorrhizal beech roots. *New Phytol.* 140: 319 – 329

Kuhn AJ, Schröder WH, Bauch J (1999) Access of calcium and magnesium into mycorrhized spruce roots. *Planta*: in press.

Le Page BA, Currah RA, Stockey RA, Rothwell GW (1997) Fossil ectomycorrhiza from the middle Eocene. *Amer J. Bot.* 84: 410 – 412.

Leshem B (1970) Resting roots of *Pinus halepensis*: structure, function, and reaction to water stress. *Bot. Gaz.* 131: 99 – 104.

Loomis WG, Schull CA (1937) *Methods in Plant Physiology*. McGraw-Hill, New York.

Mager H (1913) Versuche über die Metakutisierung. *Flora* 106: 42 – 50.

Malajczuk N, Lapeyrie F, Garbaye J (1989) Infectivity of pine and eucalypt isolates of *Pisolithus tinctorius* on roots of *Eucalyptus urophylla* *in vitro*. *New Phytol.* 114: 627 – 631.

Marschner H (1986) *Mineral Nutrition in Higher Plants*. Academic Press, New York.

Marx DH, Bryan WC, Cordell CE (1976) Growth and ectomycorrhizal development of pine seedlings in nursery soils infested with the fungal symbiont *Pisolithus tinctorius*. *For. Sci.* 22: 91 – 100.

Massicotte HB, Peterson RL, Ashford AE (1986) Ontogeny of *Eucalyptus pilularis* – *Pisolithus tinctorius* ectomycorrhizae. I. Light microscopy and scanning electron microscopy. *Can. J. Bot.* 65: 1927 – 1939.

McCully ME, Canny MJ (1988) Pathways and processes of water and nutrient movement in roots. *Plant Soil* 111: 159 – 170.

McKenzie BE, Peterson CA (1995a) Root browning in *Pinus banksiana* Lamb. and *Eucalyptus pilularis* Sm 1. Anatomy and permeability of the white and tannin zones. *Bot. Acta* 108: 127-137.

McKenzie BE, Peterson CA (1995b) Root browning in *Pinus banksiana* Lamb. and *Eucalyptus pilularis* Sm 2. Anatomy and permeability of the cork zone. Bot. Acta 108: 138 – 143.

Melin E, Nilsson H (1950) Transfer of radioactive phosphorus to pine seedlings by means of mycorrhizal hyphae. Physiol. Plant. 3: 88 – 92.

Money NP (1990) Measurement of pore size in the hyphal cell wall of *Achlya bisexualis*. Exp. Myc. 14: 234 – 242.

Müller H. (1906) Über die Metakutisierung der Wurzelspitze und über die verkorkten Scheiden in den Achsen der Monokotyledone. Bot. Zeit. 64: 53 – 84.

Oh KI, Melville LH, Peterson RL (1995) Comparative structural study of *Quercus serrata* and *Q. acutissima* formed by *Pisolithus tinctorius* and *Hebeloma cylindrosporum*. 9: 171 – 179.

Perumalla CJ, Peterson CA, Enstone, DE (1990) A survey of angiosperm species to detect hypodermal Casparian bands. I. Roots with a uniseriate hypodermis and epidermis. Bot. J. Linn. Soc. 103: 93 – 112.

Peterson CA, Enstone DE (1996) Functions of passage cells in the endodermis and exodermis of roots. *Physiol. Plant* 97: 592 – 598.

Peterson CA, Enstone DE, Taylor JH (1999) Pine root structure and its potential significance for root function. *Plant Soil* 217: 205 - 213.

Peterson CA, Lefcourt BEM (1990) Development of endodermal Casparian bands and xylem in lateral roots of broad bean. *Can. J. Bot.* 68: 2729 – 2735.

Peterson CA, Perumalla CJ (1990) A survey of angiosperm species to detect hypodermal Casparian bands. II. Roots with a multiseriate hypodermis or epidermis. *Bot. J. Linn. Soc.* 103: 113 – 125.

Peterson CA, Steudle E (1993) Lateral hydraulic conductivity of early metaxylem vessels in *Zea mays* L. roots. *Planta* 189: 288 – 297.

Peterson RL, Farquhar ML (1996) Root hairs: specialized tubular cells extending root surfaces. *Bot Rev.* 62: 1 – 40.

Piché Y, Peterson RL, Howarth MJ, Fortin JA (1983) A structural study of the interaction between the ectomycorrhizal fungus *Pisolithus tinctorius* and *Pinus strobus* roots. *Can. J. Bot.* 61: 1185 – 1193.

Plaut M. (1918) Über die morphologischen und mikroskopischen Merkmale der Periodizität der Wurzel, sowie über die Verbreitung der Metakutisierung der Wurzelhäube im Pflanzenreich. Festscher. 100-jähr. Best kgl. Württemb. Landw. Hochschule. 129 – 151.

Hohenheim.

Rayner ADM (1991) The challenge of the individualistic mycelium. *Mycologia* 83: 48 – 71.

Rayner ADM, Griffith GS, Ainsworth AM (1994) Mycelial interconnectedness. In NAR Gow, GM Gadd (eds.) *The Growing Fungus*. Chapman and Hall, London, England. pp. 1 – 40.

Read DJ, Boyd R (1985) Water relations of mycorrhizal fungi and their host plants. In PG Ayres, L Boddy (eds.) *Water, Fungi and Plants*. Cambridge University Press, Cambridge, England. pp 287 – 303.

Rhodes LH, Gerdemann JW (1975) Phosphate uptake zones of mycorrhizal and non-mycorrhizal onions. *New Phytol.* 75: 555 – 561.

Richards D, Considine JA (1981) Suberization and browning of grapevine roots. In Brouwer R (ed.) *Structure and function of plant roots*, Martinus Nijhoff / Dr. W. Junk Publishers, Boston, Massachusetts. pp. 111 – 115.

Ritter T, Kottke I, Oberwinkler F (1986) Nachweis der Vitalität von Mykorrhizen. FDA-Vitalfluorochromierung. *Biol in unserer Zeit* 16: 179 – 185.

Robards AW, Robb RE (1974) The entry of ions and molecules into roots: an investigation using electron-opaque tracers. *Planta* 120: 1 – 12.

Roser DJ (1980) Ethidium bromide: A general purpose fluorescent stain for nucleic acid in bacteria and eukaryotes and its use in microbial ecology studies. *Soil Biol. Biochem.* 12: 329 – 336.

Roser DJ, Keane PJ, Pittaway PA (1982) Fluorescent staining of fungi from soil and plant tissues with ethidium bromide. *Trans. Br. Mycol. Soc.* 79: 321 – 329.

Ruiz-Herrera J (1992) *Fungal Cell Wall: Structure, Synthesis and Assembly*. CRC Press, Boca Raton, Florida, U.S.A.

Schubert A, Marzachi C, Mazzitelli M, Cravero MC, Bonfante-Fasolo P (1987) Development of total and viable extraradical mycelium in the vesicular-arbuscular mycorrhizal fungus *Glomus clarum* Nicol. & Schenck. *New Phytol.* 107: 183 – 190.

Skinner MF, Bowen GD (1974) The uptake and translocation of phosphate by mycelial strands of pine mycorrhizas. *Soil Biol. Biochem.* 6: 57 – 81.

Smith SE, Smith FA (1990) Structure and function of the interfaces in biotrophic symbiosis as they relate to nutrient transport. *New Phytol.* 114: 1 – 38.

Smith SE, Read DJ (1997) *Mycorrhizal Symbiosis*, Second Edition. Academic Press, Inc., San Diego, California.

Söderström BE (1977) Vital staining of fungi in pure cultures and soil with fluorescein diacetate. *Soil Biol. Biochem.* 9: 59 – 63.

Sougnéz-Remy S, Waterkeyn L, Van Prag HJ (1993) L'absorption-translocation spécifique d'éléments nutritifs en relation avec la structure anatomique des radicelles de hêtre (*Fagus sylvatica*) et d'épicéa (*Picea abies*). II. Observations relatives à la structure anatomique des radicelles. *Belg. J. Bot.* 126: 184 – 190.

- St. Aubin G, Canny MJ, McCully ME (1986) Living vessel elements in the late metaxylem of sheathed maize roots. *Ann. Bot.* 58: 577 – 588.
- Szybalski W (1967) Effects of elevated temperatures on DNA and polynucleotides: denaturation, renaturation and cleavage of glycosidic and phosphate ester bonds. In AH Rose (ed) *Thermobiology*. Academic Press, Inc., London. pp. 73-122.
- Tagu D, Nasse B, Martin M (1996) Cloning and characterization of hydrophobins-encoding cDNAs from the ectomycorrhizal basidiomycete *Pisolithus tinctorius*. *Gene* 168: 93 – 97.
- Tagu D, Kottke I, Martin F (1998) Hydrophobins in ectomycorrhizal symbiosis: hypothesis. *Symbiosis* 25: 5 – 18.
- Taylor JH, Peterson CA (1999) Morphometric analysis of *Pinus banksiana* Lamb. root anatomy during a 3-month field study. *Trees*: in press.
- Tennant D (1975) A test of a modified line intersect method of estimating root length. *J. Ecol.* 63: 995 – 1001.
- Tippett JT, O'Brien TP (1976) The structure of eucalypt roots. *Aust. J. Bot.* 24: 619 – 632.



Unestam T, Sum YP (1995) Extramatrical structures of hydrophobic and hydrophilic ectomycorrhizal fungi. *Mycorrhiza* 5: 201 – 311.

Van Praag HJ, Sougnez-Remy S, Weissen F (1993) L'absorption-translocation spécifique d'éléments nutritifs en relation avec la structure anatomique des racelles de hêtre (*Fagus sylvatica*) et d'épicéa (*Picea abies*). I. Mesures de l'absorption spécifique. *Belg. J. Bot.* 126: 175 – 183.

Van Rees KCJ, Comerford NB (1990) The role of woody roots of slash pine seedlings in water and potassium absorption. *Can. J. For. Res.* 20: 1183 – 1191.

Vesk PA, Ashford AE, Markovina, A-L, Allaway WG (2000) Apoplasmic barriers and their significance in the exodermis and sheath of *Eucalyptus pilularis*-*Pisolithus tinctorius* ectomycorrhizas. In press.

Wessels JGH (1990) Role of cell wall architecture in fungal tip growth generation. In IB Heath (ed.) *Tip Growth in Plant and Fungal Cells*. Academic Press, Inc., Toronto. pp.1 – 29.

Wessels JGH (1994) Developmental regulation of fungal cell wall formation. *Annu. Rev. Phytopathol.* 32: 413 – 437.

Wilcox HE (1954) Primary organization of active and dormant roots of noble fir, *Abies procera*. Amer. J. Bot. 41: 812 – 821.

Wilcox HE (1962a) Growth studies of the root of incense cedar, *Libocedrus decurrens*. I. The origin and development of primary tissues. Amer. J. Bot. 49: 221 – 236.

Wilcox HE (1962b) Growth studies of the root of incense cedar, *Libocedrus decurrens*. II. Morphological features of the root system and growth behavior. Amer. J. Bot. 49: 237 - 245.

Wilcox HE (1968) Morphological studies of the root of red pine, *Pinus resinosa* I. Growth characteristics and patterns of branching. Amer. J. Bot. 55: 247 – 254.